CHEMOPREVENTIVE EFFECT OF HASKAP BERRY POLYPHENOLS AGAINST TOBACCO SPECIFIC NITROSAMINE-INDUCED DNA DAMAGE IN NORMAL LUNG EPITHELIAL CELLS *IN VITRO*

by

Dehigaspege Inoka Madumani Amararathna

Submitted in partial fulfillment of the requirements
for the degree of Master of Science

at

Dalhousie University
Halifax, Nova Scotia
February 2017

I dedicate this thesis to my family and teachers,

And

Also to those who fight with cancer

TABLE OF CONTENTS

LIST OF TABLES

LIST OF FIGURES

ABSTRACT

The protective effect of polyphenol-rich haskap berry extracts against tobacco-specific nitrosamine ketone (NNK)-induced DNA damage was studied *in vitro*. Normal lung epithelial BEAS-2B cells were exposed to NNK, and to its precursor, 4-[(acetoxymethyl) nitrosamino]-1-(3-pyridyl)-1-butanone (NNKOAc), to induce DNA damage. Polyphenols present in haskap berries were extracted using ethanol and water, separately. Quercetin-3-*O*-glucoside (Q3G) and cyanidin-3-*O*-glucoside (C3G) were used as the reference compounds. BEAS-2B cells were pre-incubated with non-cytotoxic concentrations of haskap extracts, Q3G, and C3G separately, and investigated for their protective effects against NNK- and NNKOAc-induced DNA damage. Pre-incubation of BEAS-2B cells with haskap extracts, Q3G, and C3G, significantly suppressed the NNK- and NNKOAc-induced DNA strand breaks, and intracellular reactive oxygen species generation. The protective effect of haskap extracts could be related to their polyphenol content and high antioxidant capacity. An experimental animal model is proposed to further investigate the chemopreventive potential of haskap polyphenols against NNK-induced lung tumorigenesis.

LIST OF ABBREVIATIONS AND SYMBOLS USED

%	Percentage
11β-HSD	11β-Hydroxysteroid Dehydrogenase
7-mGua	7-*N*-Methylguanine
7-pobdG	7-[4-(3-Pyridyl)-4-Oxobut-1-yl]-2'-Deoxyguanosine
8-OH-dGuo	8-Hydroxy Deoxyguanosine
ACP	Acid Phosphatase
ADC	Adenocarcinoma
AGT	O^6-Alkylguanine DNA Alkyltransferase
APAF1	Apoptotic Proteas Activating Factor-1
ATCC	American Type Cell Culture Collection
ATM	Ataxia Telangiectasia Mutated
B(a)P	Benzo(a)pyrene
BAX	BCL-2 Associated X Protein
BEBM	Bronchial Epithelial Basal Medium
BEGM	Bronchial Epithelial Growth Medium
BER	Base Excision Repair
BrdU	5'-Bromo-2'-Deoxy-Uridine
BSA	Bovine Serum Albumin
C3G	Cyanidin-3-*O*-Glucoside
Ca^{++}	Calcium Ion
Cdk2	Cyclin-Dependent Kinases
CHK2	Nuclear Serine/Threonine Protein Kinase
cm^2	Square Centimeter
COX-2	Cyclooxygenase-2
DCF	2',7'-Dichlorofluoresin
DI	Deionized
DMEM	Dulbecco's Modified Eagle's Medium
DMSO	Dimethyl Sulfoxide
DNA PK	DNA Protein Kinase
DPPH	2,2 Diphenyl-1-1picryl-Hydrazyl
DSBs	DNA Double Strand Breaks
DW	Dry Weight
E2F	E2 Factor
EGCG	Epigallocatechin Gallate
EGF	Epidermal Growth Factors
EGFR	Epidermal Growth Factor Receptor
EIU	Endotoxin-Induced Uveitis
EMEM	Minimum Essential Eagle Medium
ERK1/2	Extracellular Signal-Regulated Kinase1/2

Folin-C	Folin-Ciocalteu Reagent
FRAP	Ferric Reducing Antioxidant Power Assay
FW	Fresh Weight
G1	Gap 1 Phase
G2	Gap 2 Phase
GAE	Gallic Acid Equivalent
GPx	Glutathione Peroxidase
GTP	Guanosine Triphosphate
GST	Glutathione S-Transferase
H(A)	Haskap Aqueous Extract
H(E)	Haskap Ethanolic Extract
H_2DCFDA	2',7'-Dichlorofluorescein Diacetate
hEGF	Human Epidermal Growth Factor
HRP	Horseradish Peroxidase
IL-6	Interleukin-6
iNOS	Inducible Nitric Oxide Synthase
LPH	Lipopolysaccharide
M	Mitosis Phase
MAPK	Mitogen-Activated Protein Kinase
MDM2	E3 Ubiquitin-Protein Ligase
mg/ml	Milligram per Millilitre
MGMT	*O*^{6}-Methylguanine DNA Methyltransferase
mM	Milli Molar
mTOR	Mammalian Target of Rapamycin
MTX	Methotrexate
NAC	N-Acetyl-L-Cysteine
NER	Nucleotide Excision Repair
NF-kB	Nuclear Factor Kappa Activated B Cells
NNAL	4-(Methylnitrosamino)-1-(3-Pyridyl)-1-Butanol
NNAL-Glu	NNAL-Glucuronides
NNK	4-(Methylnitrosamino)-1-(3-Pyridyl)-1-Butanone
NNKOAc	4-[(Acetoxymethyl) Nitrosamino]-1-(3-Pyridyl)-1-Butanone
NO	Nitric Oxide
Nrf2	Nuclear Factor Erythroid 2-Related Factor 2
NSCLC	Non-Small Cell Lung Cancer
O^2- pobdC	*O*^{2}-[4-(3-Pyridyl)-4-Oxobut-1-yl]-2'-Deoxycytosine
O^2-pobdT	*O*^{2}-[4-(3-Pyridyl)-4-Oxobut-1-yl]-2'-Deoxythymidine
O^6-mGua	*O*^{6}-Methylguanine
O^6-pobdG	*O*^{6}-[4-(3-Pyridyl)-4-Oxobut-1-yl]-2'-Deoxyguanosine
ºC	Celsius
PAH	Polycyclic Aromatic Hydrocarbons

PBS	Dulbecco's Phosphate Buffered Saline
PCNA	Proliferating Cell Nuclear Antigen
PGE2	Prostaglandin
PI3K	Phosphatidylinositol 3-Kinase
PIP2	Phosphatidylinositol (4,5)-Bisphosphate
PIP_3	Phosphatidylinositol (3,4,5)-Trisphosphate
PKC	Protein Kinase C
PMS	Phenazine Methosulphate
POB-DNA	Pyridyloxobutylation DNA Adducts
ppm	Parts per Million
Q3G	Quercetin-3-*O*-Glucoside
Rb	Retinoblastoma Protein
RNS	Reactive Nitrogen Species
ROS	Reactive Oxygen Species
S	Synthesis Phase
SCC	Squamous Cell Carcinoma
SCLC	Small Cell Lung Cancer
sec	Seconds
SSBs	DNA Single Strand Breaks
TAE	Tris/Acetic acid/EDTA
TBE	Tris Base/Boric Acid/EDTA Buffer
TE	Trolox Equivalent
TNF-α	Tumor Necrosis Factor-Alpha
TPC	Total Phenolic Content
TPTZ	2,3,4-Tris(2-Pyridyl)-S-Triazine
Trypsin-EDTA	0.25% Trypsin – 0.53 mM Ethylenediaminetetraacetic Acid
U/ml	Unit per Millilitre
UGT	Uridine-5'-Diphospho-Glucuronosyltransferases
UPLC-ESI-MS/MS	Ultra-Performance Liquid Chromatography-Electrospray Tandem Mass Spectrometry
UVA	Ultra Violet-A
WHO	World Health Organization
α7nAchR	Alpha7 Nicotinic Acetylcholine Receptors

ACKNOWLEDGEMENT

I wish to express my heartfelt gratitude to Dr. Vasantha Rupasinghe, for his unfailing faith in my work, for his inspirational guidance, continuous supervision, suggestions, and advice. Thank you, Dr. Rupasinghe for planning to carry out all the experimental work smoothly and efficiently, and pushing me to a successful completion. Further, I convey my deepest gratitude to Dr. David Hoskin and Dr. Michael Johnston for their invaluable guidance, supervision, and support given me to complete my thesis successfully.

I wish to extend my sincere gratitude to Dr. Graham Dellaire and Dudley Chung for their invaluable assistance in establishing the carcinogenesis model of this thesis project. Immense help and guidance from Dr. Anna Greenshields during my stay at Halifax is very much appreciated. Thanks to all my colleagues of Dr. Rupasinghe's and Dr. Hoskin's labs, for their help, kindness, and friendship. It was comfortable to work with you all.

This project would have been impossible without the support from the cancer research traineeship award through the Beatrice Hunter Cancer Research Institute with funds provided by the Saunders-Matthey Cancer Prevention Foundation Award as part of The Cancer Research Training Program. The financial support received through Scotia Scholar Award, from Nova Scotia Health Research Foundation, Gordon B. Kinsman Memorial Graduate Scholarship and Graduate International Scholarship are also acknowledged gratefully. I also appreciate the LaHave Natural Farms, Blockhouse, NS, Canada, for providing me with plant materials required for the research project.

I sincerely thankful to Dr. Priyantha Yapa and Dr. Palitha Weerakkody for their help, guidance, and advice throughout my higher education path. I wish to extend my deepest gratitude to my parents and especially to my husband for their concern, love, enormous help, encouragement and patience throughout my study period. I would not be who I am today without your love and dedication. At last but not the least, my appreciation to each and every person who helped me in different ways to complete my research and thesis work successfully.

CHAPTER 1. INTRODUCTION

Worldwide, cancer has become an epidemic, and its high incidence has an annual global economic impact of USD 1.2 trillion (approximately 2% of total global gross domestic production), representing the cost of prevention, treatment and disability-adjusted life years in 2010. When considering the long-term costs for patients and their families, the estimated cost comes to USD 2.5 trillion (Knaul et al., 2012; Union for International Cancer Control, 2014). It was estimated that 14.1 million people were newly diagnosed with cancer in 2012, in which lung cancer represented about 1.8 million. Lung cancer is more common in less developed regions of the world and is more common in men than women (Ferlay et al., 2015). Tobacco smoke, ionizing radiation, soot, radon, and asbestos are a few of the Group I lung carcinogens published by the International Agency for Research on Cancer (IARC, 2012). Long-term tobacco smoking causes 70% of lung cancer deaths globally (WHO, 2016) and 90% in the United States (Carbone, 1992). The particulate phase of cigarette vapor contains at least 4,800 compounds, which include many carcinogens, such as polycyclic aromatic hydrocarbons (PAH), nicotinic nitrosamines, aromatic amines, and metals (Hoffmann et al., 2001). Although many constituents in tobacco smoke contribute to lung cancer, 4-(methylnitrosamino)-1-(3-pyridyl)-1-butanone (NNK: nicotine-derived nitrosamine ketone) plays a significant role in lung carcinogenesis (Akopyan and Bonavida, 2006; Jin et al., 2004).

Current cancer treatments, such as chemotherapy, surgery, and radiation therapy, cause many side effects (National Cancer Institute 2012; Zhang et al. 2015). Chemotherapeutics cause cytotoxicity to healthy cells and induce a broad spectrum of

degenerative diseases (MacDonald, 2009). Even if cancer is properly treated, recurrence is common (Maeda et al. 2010; Uramoto & Tanaka 2014). Therefore, prevention is an essential component in the fight against cancer. Ceasing cigarette smoking is the most effective strategy for preventing lung cancer, followed by maintaining healthy dietary habits (Clancy, 2014). Unfortunately, those cost-effective and non-toxic cancer preventive strategies are yet to be popularized and implemented in many countries (Morgan, 2007). In economic perspectives, investing USD 11 billion in cancer preventive strategies could be able to save up to USD 100 billion in cancer treatment cost annually (Knaul et al., 2012). Therefore, investigating alternative therapeutic measures in reducing the risk of lung cancer is useful, especially for high-risk- and cancer recurrence-populations.

The consumption of polyphenol-rich fruits and vegetables reduces lung cancer risk among high-risk populations (Gnagnarella et al., 2013; Vauzour et al., 2010). A population-based case control study, conducted in Shanghai, China, reported that regular consumption of green tea reduces lung cancer risk among women. A similar observation was reported with high intake of fruits and vegetables in a health follow-up study (Feskanich et al., 2000). Many studies have confirmed regular consumption of polyphenol-rich fruits and vegetables in reducing lung cancer risk among smokers (Büchner et al., 2010; Linseisen et al., 2007; Le Marchand et al., 2000). Alternatively, polyphenols have gained recent attention as an adjuvant therapeutic agent. Lecumberri et al. (2013) reviewed the potential use of green tea polyphenols in combination with chemo/ radiation therapy as an adjuvant treatment for cancer patients. Green tea polyphenols can act synergistically with conventional therapies as a radiosensitizer, and

ameliorate the side effects of conventional cancer therapies (Chem et al., 2010; Hu et al., 2011; Zhang et al., 2012). In addition, dietary supplementation of anthocyanins and resveratrol for breast cancer patients during adjuvant radiation therapy reduces radiation-induced dermatitis (Franco et al., 2012). The role of dietary plant flavonoids in genome stability and protection against DNA damage caused by various carcinogens has been reviewed (George et al., 2017). Polyphenol-rich berries are a popular dietary component in many countries, and available in fresh or processed form for consumption. Therefore, it is important to investigate the potential usefulness of berries in chemoprevention.

1.1 Hypothesis

Polyphenol-rich haskap berry extracts can prevent or suppress the NNK-induced DNA damage in normal lung epithelial cells *in vitro*.

1.2 Research Objectives

Overall objective

To investigate the efficacy of polyphenol-rich haskap berry extracts in preventing or reducing NNK-induced DNA damage in cultured normal lung epithelial cells.

Specific objectives of the research

1) To prepare polyphenol-rich extracts from haskap berry and characterize their polyphenol composition and antioxidant capacity *in vitro*; and
2) To evaluate the potential of the haskap extracts in protecting normal lung epithelial cells against carcinogen-induced DNA damage.

CHAPTER 2. LITERATURE REVIEW

This section discusses lung cancer and its classification, NNK-induced lung carcinogenesis, the effect of polyphenols in preventing lung carcinogenesis and the botanical description of the haskap plant.

2.1 Lung cancer

Lung cancer is a heterogeneous disease arises when genetic, and epigenetic alterations happen in lung epithelia (Zhan et al., 2012). Most lung tumors originate as a result of frequent exposure to exogenous carcinogens, such as tobacco smoke, vehicle exhaust, and other environmental carcinogens (Bailey-Wilson, 2008). Based on clinical and therapeutic characteristics, lung cancer is broadly divided into small cell lung cancer (SCLC) and non-small cell lung cancer (NSCLC). NSCLC is further divided to squamous cell carcinoma (SCC), Adenocarcinoma (ADC) and large cell carcinoma. Combination chemotherapy is the most efficient treatment given for patients with SCLC, whereas lung surgery works better for NSCLC patients with early stage disease (Linnoila and Aisner, 1995; Shames et al., 2008). The classification and characteristics of lung cancer are given in Table 1. The incidence of SCLC and SCC are strongly related to tobacco smoking (Linnoila and Aisner, 1995; Yang et al., 2002). With the introduction of low-tar containing filter-tipped cigarettes, the incidence of ADC has become more frequent (B'chir et al., 2007; Brooks et al., 2005). It is suggested that filter-tipped cigarettes increase the exposure of the bronchioalveolar junction to nitrosamines present in smoke. Usually, ADC arises near the bronchioalveolar junction (B'chir et al., 2007). A cohort study conducted in Iowa with postmenopausal women has shown a clear relationship between ADC formation and smoking (Yang et al., 2002).

Table 1 A brief classification of lung cancer with main characteristic features of each type.

Classification	Location on the lung	Characteristics
		SCLC
SCLC	Mostly perihilar found in bronchus	Macroscopic: soft, friable white tumors with necrotic tissues Cytology: small cells with limited or no cytoplasm. Cells are round- or spindle-shaped with granular nuclear chromatin ("salt and pepper" nature)
		NSCLC
SCC	Usually located centrally on the main stem, lobar or segmental bronchi	Cytology: keratinized epithelial cells having intercellular bridges ("squamous or keratin pearl" formation)
ADC	Mostly peripheral solid tumors	Macroscopic: gland formation and mucus production Cytology: single or clump of cells arranged as acini, pseudopapillary, papillary or solid tumor. Cells have prominent cytoplasm with round shaped nuclei
Large cell carcinoma	Mostly peripheral	Macroscopic: poorly differentiated large mass of cells Cytology: cellular aggregates in samples. Nuclei are large and prominent, vary from round to irregular in shape. Cells have high nuclear to cytoplasm ratio

Source: Linnoila and Aisner, 1995; Travis et al., 2004, 2015

Long-term exposure to direct or indirect tobacco smoke has been identified as a primary cause of lung cancer around the world. More than 70 carcinogens, such as benzo(a)pyrene [B(a)P], arsenic, cadmium, chromium, nickel, and acrylonitrile, which are known to initiate or promote cancer, are present in tobacco smoke (Health Canada, 2011; Hoffmann et al., 2001). Among them, NNK has been identified as a major compound causing lung cancer (Jin et al., 2006; Wu et al., 2015). The precursor of NKK, 4-[(acetoxymethyl)nitrosamino]-1-(3-pyridyl)-1-butanone (NNKOAc), was also studied in the present study.

2.2 Metabolism of NNK and NNKOAc

2.2.1 NNK

The aromatic compound NNK (CAS number: 64091-91-4) is a pale-yellow crystalline powder with a molecular formula of $C_{10}H_{13}N_3O_2$ and molecular weight of 207.22912 g/mol. Nitrosamines are formed during the curing, fermentation and storage of tobacco leaves by N-nitrosation of the *Nicotiana* alkaloids. Alternatively, NNK can generate during smoking (Hoffmann 2001; Hoffmann et al. 1994). The chemical structure of NNK is illustrated in Figure 1.

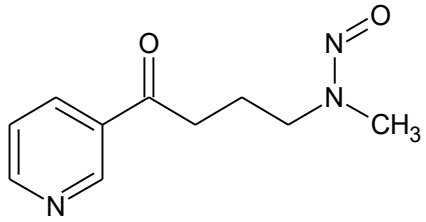

Figure 1 The chemical structure of NNK.

All tobacco products contain NNK, and it is unique to tobacco (Hecht et al., 2016). Humans can be exposed to tobacco-specific nitrosamines through the direct inhalation of mainstream tobacco smoke and passive inhalation of environmental tobacco

smoke, chewing tobacco leaves and by snuff dipping (Hecht et al., 2016; Hoffmann and Hecht, 1985). Among other nitrosamines, NNK is the most potent tobacco-specific carcinogen involved in lung cancer (Hecht et al., 2016; Hoffmann and Hecht, 1985; Lin et al., 2011).

2.2.2 NNKOAc

A precursor of NNK, NNKOAc, has been used in many studies to bypass the complexities in NNK metabolism and to induce nuclear DNA damage in cells (Cloutier et al., 2001; Proulx et al., 2005). NNKOAc (CAS number: 127686-49-1) is an aromatic compound with a molecular formula of $C_{12}H_{15}N_3O_4$ and molecular weight of 265.27 g/mol. It is a white powder. The chemical structure of NNKOAc is presented in Figure 2.

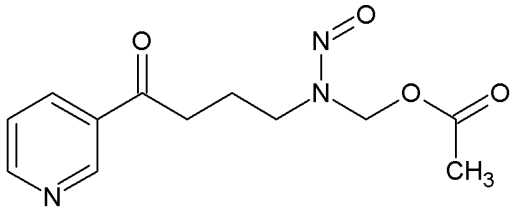

Figure 2 The chemical structure of NNKOAc.

2.2.3 Metabolism of NNK in cells

As a procarcinogen, NNK is activated by cofactors, such as cytochrome pigment 450 (CYP450) enzymes, present in cells. Three central metabolic pathways are (Figure 3) involved in NNK metabolism. They are carbonyl reduction, oxidation of the pyridine nitrogen molecule and α-hydroxylation of the methyl or methylene carbons (Hecht et al., 2016).

The carbonyl reduction pathway is the dominant pathway (Yalcin and Monte, 2016), converting a great portion of NNK into 4-(methylnitrosamino)-1-(3-pyridyl)-1-butanol (NNAL) via carbonyl reductases (11β-hydroxysteroid dehydrogenase [11β-

HSD]) (Maser et al., 1996). The resultant NNAL conjugates with glucuronic acids and forms NNAL-glucuronides (NNAL-Glu). This reaction is catalyzed by uridine-5'-diphospho-glucuronosyltransferases (UGT) (Hecht et al., 1993; Morse et al., 1990). NNAL-Glu is nontoxic and excreted through urine (Carmella et al., 1993; Wiener et al., 2004). However, NNAL is carcinogenic and partially oxidized back to NNK. Also, NNAL undergoes α-hydroxylation via CYP450 enzymes, generating electrophilic intermediates that can react with DNA, forming bulky pyridyloxobutylation DNA (POB-DNA) adducts (Hecht et al., 1993).

Pyridine N-oxidation is a detoxification process in which both NNK and NNAL oxidize at the nitrogen atom of the pyridine ring and form nontoxic NNK-N-oxide and NNAL-N-oxide, respectively. The oxidation reaction of NNK and NNAL occurs in lung microsomes, and the resulting metabolites are excreted through urine in rodents and primates (Carmella et al., 1997; Hecht et al., 1993, 2016; Yalcin and Monte, 2016).

The α-hydroxylation of NNK and NNAL form reactive electrophilic metabolites. Methylene or methyl carbon atoms adjacent to the N-nitroso nitrogen of NNK and NNAL are hydroxylated by CYP450 (Hecht et al., 1993). The resultant electrophilic metabolites can covalently bind to DNA and induce methylation, pyridyloxobutylation and pyridylhydroxybutylation of nucleobases in DNA, forming bulky DNA adducts that cause mutations in oncogenes and tumor suppressor genes (Yalcin and Monte, 2016). There are several cytochrome isoforms involved in the activation of NNK (Wu et al., 2008).

The process of α-methylene hydroxylation of NNK yields α-methylenehydroxy NNK. Human liver microsomal enzymes, CYP2A6 and 3A4, are involved in α-

methylene hydroxylation (Patten et al., 1996). They convert NNK to keto aldehyde and methane diazohydroxide, which later reacts with DNA, producing methyl DNA adducts; mainly 7-*N*-methylguanine (7-mGua) and O^6-methylguanine (O^6-mGua), as well as small amounts of O^4-methylthymine (Devereux et al., 1988; Hecht and Hoffmann, 1988; Loechler et al., 1984). Keto aldehydes oxidize into a keto acid, a urinary metabolite which is excreted from the body (Peterson et al. 1991).

The α-hydroxylation of NNK at the methyl carbon atom produces α-hydroxymethyl NNK. Several liver microsomal enzymes, such as CYP1A2, 2E1 and 2D6, are involved in methyl hydroxylation (Patten et al., 1996). α-Hydroxymethyl NNK spontaneously loses formaldehyde, producing 4-3- pyridyl-4-oxobutane-1-diazohydroxide, which reacts with water, yielding a urinary metabolite, keto alcohol that is excreted from the body (Hecht, 1998). Additionally, 4-3- pyridyl-4-oxobutane-1-diazohydroxide is capable of forming POB-DNA adducts, leading to lung cancer (Yalcin and Monte, 2016). There are four types of POB-DNA adducts, designated 7-[4-(3-pyridyl)-4-oxobut-1-yl]-2'-deoxyguanosine (7-pobdG), O^2-[4-(3-pyridyl)-4-oxobut-1-yl]-2'-deoxycytosine (O^2- pobdC), O^2-[4-(3-pyridyl)-4-oxobut-1-yl]-2'-deoxythymidine (O^2-pobdT) and O^6-[4-(3-pyridyl)-4-oxobut-1-yl]-2'-deoxyguanosine (O^6-pobdG), identified so far (Peterson, 2010).

2.2.4 Metabolism of NNKOAc

In cell culture systems, NNKOAc generates α-hydroxymethyl NNK, which spontaneously yields 4-3-pyridyl-4-oxobutane-1-diazohydroxide. The resulting diazohydroxides react with DNA, forming POB-DNA adducts (Figure 3). Therefore, NNKOAc mimics the DNA damage pattern of NNK (Cloutier et al., 2001).

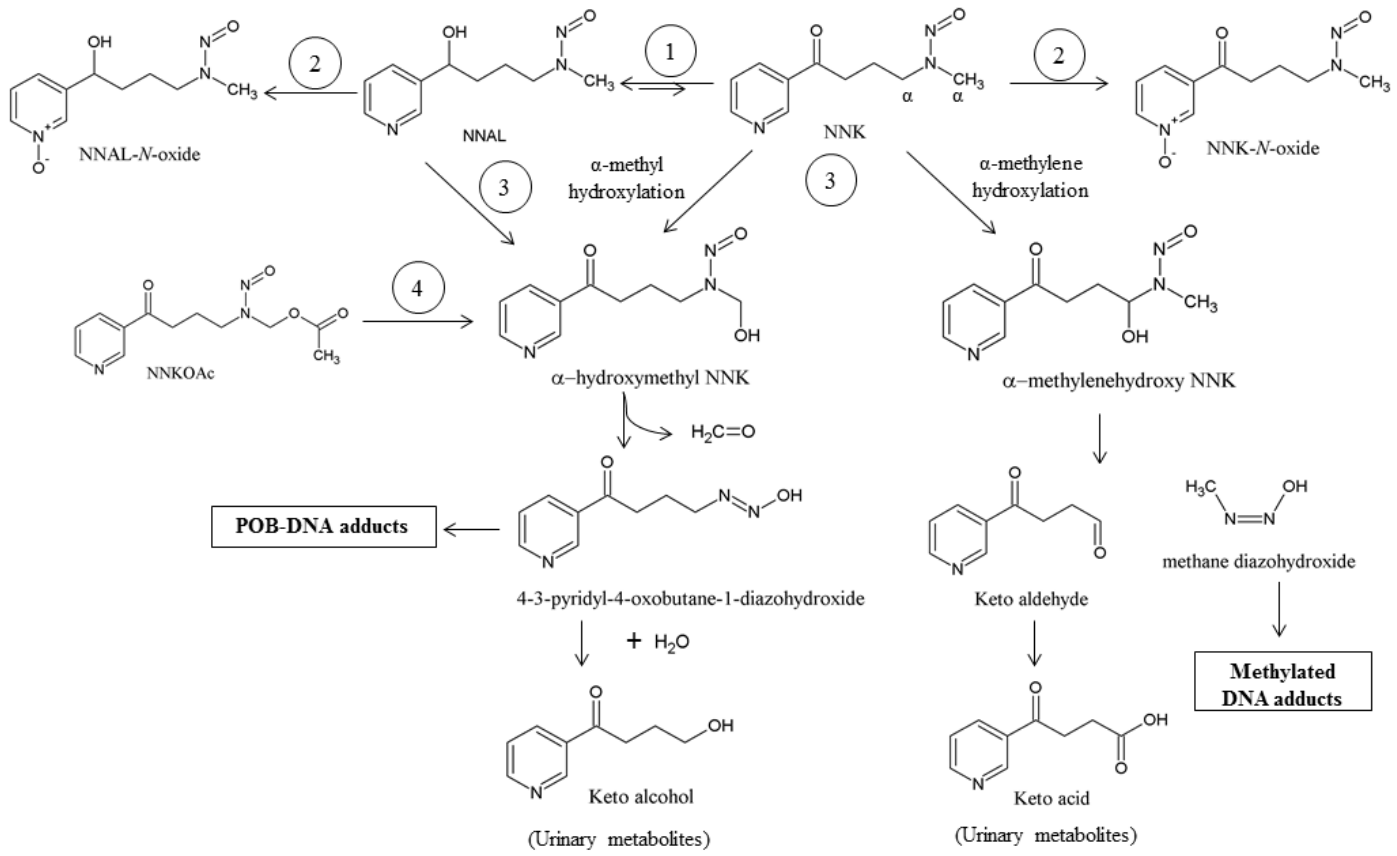

Figure 3 NNK undergoes through three main metabolic pathways in the body.

1) Carbonyl reduction, the major metabolic pathway by which NNK converts into NNAL initially; 2) pyridine ring oxidation, the oxidation of pyridine N atom forming non-toxic metabolites; and 3) α-hydroxylation, the hydroxylation of methyl and methylene carbons adjacent to the N-nitroso nitrogen, resulting in more reactive electrophilic metabolites. 4) The esterase enzymes activate NNKOAc, which forms POB-DNA adducts. Adapted from Hecht, 1999; Hecht and Hoffmann, 1988; Hecht et al., 1993; Yalcin and Monte, 2016.

However, activation of NNKOAc does not depend on cytochrome enzymes. It is activated by esterase enzymes to generate α-hydroxymethyl NNK (Ma et al., 2015).

2.3 NNK-induced lung carcinogenesis

The somatic mutation of onco-, tumor suppressor-, cell cycle regulatory- and DNA repair-genes is common in cancer (Cooper, 2005). NNK induces lung carcinogenesis through genetic and epigenetic modifications of genes and activation of cell surface receptors present in lung epithelial cells (Cooper, 2005; Lin et al., 2011; Xue et al., 2014). Long-term smoking can disturb the balance in metabolic activation and detoxification of NNK. The accumulation of reactive metabolites causes the formation of DNA adducts. However, DNA repair through nucleotide excision repair (NER) and base excision repair (BER) can reconstruct the damaged DNA (Peterson, 2010; Sheets et al., 2006). Some cells can escape from DNA repair mechanisms, leading to miscoding of genes and permanent gene mutation (Hecht, 1999). The proto-oncogene mutation and tumor suppressor gene inactivation are common among lung cancer patients having a smoking history.

2.3.1 NNK-induced gene mutation in relation to lung cancer

2.3.1.1 Oncogene mutation

The mutation of the *KRAS* oncogene is shared among smokers and in NNK-injected experimental mouse models (Ding et al., 2008; Keohavong et al., 2011; Mascaux et al., 2005). Metabolically active NNK can bind with the deoxyguanosine nucleotide bases of the coding region of *KRAS* gene, leading to G to T transversions, which are more common among adenocarcinoma patients having a smoking history. For example, codon (12^{th} codon) GGT, which codes for glycine amino acid, alters into GTT, and TGT, which

code for valine and cysteine amino acids due to G to T transversion, respectively (Wen et al., 2011). Mutation of the *KRAS* gene at codon 12 was reported in NNK injected FVB/N mouse lung tumors (Keohavong et al., 2011). These modifications in the gene sequence lead to activation of the *KRAS* oncogene and trigger the expression of its resultant protein RAS. In the cytoplasm, RAS protein binds with guanosine triphosphate (GTP) and activates a cascade of signal transduction pathways (RAS/RAF-1/mitogen-activated protein kinase [MAPK] pathway, PI3K/AKT pathway), which activate transcription factors MYC, FOS, and JUN (Dhillon et al., 2007; Fernández-Medarde and Santos, 2011; Meloche and Pouysse, 2007) . The activation of these genes encourages epithelial cell proliferation, survival and the inhibition of apoptosis. However, Yamakawa et al. (2016) found that the activation of extracellular signal-regulated kinase 1/2 (ERK1/2) signaling pathway does not only depend on *KRAS* gene mutation, but also on other signaling pathways (Figure 4).

2.3.1.2 Tumor suppressor gene mutation

Tumor suppressor genes act as "guardian genes" to protect cells from becoming cancerous (Lane, 1992). Mutation and inactivation of the tumor suppressor gene, *TP53,* is more common among smokers than non-smokers (Ding et al., 2008). The *TP53* gene produces a nuclear protein p53 that is involved in multiple cellular functions, such as DNA repair, cell cycle regulation and programmed cell death (Cooper, 2005). The expression of p53 is lower in healthy cells but is upregulated under stress conditions. The p53 protein acts as a transcription factor for *P21* and growth arrest and DNA damage-inducible 45 (*GADD45*) genes, which suppress the activation of cyclin-dependent kinases (cdk2) at cell cycle checkpoints Gap 1/Synthesis (G1/S) phase and Gap 2/Mitosis (G2/M)

phase (Zhan et al., 1993, 1999). Therefore, p53 prevents the binding of cdk2 with cyclin E and cyclin B at each phase. Hence, p53 inhibits the cell cycle progression from G1 to S- and G2 to M phases in damaged cells. Meanwhile, DNA damage activates damage repair proteins, ataxia telangiectasia mutated (ATM), DNA-protein kinase (DNA-PK) and nuclear serine/threonine protein kinase (CHK2), to phosphorylate p53 (Banin et al., 1998; Lees-Miller et al., 1990; Zannini et al., 2014). The activation of p53 induces the ribonucleotide reductase, P53R2 which facilitates DNA repair by transporting deoxynucleotides to the damaged DNA site (Nakano et al., 2000). If the recovery of cell damage is not possible, p53 induces cell apoptosis by activating BCL-2 associated X protein (BAX) and apoptotic protease activating factor-1 (APAF1) (Fridman and Lowe, 2003). BAX protein interacts with the mitochondrial membrane and induces the release of cytochrome c into the cytoplasm. In the cytoplasm, cytochrome c binds with APAF1 and activates cysteine-aspartic acid protease-9 (caspase-9), causing apoptosis (Acehan et al., 2002; Mcilwain et al., 2013). Therefore, mutation of *TP53* gene can suppress the cell cycle regulation, impair the DNA damage repair and inhibit apoptosis, causing unregulated cell growth, leading to lung carcinogenesis.

2.3.1.3 Mutation of the other related genes

In addition to the direct gene mutations, NNK-induced epigenetic modifications in tumor suppressor- and DNA repair-genes cause lung carcinogenesis. The inactivation of *P16*, another tumor suppressor gene, by promoter hypermethylation occurs in adenocarcinomas (Kawabuchi et al., 1999; Tam et al., 2013). *P16* induces the Cdks, which bind with cyclin during cell cycle progression and phosphorylate retinoblastoma protein (Rb), preventing its association with E2 factor (E2F) transcription factor. Free

E2F activates cell cycle genes and induces cell proliferation (Ohtani et al., 2004; Rayess et al., 2012). On the other hand, promoter hypermethylation of the DNA repair gene, O^6-methylguanine DNA methyltransferase (MGMT), has been identified in the early stages of adenocarcinomas (Pulling et al., 2003). The respective gene product O^6-alkylguanine DNA alkyltransferase (AGT) helps in repairing O^6-alkylguanine DNA adducts by transferring the methyl group from guanine to a cysteinyl residue on the protein (Pegg, 2000). Promoter hypermethylation reduces the expression of AGT (Devereux et al., 1988), resulting in the accumulation of DNA mutations in oncogenes and tumor suppressor genes.

2.3.2 NNK activates cell surface receptors and cell signal transduction pathways

Similar to nicotine, NNK is an agonist of alpha7 nicotinic acetylcholine receptors (α7nAchR) and enables the voltage-gated calcium ion (Ca^{++}) channel, causing membrane depolarization (Al-Wadei and Schuller, 2009; Improgo et al., 2013). The Ca^{++} ion influx stimulates several cellular transduction pathways, such as PI3K/AKT pathway (West et al., 2003), PKC pathway and RAS/RAF/MAPK pathway (Dasgupta et al., 2006; Schuller et al., 2003), which induce transcription factors FOS, JUN and MYC, leading to cell proliferation (Al-Wadei and Schuller, 2009), survival and suppression of apoptosis (Xue et al., 2014) (Figure 3). It has been found that Ca^{++} ion antagonists prevent NNK-induced lung epithelial cell transformation *in vitro* (Boo et al., 2016).

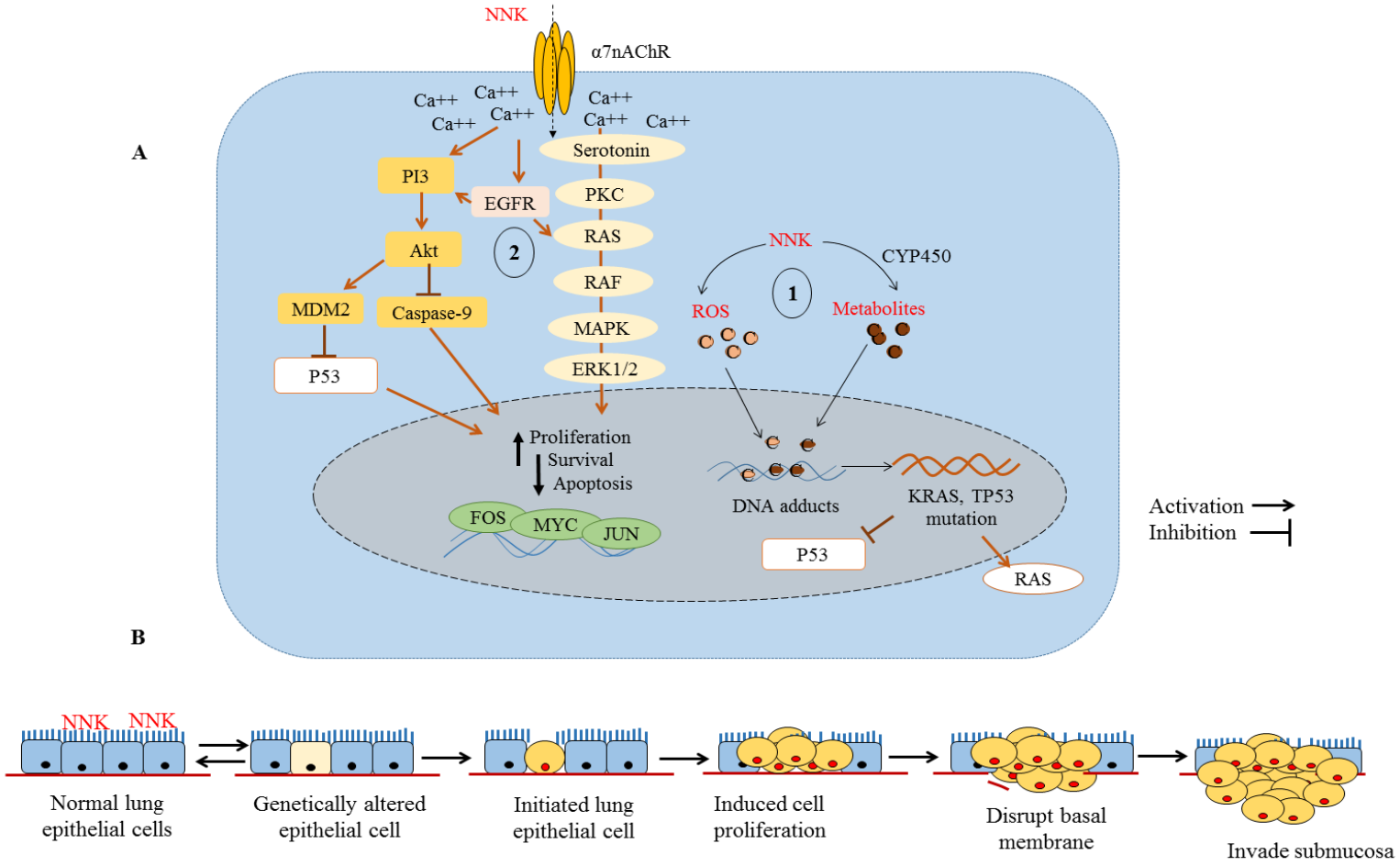

Figure 4 The mechanism of NNK-induced carcinogenesis in lung epithelial cells.

(A) There are two primary carcinogenesis mechanisms related to NNK. 1) NNK forms reactive electrophilic metabolites, which react with nuclear DNA, creating methylated- and POB-DNA adducts on oncogenes (*KRAS*) and tumor suppressor genes (*TP53*). The mutation of *KRAS* gene enhances the expression of RAS protein, which induces a cascade of signal transduction pathways in the cytoplasm leading to the activation of transcription factors FOS, JUN and MYC in the cell nucleus. Activated RAS activates the proto-oncogene serine/threonine-protein kinase (RAF), which after phosphorylation activates mitogen-activated protein kinases (MAPK). Furthermore, RAS can activate phosphatidylinositol 3-kinase (PI3K), which converts phosphatidylinositol (4,5)-bisphosphate (PIP_2) into phosphatidylinositol (3,4,5)-trisphosphate (PIP_3) on the cell surface, stimulating the activity of serine/threonine kinase (AKT/PKB). Activated AKT induces E3 ubiquitin-protein ligase **(**MDM2), which negatively regulates p53 tumor suppressor protein in cells. AKT also phosphorylates and activates mammalian target of rapamycin (mTOR), stimulating cell growth. Also, AKT suppresses caspase-9 activation and prevents apoptosis. 2) NNK is an agonist for α7nAchRs located on the cell surface. NNK binds with α7nAchRs receptors and causes Ca^{++} influx into the cell. Intracellular Ca^{++} induces the release of serotonin and mammalian bombesin, which activates the protein kinase C (PKC)-induced signaling cascade, leading to the activation of MAPKs, which stimulate cell proliferation and inhibit apoptosis. High concentrations of Ca^{++} in the cytoplasm triggers the release of epidermal growth factors (EGF), activating the epidermal growth factor receptor (EGFR) signaling cascade. EGFR activates the RAS/RAF signaling pathway and the PI3K/AKT signal transduction pathway, leading to cell proliferation, survival, and inhibition of apoptosis. Literature used to create the figure are cited in the text.

(B) When healthy lung epithelial cells are chronically exposed to NNK, the balance between NNK-activation and -detoxification breaks down, leading to persistent genetic and epigenetic alterations in the cells. Mostly, this damage is identified and repaired by the cell cycle regulatory and DNA repair proteins, and if not, apoptosis destroys the damaged cells. In certain situations, cells can escape from these checkpoints and acquire independence, leading to uncontrolled cell proliferation. Uncontrolled cell division can lead to hyperplasia, dysplasia and cell growth that extends beyond the basement membrane and invades the submucosa of the lung tissues.

Therefore, NNK-induced lung carcinogenesis depends on two primary carcinogenic mechanisms. Firstly, NNK causes genomic instability in lung epithelial cells through point mutation and promoter hypermethylation. Secondly, NNK activates membrane-bound cell surface receptors and downstream signal transduction pathways, inducing cell proliferation and survival (Figure 4). When lung epithelial cells are exposed to NNK, oncogene and tumor suppressor genes mutate along with the activation of other carcinogenic pathways, leading to uncontrolled cell proliferation and tumorigenesis (Soria et al., 2003). Mutagenic DNA damage is an early step in tobacco-related lung carcinogenesis (Wang et al., 2012).

2.4 Definition and classification of plant polyphenols

Polyphenols have gained attention due to their potential health–benefiting properties of reducing the risks for many human chronic diseases. Fruits, vegetables, cereals, and beverages, such as tea, coffee, wine, are familiar polyphenol-rich dietary sources. For plants, polyphenols provide protection against pathogens and environmental stresses and give signaling characteristics, such as fragrance, color, and flavor, which help plants to maintain interactions with the surrounding environment (Bravo, 1998; Rupasinghe et al., 2014). More than 8000 phenolic structures have been identified so far (Cheynier, 2005; Tsao, 2010), ranging from simple molecules (monomers and oligomers) to higher molecular weight polymeric structures (Cheynier, 2005). Figure 5 illustrates the classification of polyphenols, based on the nature of their chemical structure.

All the polyphenols contain at least one aromatic ring with one or more hydroxyl groups (Ferrazzano et al., 2011; Tsao, 2010). Flavonoids contain two aromatic rings (A and B rings) linked by three carbon atoms confined by an oxygenated heterocyclic ring

(C-ring). The structures of commonly available polyphenols and their dietary sources are presented in Figure 6.

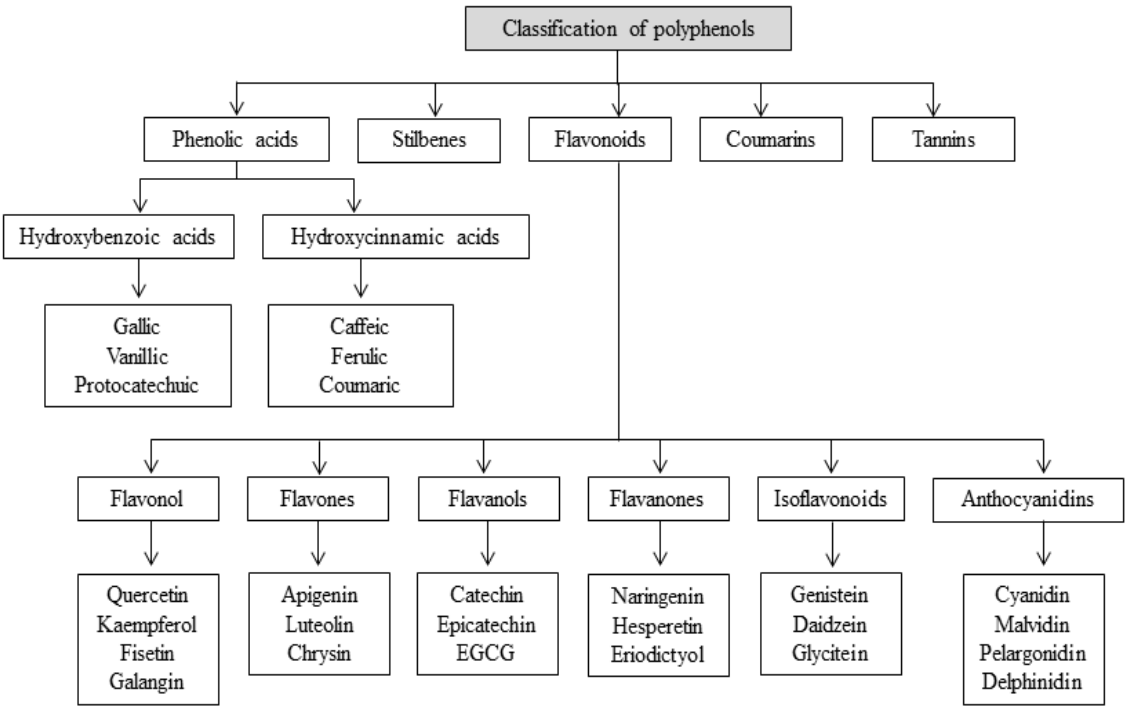

Figure 5 A general classification of commonly found dietary polyphenols.

*EGCG, epigallocatechin gallate

Adapted from Pandey and Rizvi, 2009; Rupasinghe et al., 2014

2.5 Protective effect of polyphenols against NNK-induced carcinogenesis

2.5.1 Polyphenols can maintain genetic integrity

The phenolic hydroxyl groups of polyphenols are capable of donating hydrogen molecules to free radicals, transforming them into stable molecules in the cells (Valentão et al., 2003). Oxidative DNA lesions induced by NNK (the formation of 8-hydroxy deoxyguanosine [8-OH-dGuo] DNA adducts) were reduced in mice fed with green tea and EGCG (Xu et al., 1992). By stabilizing intracellular oxidative radicals, polyphenols reduce the autoxidation and accumulation of radicals in cells, preventing oxidative DNA

damage (Guo et al., 1996). The main constituent of green tea, EGCG significantly reduced NNK-induced DNA single strand breaks (SSBs) in cultured lung epithelial cells (Weitber and Corvese, 1999). In addition, Liu and Castonguay (1991) have observed the protective effect of catechin (present in tea) against NNK in rat hepatocytes. Pretreatment of rat hepatocytes with catechin inhibits the α-hydroxylation of NNK and suppresses NNK-induced SSBs. Duthie (2007) reviewed the berry extracts and reported that they maintained genetic integrity in both *in vitro* and *in vivo* studies.

2.5.2 Polyphenols involved in the expression of enzymes associated with NNK metabolism

Polyphenols have the ability to engage the activation- and detoxification-enzymes of NNK (Figure 3). Citrus flavonoids, quercetin, and naringenin inhibit the α-hydroxylation of NNK in hamster liver and lung microsomes *in vitro*. Both flavonoids suppress the activity of CYP450 enzymes (Bear and Teel, 2000). Proanthocyanidins extracted from grape seeds have a protective effect against NNK-induced carcinogenesis in MCF10A human breast epithelial cells by regulating the level of 11β-HSD, which enhances the carbonyl reduction of NNK in cells, and by suppressing the activity of CYP1A1 and 1B1, which prevent the formation of reactive electrophilic metabolites (Song et al., 2010). Russell et al. (2015) observed that delphinidin reduces dibenzo(*a,l*)pyrene-induced adduct formation by suppressing CYP1A1 1A2 and 1B1, reacting with carcinogenic metabolites.

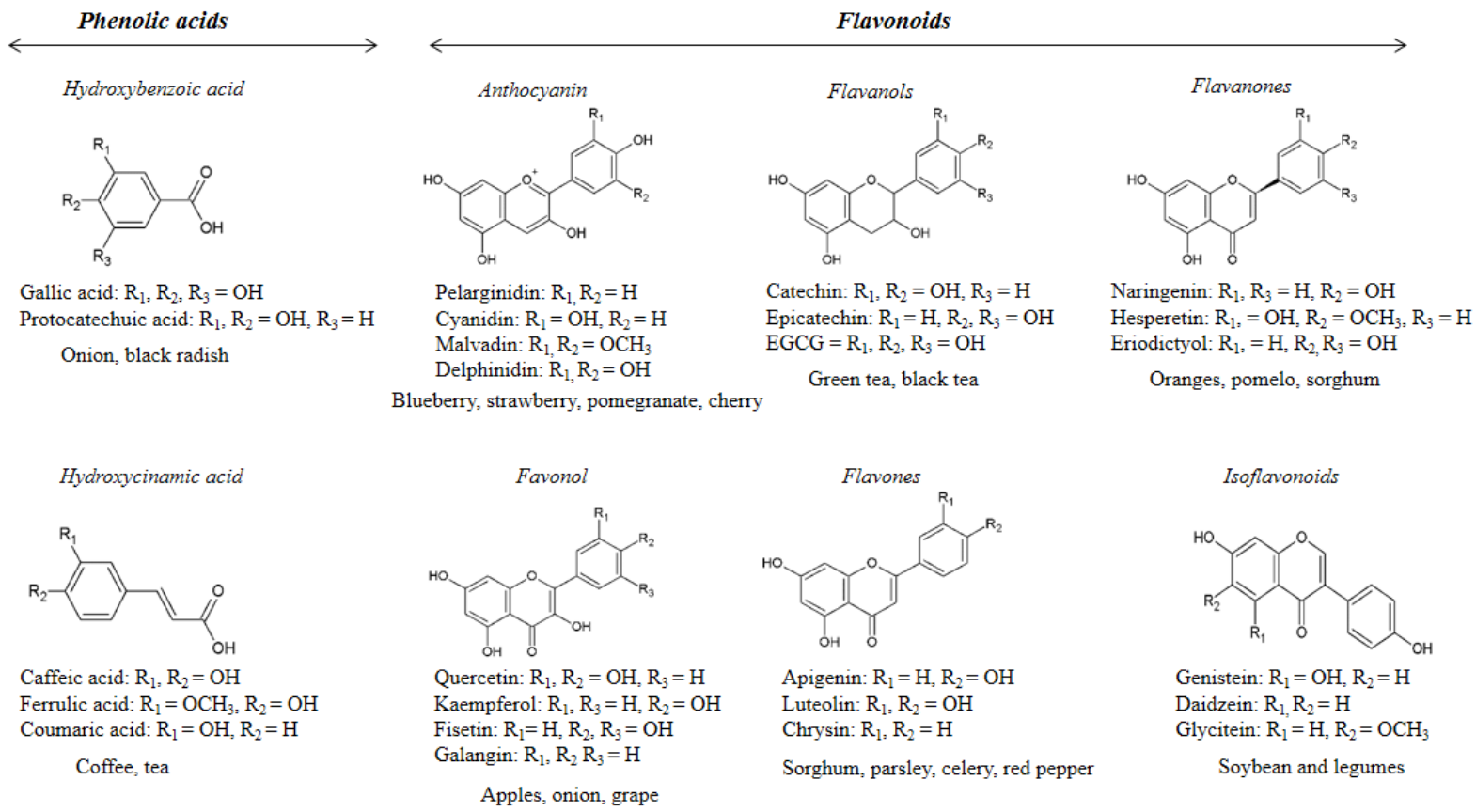

Figure 6 Structural differences among major polyphenols found in foods.

Adapted from Bellik et al., 2012; Markakis et al., 2015; Pan et al., 2001; Patel et al., 2007; Zhu et al., 2014

In addition, polyphenols have the ability to induce phase II enzymes, which detoxify endogenous and xenobiotic electrophilic metabolites through glucuronidation, sulfation, methylation, acetylation, glutathione and amino acid conjugation (Jancova et al., 2010). For example, genistein, present in soybeans, induces phase II detoxifying enzymes, such as glutathione S-transferase (GST), UGT and quinone reductases (QR), in cell culture models and *in vivo* rat experimental models (Appelt and Reicks, 1997; Froyen et al., 2009). The anthocyanin-rich rice bran extracts show a protective effect against aflatoxin B1-induced hepatic carcinoma in Wistar rats. Rice bran modulates the activation of aflatoxin B1 by suppressing CYP1A2, 3A, and enhancing the activity of UGT, NAD(H); quinone oxidoreductase (NQOR) and GST phase II enzymes (Suwannakul et al., 2015). Similarly, anthocyanin-rich extracts from *Hibiscus sabdariffa* calyxes restore carbon tetrachloride (CCL_4)-suppressed UGT and GST in albino rats. Additionally, the extracts suppress oxidative stress by reversing CCL_4-reduced antioxidant enzyme activity [superoxide dismutase (SOD), catalase (CAT), and glutathione reductase (GR)] (Ajiboye et al., 2011). UGT is involved in detoxification of the NNK metabolite NNAL, through glucuronidation (Figure 3).

2.5.3 Polyphenols regulate cell surface receptors and signal transduction pathways activated by NNK

The hydrophobic benzoic ring of polyphenols has the potential to react with proteins. Also, the hydroxyl groups present in polyphenols have the ability to form hydrogen bonds with proteins. This property helps them alter the regulation of membrane-bound enzymes and receptors. Quercetin and resveratrol, which are abundantly present in apples and grapes, have been identified as potent antagonists of

aryl hydrocarbon receptors (AhR) (Murakami et al., 2008; Revel et al., 2003). The AhRs regulate the expression of CYP450 enzymes and transcription factors that can be activated by polycyclic aromatic hydrocarbons (PAHs) and cause lung carcinogenicity (Cos et al., 1998; Denison and Nagy, 2003; Denison et al., 2002; Murakami et al., 2008; Parr and Bolwell, 2000; Revel et al., 2003). Combined treatment with quercetin, luteolin reduces α9nAchR expression in MDA MB 231. Similarly and EGCG down-regulates the α9nAchR expression in MCF-7 breast cancer cells (Shih et al., 2010; Tu et al., 2011). Genistein is an isoflavonoid that suppresses the MAPKs induced by nicotine and the phosphorylation of α7nAChR in SH-SY5Y neuroblastoma cells (Charpantier, 2005). Genistein also increases the expression of nuclear factor E2-related protein 2 (Nrf2), which interacts with antioxidant response element (ARE) (Zhai et al., 2013). Most of the genes that encode phase II enzymes contain an ARE sequence in their promoter regions (Li et al., 2011). Fisetin, a flavonoid commonly found in apple and strawberries (Khan et al., 2013), suppresses the PI3K/AKT and mTOR signaling cascades in NSCLC, A594, and H1792 cells and suppresses cell proliferation (Khan et al., 2012). The anthocyanins extracted from black rice have the potential to reduce the expression of PI3K, AKT, RAS and JUN proteins and suppress the proliferation of CAL 27 human oral cancer cells (Fan et al., 2015).

Table 2 Evidence for polyphenols in reducing NNK-induced tumorigenesis in vivo.

Animal model	Reagent or chemical	Observation	Ref.
A/J mice	EGCG	Reduced tumor multiplicity. Attenuated the expression of DNMT1, p-AKT, and γ-H2AX in lung epithelial cells.	(Jin et al., 2015)
Sprague-Dawley rats	Cape gooseberry extract	Reduced pulmonary hyperplasia. Reduced the expression of cell proliferation marker Ki-67 Enhanced the p53 tumor suppressor gene expression	(El-Kenawy et al., 2015)
A/J mice	Black tea and green tea	Reduced the incidence and multiplicity of lung tumors	(Landau et al., 1998)
A/J mice	Polyphenol E	Inhibited the progression of lung adenoma to adenocarcinoma Reduced PCNA – cell proliferation Induced caspase-3 expression - apoptosis Inhibit the phosphorylation of c-Jun and ERK 1/2	(Lu et al., 2006)
A/J mice	Adlay seed	Reduced lung tumor multiplicity	(Chang et al., 2003)
A/J mice	Theaflavin	Reduced tumor multiplicity and volume	(Yang et al., 1997)
A/J mouse	Hesperidin rich mandarin juice	Suppressed tumor multiplicity Reduced the expression of PCNA in lung tissues	(Kohno et al., 2001)
Swiss albino mice	Black tea	Reduced diethylnitrosamine- induced lung tumorigenesis	(Shukla and Taneja, 2002)
F344 rats	Catechin	Reduced SSBs and methylation of DNA (O^6-mGua)	(Liu and Castonguay, 1991)
F344 rats	Black tea and caffeine	Reduced the formation of adenomas and adenocarcinoma	(Chung et al., 1998)

Polyphenol E contains 65% (-) epigallocatechin-3-gallate; PCNA, proliferating cell nuclear antigen; c-Jun, protein product of *JUN* gene

2.6 Haskap (*Lonicera caerulea* L.)

Haskap berries, also known as honeyberries or blue honeysuckle berries, are a berry fruit newly introduced to North America. The indigenous Ainu people in Hokkaido Island of Japan have given it the name "Haskap," which means "bearing many fruits on branches." They recognized the value of haskap and treated it as "the elixir of life" (Thompson, 2006). Wild haskap is a circumpolar species belonging to the *Lonicera* genus, and is native to the Northern boreal forests spread across Canada, Russia, and Japan. Russian cultivars are good survivors of extremely low-temperature conditions (-46 °C) and the flowers can withstand -10 °C at full bloom (Thompson, 2006; Vavilov and Plekhanova, 2000). Early fruiting and fruit ripening, higher ascorbic acid content, richness in bioactive flavonoids and outstanding frost tolerance are key features of the haskap plant, which earns it greater attention as a potential commercial fruit crop (Vavilov and Plekhanova, 2000).

2.6.1 Botanical description

Kingdom:	Plantae
Subkingdom:	*Tracheobionta* – vascular plants
Super division:	*Spermatophyta* – seed plants
Division:	*Magnoliophyta* – flowering plants
Class:	*Magnoliopsida* – dicotyledons
Subclass:	*Asteridae*
Order:	*Dipsacales*
Family:	*Caprifoliaceae*
Genus:	*Lonicera* L.
Species:	*Lonicera cearulea* L. – Honeysuckle berry/haskap

Haskap is a perennial, deciduous shrub having an upright to spreading growth habit. Wild types of haskap grow up to 0.8 – 3.0 m tall, but domesticated shrubs are typically 1.0 m wide to 1.8 m in height. Flowers are small, pale yellow or cream colored and mostly self-incompatible. Fruits are oval to long in shape, deep purple to dark blue in color, and covered with a white, waxy bloom. Fruits are soft and, hence, tend to rupture at harvesting. Fruits have a unique flavor, which varies among species, from a pleasant mild taste, tart-sweet, mildly tart, very sour to slightly or very bitter (Hummer, 2006; Thompson, 2006).

2.6.2 The polyphenolic profile of commercially grown haskap species in Canada

Haskap berries are well-known for their phenolic phytochemicals and antioxidant potential. The berries contain a diversity of phytochemicals, mainly anthocyanins and phenolic acids (Khattab et al., 2016; Rupasinghe et al., 2015; Takahashi et al., 2014). The polyphenol profile of haskap fruits is affected by factors, such as genotype, ripening stage, harvesting period, postharvest handling and growing environment (Kaczmarska et al. 2015; Khattab et al. 2015; Ochmian et al. 2012; Skupień et al. 2009), as documented in Table 3.

Table 3 Polyphenol profile of the commonly grown haskap varieties in Canada (mg/100 g fresh weight of haskap berries).

Type of phytochemical	Borealis	Berry Blue	Tundra	Indigo Gem
Phenolic acids				
Chlorogenic acid	0.9	23.1- 44.0	26.0 - 42.0	22.4 – 35.0
Neochlorogenic acid	ND	4.0	5.0	2.0
Caffeic acid	0.2	0.1	0.2	0.1
Flavan –3-ols				
Epigallocatechin	0.1	0.1	0.1	0.6
Catechin	2.5	1.7	3.5	2.9
Epicatechin	1.2	1.7	0.7	1.5
Epigallocatechin gallate	0.1	0.2	0.2	0.2
Flavonols				
Quercetin-3-*O*-glucoside	3.6	4.0 - 4.2	1.4 – 10.0	2.8 – 8.0
Quercetin-3- *O*-rutinoside	24.3	16.7 – 31.0	19.9 – 22.0	21.6 – 34.0
Quercetin-3-*O*-arabinoside	2.9	2.0	1.4	1.1
Anthocyanins				
Cyanidin-3-*O*-glucoside	170.0	140.8 – 342.0	104.7 – 597.0	143.9 – 649.0
Cyanidin-3-*O*-rutinoside	39.2	26.1 – 37.0	10.0 - 64.9	15.0 - 38.6
Cyanidin-3-*O*-galactoside	0.4	0.2	0.8	0.0
Peonidin-3-*O*-glucoside	13.7	3.0 - 9.5	6.7 – 22.0	8.2 – 25.0
Pelargonidin-3-*O*-glucoside		12.0	5.0	6.0
Delphinidin-3-*O*-glucoside	0.4	0.4	0.3	0.4
Delphinidin-3-*O*-ruinoside	0.2	0.1	0.1	0.1

(Khattab et al., 2016; Rupasinghe et al., 2015)

2.6.3 Medicinal properties of haskap plant

Haskap is popular in Russian, Chinese, Japanese and Indian folk medicine. Its berries are used in treating high blood pressure, diabetes, and glaucoma. Also, berries are believed to decrease the risk of heart attack, prevent anemia, heal malaria and gastrointestinal diseases, prevent osteoporosis, slow aging and increase skin elasticity (Lefol, 2007). Recent studies have confirmed the pharmaceutical value of haskap fruit

extracts. Polyphenol-rich haskap extracts have shown anti-inflammatory, antioxidant and antitumor properties *in vitro* and *in vivo* (Table 4).

Table 4 The recent findings of haskap berry related to its pharmaceutical properties.

Experimental Model	**Observation**	**Ref.**
HaCaT human keratinocytes exposed to UVA	Pre-and post-treatment of cells reduced UVA-induced ROS generation, lipid peroxidation, and elevated cellular glutathione level.	(Svobodova et al., 2008)
THP-1 macrophages differentiated from human leukemic monocytes	Reduced the pro-inflammatory cytokines such as IL-6, TNF-α, PGE2, and COX-2 induced by LPS.	(Rupasinghe et al., 2015)
RAW264.7 LPS-induced mouse macrophage	Reduced TNF-α, PGE2, and NO formation and inhibited iNOS and COX-2 protein expression.	(Jin et al., 2006)
Male SD/SPF rats given high-fat diet	Decreased the postprandial blood lipid, blood glucose, and adipose tissue	(Takahashi et al., 2014)
Walker 256 carcinoma bearing Wister rats	Reduced the tumor volume	(Gruia et al., 2008)
Lewis rats with LPS-induced EIU	Reduced the inflammatory cells and pro-inflammatory cytokines in the aqueous humor of rats. Suppressed the activation of NF-kB.	(Jin et al., 2006)

UVA, ultra violet-A; ROS, reactive oxygen species; LPH, lipopolysaccharide; IL-6, interleukin-6; TNF-α, tumor necrotic factor-α; PGE2, prostaglandin; COX-2, cyclooxygenase-2; NO, nitric oxide; iNOS, inducible nitric oxide synthase; EIU, endotoxin-induced uveitis; NF-kB, Nuclear factor kappa activated B cells

These findings suggest the pharmaceutical value of haskap berry polyphenols in human diseases. However, very few studies have been conducted to evaluate the potential of using haskap berries in relation to cancer prevention.

CHAPTER 3. MATERIALS AND METHODS

3.1 Instruments and chemical reagents

A class II-type A2 biological safety cabinet (LR2-452, ESCO Technologies Inc. Horsham, PA, USA), inverted microscope (eclipse TS100F, Nikon Instruments, Melville, NY, USA) water bath (ISOTEMP 205, Fisher Scientific, Mountain View, California, USA), CO_2 incubator (3074, VWR International, Edmonton, AB, Canada) centrifuge (Sorvail Legend Micro 21 R, Thermo Fisher Scientific Inc., Waltham, MA, USA), rotary evaporator (Heidolph RotaChill, UVS400-115, Thermo Electron Corporation, Milford, MA, USA), microplate reader (Tecan Infinite® M200 PRO, Morriscille, NC, USA), nitrogen evaporator (N-EVAP™ 111, Organomation Associates Inc., Berlin, MA, USA), micro centrifuge (Sorvail ST 16, Thermo Fisher Scientific Inc., Waltham, MA, USA), mini shaker (980334, VWR International, Edmonton, AB, Canada), heat block (Isotemp® 2001, Fisher Scientific, Ottawa, ON, Canada), freeze dryer (Dura-Dry™ MP FD-14-85BMP1, DJS Enterprises, Markham, Ontario, Canada), commercial blender (HBB909, Hamilton Beach Brands Inc., Glen Allen, VA, USA) and confocal microscope (Zeiss Axiovert 200M coupled with Hamamatsu Orca R2 Camera, Olympus Microscopes, Thornwood, NY, USA) were used for the experiments.

Bronchial Epithelial Basal Medium (BEBM) and Bronchial Epithelial Growth Medium (BEGM) were purchased from Lonza Clonetics® Walkersville, MD, USA. Dulbecco's phosphate buffered saline (PBS, cat # D8537), NNK (cat # 78013), fibronectin from human plasma (cat # F2006), bovine serum albumin (BSA, cat # A8022), dimethyl sulfoxide (DMSO, cat #D2438), 0.25% Trypsin – 0.53 mM ethylenediaminetetraacetic acid (Trypsin- EDTA) (cat # T3924), Triton X-100 (cat #

T8787), polyvinylepyriilodone (cat # P0930), penicillin-streptomycin (cat # P0781), phosphatase substrate (cat # S0942), phenazine methosulfate (PMS, cat # P9625), methotrexate (MTX, cat # M9929) Dulbecco's Modified Eagle's Medium (DMEM, cat # D5671) Minimum Essential Eagle's Medium (EMEM, cat # M2279), Folin-Ciocalteu reagent (Folin-C, cat # F9252), 2,2 diphenyl-1-1picryl-hydrazyl (DPPH, cat # D9132), 2,3,4-tris(2-pyridyl)-s-triazine (TPTZ, cat # T1253) and agarose (cat # A9539) were purchased from Sigma® Life Science, St. Louis, MO, USA. NNKOAc (cat # 167550) was purchased from Toronto Research Chemicals, North York, ON, Canada. Alexa fluor® 594 donkey anti-mouse (cat# A21203) and anti-phospho-histone H2A.X (ser139, clone JBW301, cat # 05-636) were purchased from Life Technologies, Eugene, OR, USA and EMD Millipore, Etobicoke, ON, Canada respectively. Bovine collagen type I (PureCol® 5409) was purchased from Advanced BioMetrix, Carlsbad, CA, USA. Glass coverslips (1.5, 18 ×18 mm, cat # B10143263NR15) were purchased from VWR International, Radnor, PA, USA).

Experiments were conducted in four stages; 1) preparation of polyphenol-rich haskap extracts, 2) evaluation of the polyphenol profile and antioxidant capacity of extracts, 3) development of the carcinogenic model using two nitrosamines and finally, 4) determination of the cytoprotective properties of haskap extracts against carcinogenesis.

3.2 Preparation of haskap berry extracts and determination of polyphenols

3.2.1 Preparation of polyphenol-rich extracts

Well ripe fresh haskap fruits (Brix value 14-16%) were obtained from the LaHave Natural Farms (Blockhouse, NS, Canada) and frozen at -20 ºC. The variety 'Indigo-gem 915' was selected for the study since it was the most popular variety among growers.

Two polyphenol-rich extracts were prepared using; 1) anhydrous ethanol and 2) deionized water (DI water).

Preparation of ethanolic extracts [H(E)]

The extracts were prepared according to a previously described method (Rupasinghe et al., 2015). The frozen haskap berries (50 g) were immediately ground in absolute ethanol (1: 5, w/v) using a commercial blender in a semi-dark environment (for 20 min). The resulting ethanolic extract was filtered through P2 grade filter papers (09-805-5C, Fisher Scientific, Ottawa, ON, Canada) under vacuum in the semi-dark. The remains were washed with ethanol until a clear filtrate was obtained. Filtrates were rotary evaporated using a 45 ºC water bath and -9 ºC chiller temperatures at 80 - 100 rpm in the dark. The remaining ethanol was evaporated by a gentle flow of nitrogen, using a dry evaporator (N-EVAP™ 111, Organomation Associates Inc., Berlin, MA, USA), followed by freezing at -20 ºC overnight. The frozen samples were dried in a freeze-dryer (Dura-Dry™ MP FD-14-85BMP1, DJS Enterprises, Markham, ON, Canada) under 3600 mT vacuum at -20 ºC for 48 h. The crude extracts were further purified to obtain sugar-free polyphenol-rich extracts by solid phase column chromatography (O'Kennedy et al., 2006). Briefly, 1 g of freeze-dried sample was dissolved in 1 ml of 20% ethanol and loaded to the preconditioned Sepabeads Resin stationary column (cat # 207-1, Sorbent Technologies, Atlanta, GA, USA). The column consisted of the brominated styrenic adsorbent with >250 µm particle size, 210A porosity, 630 m^2/g surface area, 43 – 53% water content and 780 g/L bulk density. The water-soluble sugar fraction was slowly eluted with deionized water while the Brix value was measured (≤ 0.1) by refractometer to confirm the sugar level. The non-sugar fraction was eluted with 20%, 70% and 95% in

an ethanol gradient. The elute was rotary evaporated and freeze-dried, as described before, to obtain a polyphenol-rich haskap extract. Three individual extracts were prepared in ethanol as three replicates, and powdered polyphenol-rich extracts were stored at -80 ºC in dark airtight containers.

Preparation of aqueous extracts [H(A)]

Frozen fruits were ground for 20 min using a commercial blender (HBB909, Hamilton Beach Brands Inc., Glen Allen, VA, USA) and filtered through eight layers of cheesecloth at room temperature in the dark. The remains were washed with DI water until a clear filtrate was obtained. The filtrate was centrifuged at 1000 × g for 10 min in the dark, and the supernatant was frozen at -20 ºC overnight. The frozen samples were freeze dried under 3600 mT vacuum at -20 ºC for 48 h. The resulting crude extracts were stored at -80 ºC in dark airtight containers. Free sugar was eluted from the crude extracts to obtain polyphenol-rich extracts, following the same procedure explained before.

3.2.2 Measurement of major polyphenols present in each haskap extract

The total polyphenols were measured in haskap extracts by ultra-performance liquid chromatography-electrospray tandem mass spectrometry (UPLC-ESI-MS/MS) (Rupasinghe et al., 2015). Briefly, extracts were dissolved (10 mg/ml) in methanol containing 1% acetic acid to obtain a final concentration of 10,000 ppm. Dissolved samples were filtered through 0.22 µm syringe filter and analyzed.

3.2.3 Determination of the total phenolic content (TPC)

TPC in 'Indigo-Gem 915' extracts was tested by the Folin-C assay in 96-well plate (COSTAR 9017, Fisher Scientific, Ottawa, ON, Canada) as described by Rupasinghe et al. (2012). The polyphenol-rich extracts were dissolved in methanol to

determine TPC. The diluted sample (200 µg/ml) was mixed with 0.2 N Folin-C and incubated at room temperature for 5 min in the dark. Then 7.5% sodium carbonate solution was added and incubated for 2 h at room temperature before reading at 760 nm. The final reaction mixture consisted of 20 µl sample or gallic acid standard, 100 µl of Folin-C and 80 µl of sodium carbonate per well. A standard curve was prepared using gallic acid (10 – 250 mg/L) and TPC was expressed as mg gallic acid equivalent/g dry weight (mg GAE/g DW). The solutions were made fresh under reduced light and the reaction was carried out under dark conditions.

3.2.4 Evaluation of the antioxidant capacity

The antioxidant capacity of haskap extracts was determined by Ferric Reducing Antioxidant Power assay (FRAP) and the free radical scavenging assay using DPPH radical (DPPH assay).

FRAP assay

The antioxidant capacity of samples was determined by measuring the electron donation potential of samples, as described by Benzie and Strain (1996), and modified by Rupasinghe (2010). Polyphenol-rich extracts were dissolved in methanol to a final concentration of 200 µg/ml. A working solution consisting of 300 mM acetate buffer (pH 3.6), 20 mM ferric chloride, and 1 mM TPTZ solution (10:1:1, v/v/v) was made freshly and added (180 µl) to 20 µl of sample or standard in 96-well microplate. The absorbance value was measured at 593 nm after a 6-min incubation at room temperature in the dark. The antioxidant capacity of extracts was calculated based on the Trolox standard curve (5 – 450 µM). The Trolox equivalent antioxidant capacity was expressed as µmole Trolox equivalent/g dry weight (µmole TE/g DW).

DPPH· assay

The assay was adapted from Blois (1958) to be performed in 96-well microplate. Briefly, 0.2 mM DPPH reagent was prepared. Haskap extracts were dissolved into a concentration gradient (50, 100, 200, 400, 800 and 1600 µg/ml), and 150 µl of DPPH reagent was pipetted into each well containing 150 µl of sample. The inhibition percentage was calculated by the following equation.

$$\%\ inhibition = \frac{(Ab\ blank - Ab\ sample)}{Ab\ blank} X\ 100$$

Ab sample represents the absorbance value of the sample containing the haskap extracts and Ab blank represents the absorbance value of the sample that did not contain haskap extracts. The antioxidant capacity of haskap extracts was expressed as IC_{50}, which is defined as the concentration of tested material required to cause a 50% decrease in initial DPPH concentration. The IC_{50} value was calculated using the % inhibition vs. antioxidant concentration curve.

3.2.5 Determination of the stability of haskap extracts in cell culture medium

Haskap extracts were dissolved in DMSO for cell culture and stored at -80 ºC. An Amplex® Red hydrogen peroxide/peroxidase assay kit (A22188, Thermo Fisher Scientific, Waltham, MA, USA) was used to determine the possible oxidation degradation of the haskap polyphenols in the cell culture medium. Haskap extracts were dissolved in standard cell culture media (250 µg/ml); BEBM, DMEM, and EMEM, separately. Additionally, Trolox (25 µg/ml) and N-acetyl-L-cysteine (NAC, 25 µg/ml) were added separately to the media along with haskap extracts, to determine their protective effects. Treatment combinations were prepared in 96-well plates, which were incubated at 37 ºC, 5% CO_2, in the dark for 8 h. Then, each sample was transferred into

another microplate containing the working solution (1:1, v/v), which consisted of 50 µl of 10 mM 10-acetyle-3,7-dihydroxyphenoxazine (Amplex® Red) reagent, 100 µl of 10 U/ml horseradish peroxidase (HRP) and 4.85 ml 1× reaction buffer (sodium phosphate, pH 7.4). The reaction mixture was incubated at room temperature in the dark for 30 min, and the formation of resorufin was measured at 570 nm excitation/585 nm emission. The level of H_2O_2 in the cell culture medium was calculated based on the H_2O_2 standard curve (0 – 5 µM). In the presence of peroxidase enzyme, the Amplex® Red reagent reacted with hydrogen peroxide (1:1 stoichiometry), producing resorufin, a red colored fluorescent product. Therefore, the oxidative degradation of haskap extracts was detected by measuring the level of resorufin in the cell culture medium.

3.3 Cell culture

3.3.1 Human lung epithelial cell line.

The non-tumorigenic bronchial epithelial cell line, BEAS-2B (ATCC® CRL-9609™) was purchased from American Type Cell Culture Collection (ATCC, Manassas, VA, USA). BEAS-2B cells were derived from the normal human bronchial epithelium of a healthy individual and transfected with 12-SV40 adenovirus hybrid Ad12SV40. Cells were grown according to the guidelines recommended by ATCC (ATCC, 2016).

BEAS-2B cells were cultured in T-75 flasks, coated with a mixture of 0.03 mg/ml bovine collagen type I, 0.01 mg/ml BSA and 0.01 mg/ml fibronectin, dissolved in BEBM. BEGM bullet kit was used as the cell culture medium, consisting of BEBM supplemented with bovine pituitary extract, retinoic acid, insulin, transferrin, triiodothyronine, hydrocortisone, epinephrine and human epidermal growth factor (hEGF). Penicillin and streptomycin (1:50, v/v) were added. BEAS-2B cells were

maintained at 37 ºC, 5% CO_2 and in a 100% humidified environment throughout the experiment. Sub-culturing was carried out before confluence was reached. The medium was aspirated from the flask, and the cell monolayer was rinsed with $CaCl_2$ and $MgCl_2$ free PBS. Then, Trypsin-EDTA, containing 0.5% polyvinylpyrrolidone, was added and incubated at 37 ºC, 5% CO_2 for 5 – 10 min until the cells detached from each other. Dispersed cells were gently aspirated out with an additional amount of fresh BEGM medium, transferred into a centrifuge tube and centrifuged at 125 × g for 5 min. The pellet was resuspended in fresh culture medium and then transferred into a newly coated T-75 flask (1500 – 3000 cells/cm^2). All the experiments were conducted between the 5 and 30 passages of BEAS-2B cells.

3.4 Optimization and development of the NNK- and NNKOAc-induced carcinogenic model in BEAS-2B cells

The sub-lethal concentrations of NNK and NNKOAc were evaluated in a dose- and time-dependent manner using MTS and γH2AX assays. A chemotherapeutic drug, MTX (BC Cancer Agency, 2016) was used as a positive control. The same assays were performed to determine the non-cytotoxic concentration of haskap extracts.

3.4.1 Determination of the BEAS-2B cell viability

The effect of NNK and NNKOAc on BEAS-2B cell viability

The BEAS-2B cells were cultured in 96-well microplates and incubated for 24 h. After 24 h, they were treated with NNK (1, 10, 75, 150, 250, 350, 500 and 600 µM) and NNKOAc (10, 25, 50, 75 and 100 µM), and incubated for 4 h and 3 h, respectively. Based on the results, the effect of NNK on cell viability was further tested for 24, 48 and 72 h at 100, 200 and 300 µM concentrations.

The effect of haskap extracts on BEAS-2B cell viability

Initially, cells were treated with 1, 10, 50, 100, 150 and 200 µg/ml H(E) extract, for 3 h before determining the cell viability.

The effect of MTX as a positive control in carcinogenic model development

MTX was used as a positive control in designing NNK- and NNKOAc-induced carcinogenesis model development. The effect of MTX (25, 50, 75, 100 and 200 µM) on the viability of BEAS-2B cells was determined at 12 and 24 h after treatment.

In all the above assays, DMSO (0.05% of final concentration) was implemented as the vehicle control since it was used as the solvent for all the tested compounds. Also, blanks were (cell-free system) run for each measured concentration to eliminate the background effect. Three independent experiments were carried out with four replicates per experiment.

3.4.2 Determination of the DNA double-strand breaks (DSBs)

Dose- and time-dependent DSBs were determined by γH2AX assay, to assess the sub-lethal concentrations of NNK and NNKOAc, and non-cytotoxic concentrations of haskap extract.

Cells were seeded on sterilized, coated glass coverslips, kept in 6-well plates and incubated for 24 h. Based on the cell viability data, they were treated with NNK (200 and 300 µM, for 72 h), NNKOAc (10, 25, 50, 75 and 100 µM for 3 h) and haskap extract (5, 10, 20 and 50 µg/ml for 3 h). The positive control MTX (200 µM for 24 h) and the DMSO vehicle control (0.05%) were included for comparison.

3.5 Investigation of the cytoprotective effect of polyphenols on BEAS-2B cell viability

The time and dose combinations for NNK (200 µM for 72 h), NNKOAc (100 µM for 3 h) and hasakp extract (50 µg/ml for 3 h) were selected, based on previous preliminary optimization experiments. Quercetin-3-*O*-glucoside (Q3G, 50 µM for 3 h) and cyanidin-3-*O*-glucoside (C3G, 50 µg/ml for 3 h) were used for the comparisons. The above-mentioned concentrations were used in cytoprotective assays to determine the protective effect of polyphenol-rich haskap extracts.

3.5.1 Cell viability assays

The effect of polyphenols; H(E), H(A), Q3G, C3G, NNK and NNKOAc on BEAS-2B cell viability was determined by MTS and acid phosphatase assays.

MTS Assay

Epithelial cells were cultured in 96-well transparent flat bottom microplates at a density of 1×10^4 cells/100 µl/well and incubated for 24 h. Then the cells were incubated with H(E)-, H(A)-extracts, C3G, Q3G, NNK, and NNKOAc separately. A DMSO (0.05%) vehicle control and medium were also included. At the end, MTS reagent (10 µl, freshly prepared in the dark by adding 2 ml of MTS to 100 µl PMS), was added to each well and incubated at 37 ºC for 3 h. MTS does not penetrate the live cell membrane, but PMS can penetrate through the cell membrane and be reduced in metabolically active live cells by NADH (NAD(P)H-dependent dehydrogenase enzymes). Reduced PMS donates electrons to MTS in the culture medium, converting it to red colored formazan. Formazan is soluble in the tissue culture medium and absorbance was measured at 490 nm. The cell viability was calculated as below:

$$\%\ cell\ viability = \frac{Absorbance\ value\ of\ the\ treated\ cells - Blank *}{Absorbance\ value\ of\ the\ DMSO\ control\ cells - Blank *} X\ 100$$

*Blank, the absorbance of the tested compounds without cells.

Acid phosphatase assay

Cultured BEAS-2B cells 1×10^4 cells/well were incubated with respective polyphenol and carcinogen, separately. After each treatment, cells were centrifuged at 250 × g for 10 min, aspirated out the culture medium gently and washed with Ca^{++} and Mg^{++} ions free PBS. Cells were incubated with sterilized phosphatase buffer (pH 5.5, 100 µl/well), containing 0.1 M sodium acetate, 0.1% Triton X-100 (v/v) and 4 mg/ml *p*-nitrophenyl phosphate for 2 h. The acid phosphatase reaction was stopped with 1 N NaOH (10 µl) and the absorbance was measured at 405 nm. The cell viability was calculated by the phosphatase activity using the following equation.

$$\%\ acid\ phosphatase\ activity = \frac{(Absorbance\ value\ of\ the\ treatment - Blank *)}{(Absorbance\ value\ of\ the\ DMSO\ control - Blank *)} X\ 100$$

*Blank, the absorbance of the phosphatase buffer without cells.

3.6 Cytoprotective effect of haskap extracts against NNK and NNKOAc

Cultured BEAS-2B cells were pre-incubated with H(E) 50 µg/ml, H(A) 50 µg/ml, Q3G 50 µM and C3G 50 µg/ml for 3 h. The pre-incubated cells were exposed to 200 µM of NNK for 72 h and 100 µM NNKOAc for 3 h separately to determine the cytoprotective effects of each polyphenol against NNK- and NNKOAc-induced toxicity. The cytoprotective effect was determined by evaluating the reduction of DNA damage and a decrease of ROS level using various assays explained below.

3.6.1 Gamma H2AX assay

Cells were cultured on sterilized, coated glass coverslips (5×10^4 cells/well), kept in 6-well plates and incubated for 24 h. They were treated with haskap extracts, Q3G, C3G, NNK and NNKOAc separately and in combination, as explained earlier. After each treatment, cells were washed using cold PBS and fixed in 3.7% paraformaldehyde dissolved in PBS at room temperature for 20 min in the dark. The fixed cells were rinsed with PBS three times and immersed in 0.5% Triton X-100 dissolved in PBS. The cells were incubated on a shaker at room temperature, to induce cell membrane permeability. Triton X-100 was removed with PBS and non-specific sites were blocked by inverting the cell-side of the coverslips on a drop of 4% BSA on parafilm. A humidifying chamber (100% humidity) was used at room temperature to avoid desiccation. Blocking was done at room temperature for 20 min, followed by staining with anti-phospho-histone H2A.X primary antibody (1:250 in 4% BSA) for 1 h at room temperature in the humidity chamber. Stained cells were rinsed three times with PBS for 10 min each and stained with Alexa fluorophore® 594 donkey anti-mouse IgG, (1:500 in 4% BSA), the secondary antibody, at room temperature (dark) for 45 min. Cells were washed again with PBS, blotted thoroughly and mounted on a microscope slide (cell side down). Vectorsheild®, containing 4',6-diamidino-2-phenylindole (DAPI, cat # H1200, Vector Laboratories Inc, Burlingame, CA, USA), was used as the mounting medium. The sides of the coverslips were sealed properly with clear nail polish and dried at room temperature in the dark before storing at 4º C in a light tight box. Images were taken at 100× object using a flourescence inverted microscope (Axiovert 200M, ZEISS, Gottingen, Germany).

3.6.2 Comet assay

The single cell gel electrophoresis assay was performed to evaluate the DNA damage in cells using COMET SCGE assay kit (Cat # ADI-900-166, ENZO Life Sciences, Inc., CA-Brockville, ON, Canada). Cells were grown in 6-well plates at a density of 2×10^5 cells/well and incubated for 24 h. After each treatment, cells were harvested and centrifuged at 125 × g for 5 min. The cell pellet was washed once in cold Ca^{++} and Mg^{++} ion free PBS and suspended again in cold PBS (1×10^4 cells/ml). The LMA agarose was melted in boiling water and cooled in a 37 ºC water bath for 20 min. Treated cells were mixed with molten LMA agarose at room temperature at a ratio of 1: 10 (v/v) and immediately pipetted (75 µl) onto glass slides and gently spread to make a thin layer. The slides were immersed in prechilled lysis solution [2.5 M NaCl, 100 mM EDTA (pH 10), 10 mM Tris Base, 1% sodium lauryl sarcosinate, 1% Triton X-100] and incubated at 4 ºC for 45 min, following solidification. The unwinding of DNA was facilitated by dipping the slides in freshly prepared 0.3 M NaOH containing 1 µM EDTA (pH > 13). Slides were kept in NaOH for 20 min in the dark at room temperature, followed by two washes in Tris base/boric acid/EDTA (TBE) buffer (cat # B52, Thermo Fisher Scientific, Waltham, MA USA) for 5 min each. Slides were transferred to a leveled gel electrophoresis apparatus and covered with 1× TBE buffer (run at 20 volts for 15 min). Then slides were immersed in 70% ethanol for 5 min and air-dried in the dark, followed by staining in CYGREEN® dye (diluted in 1: 1000 in deionized water) for 30 min at room temperature in the dark. The slides were briefly rinsed in distilled water for three times and dried well prior to imaging.

3.6.3 DNA fragmentation.

Fragmented DNA were detected by agarose gel electrophoresis and photometric enzyme-linked immunosorbent assay (ELISA).

Agarose gel electrophoresis

GeneElute™ Mammalian Genomic DNA Miniprep Kit (cat # GIN70, Sigma-Aldrich St. Louis, MO, USA) was used to extract the nuclear DNA from treated cells. Cells were grown at 2×10^5 cells/well density in coated 6-well plates and incubated for 24 h, followed by treating them with each extract and compound accordingly. At the end, cells were harvested with trypsin-EDTA and centrifuged at 300 × g for 5 min. The cell pellet was suspended thoroughly in the suspension solution provided with the kit and treated with RNase A to minimize RNA contamination. Proteinase K was added to destroy proteins, then the cells were lysed (lysis solution C, given with the kit) and thoroughly vortexed for 15 sec before being incubated at 70 ºC for 10 min. The cell lysate was mixed thoroughly with anhydrous ethanol to get a homogenous solution, loaded onto the treated binding columns and centrifuged at 6500 × g for 1 min. The column with DNA was rinsed twice with the wash solution (provided) and DNA was eluted by centrifugation at 6500 × g for 1 min. The eluted nuclear DNA was stored at 4 ºC. Samples (5 µg) were mixed with DNA loading buffer (cat # G2526, Sigma-Aldrich, St. Louis, MO, USA), and carefully loaded into wells of 1.2% agarose gel in Tris/acetic acid/EDTA (TAE) buffer containing GelRed™ nucleic acid gel stain (cat # 41003, Biotium Inc. Fremont, CA, USA). The agarose gel was run at 40 volts for 4 h. A DNA ladder (cat # D0428, Sigma-Aldrich) was loaded as a DNA marker and visualized by UV light (GelDoc™ EZ Imager, BioRad Laboratories, Mississauga, ON, Canada).

Enzyme Linked Immunosorbent Assay (ELISA)

DNA fragmentation was further tested with an ELISA assay (cat # Roche 11585045001, Sigma-Aldrich, St. Louis, MO, USA). BEAS-2B cells were suspended at a density of 4×10^5 cells/ml in BEGM medium containing 5'-bromo-2'-deoxy-uridine (BrdU, 10 µM final concentration). The cell suspension was incubated at 37 ºC in 5% CO_2 for 2 h followed by centrifugation at 250 × g for 10 min. The cell pellet was dispersed in BEGM medium (1×10^5 cell/ml) and cells were cultured in 96-well, round bottom microplates. Treatments (2× concentration) were added to each well and incubated. The plate was centrifuged at 250 × g for 10 min before the supernatant was removed, and then the cells were incubated with 200 µl incubation solution at room temperature for 30 min. The supernatant was collected (100 µl) by centrifugation at 250 × g for 10 min. A 96-well flat bottom plate was coated with the anti-DNA coating solution and incubated at 37 ºC for 1 h. The coating solution was aspirated; non-specific binding sites were blocked with incubation solution at room temperature for 30 min. The incubation solution was removed, and wells were cleaned with wash solution. The BrdU-labeled samples were transferred into each well of the coated plate and incubated overnight at 4 ºC. Then remaining samples were removed, and the plate was rinsed three times with wash solution. The microplate was microwaved for 5 min at medium heat with 250 µl wash solution and cooled down at 4 ºC. The anti-BrdU-POD solution was added to each emptied well (incubated at room temperature for 90 min) followed by another three washes. The substrate solution was pipetted into each well, incubated in the dark on a shaker until color development (5 - 6 min), followed by the addition of stop solution (concentrated sulfuric acid). The plate was incubated on the shaker for another 1 min and

the absorbance was measured at 450 nm. A blank, containing the substrate solution and stop solution, was included each time.

3.6.4 Determination of the ROS

The generation of ROS was determined using a DCFDA cellular ROS detection assay kit (cat # ab113851, Abcam Inc, Toronto, ON, Canada), following the manufacturer's guidelines. Briefly, cells were cultured at 2.5×10^4 density/well in clear bottom dark-sided 96-well microplates and incubated for 24 h. Then cells were treated accordingly. The cells treated with NNKOAc, H(E), H(A), Q3G and C3G were stained with 10 µM 2',7'-dichlorofluorescein diacetate (H_2DCFDA) for 45 min at 37 ºC before treatments. The cells treated with NNK (72 h) were stained for 45 min before completion of the treatment, by overlaying 25 µM freshly prepared H_2DCFDA on top of the treated cells. The H_2DCFDA is membrane permeable and is deacetylated in the cytoplasm by cellular esterase to a nonfluorescent ionic compound 2',7'-dichlorofluoresin (H_2DCF). With the presence of ROS (hydroxyl and peroxyl radicles), H_2DCF was oxidized to 2',7'-dichlorofluoresin (DCF), a highly fluorescent compound. The fluorescence intensity was measured at 485 nm excitation and 535 nm emission.

3.7 Statistical analysis

The complete randomized design was used as the experimental design. All the experiments were conducted in quadruplicate and independently, three times. One-way ANOVA ($p < 0.0001$) was performed using Minitab® 17.0 statistical software. Mean comparison (at $p < 0.05$) was resolved by means of confidence intervals using Tukey's and Duncan's multiple mean tests. Results were expressed as mean ± standard deviation.

CHAPTER 4. RESULTS

4.1 Haskap berries are rich in polyphenols

The polyphenols present in two commercially grown haskap varieties, 'Indigo Gem 915' and 'Tundra', were extracted separately in absolute ethanol [H(E)] and deionized water [H(A)], and analyzed to characterize their phenolic profiles (Table 1). The haskap berries were found to contain a diversity of polyphenols, including flavonoids and phenolic acids. Anthocyanin was the most predominant flavonoid, including C3G followed by cyanidin-3-rutinoside. The C3G accounts for 82 – 85% of the flavonoids in all four extracts. The variety 'Indigo Gem 915' contained the highest C3G content, and its aqueous extract had the highest [205 mg/100 g fresh weight (FW)]. The flavonol, quercetin rutinoside was also found in both varieties and varied from 9 – 12 mg/100 g FW among the four extracts. The haskap berries also contained chlorogenic acid and many other simple phenolic acids, but approximately 96% of the phenolic acids consisted of chlorogenic acid. The variety 'Indigo Gem 915' had a considerably higher level of anthocyanin than the variety 'Tundra'. However, aqueous extracts of both varieties contained a greater quantity of flavonoids, particularly, anthocyanins than their ethanolic extracts. The polyphenols extracted from 'Indigo Gem 915' were used for the investigation of chemopreventive potential against lung carcinogenesis.

4.2 TPC of the polyphenol-rich 'Indigo Gem 915'

The TPC of H(E) and H(A) extracts of the variety 'Indigo Gem 915' was analyzed using the Folin–C method. The TPC varied from 344 to 430 mg GAE/g DW among the three separate polyphenol-rich H(E) extracts, with a mean value of 379 ± 7 mg

GAE/g DW. The H(A) extracts showed a higher level of TPC, ranging from 336 to 468 mg GAE/g DW, with a mean value of 386 ± 23 mg GAE/g DW.

4.3 Antioxidant capacity of the variety 'Indigo Gem 915'

The FRAP and DPPH• radical scavenging assays measured the *in vitro* antioxidant capacity of ethanolic and aqueous extracts of the 'Indigo Gem 915'. The FRAP values varied from 1121 to 1918 µmol TE/g DW, with a mean value of 1604 ± 60 µmol TE/g DW among three H(E) extracts. The FRAP values of aqueous extracts ranged from 1208 – 2655, with a mean value of 2033 ± 196 µmol TE/g DW. The antioxidant capacity of H(A) was significantly higher ($p = 0.045$ at 95% CI) than that of the H(E). The IC_{50} values from DPPH• radical scavenging assay were 0.8 mg DW/ml and 0.7 mg DW/ml in H(A) and H(E) extracts, respectively.

4.4 Haskap extracts were stable in BEAS-2B cell culture medium

Oxidative degradation of the haskap extracts was determined and compared for each cell-free medium after 8 h incubation under cell culture conditions. Trolox, a water-soluble antioxidant vitamin E analog, and NAC, a water-soluble antioxidant (LeyZafarullah et al., 2003), were also incorporated along with haskap, into each cell culture medium. The formation of H_2O_2 in the BEBM medium containing haskap extracts (10 – 11 µM) was significantly ($p < 0.0001$) lower than the other cell culture media, such as DMEM and EMEM, except for DMSO (11 µM) solvent control ($p < 0.0001$). Therefore, the BEBM medium constituents protected the oxidative degradation of polyphenol-rich haskap extracts. The addition of NAC significantly reduced the H_2O_2 formation in the haskap dissolved BEBM medium, compared to Trolox (Figure 7). The

pH of BEBM dissolved with haskap extracts was approximately 7.3 and all the other treatments recorded a similar pH range (7.0 – 7.6) after the treatment period.

4.5 The NNK- and NNKOAc-induced DNA damage in BEAS-2B cells

The cell viability and the intensity of DSBs which occurred in BEAS-2B cells were evaluated to develop the NNK- and NNKOAc-induced lung carcinogenesis model. Formation of DSBs induced the rapid phosphorylation of histone H2AX protein (γH2AX), which was detectable near the breaks. These breaks were detected by immunostaining and used as biomarkers of DNA damage. A cytoprotective dose of the haskap extracts was selected and evaluated with sub-lethal concentrations of NNK and NNKOAc, to understand the chemopreventive potential of haskap berry fruit (Figure 8).

4.5.1 Haskap extracts were not cytotoxic to BEAS-2B cells

As presented in Figure 8, low concentrations (1 – 50 µg/ml) of H(E) extract did not inhibit the BEAS-2B cell growth. The percent viability of cells was >80% at the low doses of H(E) extract and a similar outcome was seen even after 24 h incubation (Appendix 1). When the cells were incubated with higher concentrations (100 – 200 µg/ml) of H(E) extract, cell viability decreased. However, the IC_{50} value of H(E) was 189 µg/ml after 3 h. Therefore, 1, 5, 20, 50 µg/ml concentrations were investigated to determine whether these doses could enhance DSBs in BEAS-2B epithelial cells. None of the test levels induced a significant ($p > 0.05$) level of DSBs in epithelial cells, compared to the DMSO (0.05%) vehicle control, but were significantly ($p < 0.0001$) lower from the MTX, as expected. Therefore, 50 µg/ml was selected as a non-cytotoxic concentration of haskap to investigate its protective effect against two lung carcinogens.

4.5.2 The effect of NNK on BEAS-2B cells

Exposure to 600 µM NNK did not reduce cell viability at 4 h (Appendix 2). The percent viability was approximately >80% at 100, 200 and 300 µM of NNK even after 24 and 48 h incubation (Figure 8). However, long term exposure (72 h) to a higher concentration (300 µM) of NNK significantly ($p < 0.0001$) reduced the epithelial cell viability (36%). Therefore, DSBs were tested at higher NNK concentrations (200 and 300 µM) after 72 h exposure and the formation of γH2AX foci was quantified. The formation of DSBs was high in NNK-treated cells, compared to DMSO-treated controls, but differences were not significant between 200 µM and 300 µM. Therefore, 200 µM of NNK for 72 h, which showed more than 70% cell viability, was selected as a sub-lethal concentration and tested in the chemopreventive cell model.

4.5.3 The effect of NNKOAc on BEAS-2B cells

Exposure to 200 µM NNKOAc for 4 h did not reduce the BEAS-2B cell viability, but DNA damage was greater and uncountable due to overlapping foci (Appendix 3). The percent viability of epithelial cells treated with up to 100 µM NNKOAc for 3 h was >90% and a concentration-dependent (10, 25, 50, 75, 100 µM) increase in DSBs in BEAS-2B cells was observed for NNKOAc comparable to its DMSO vehicle control (Figure 8). Therefore, NNKOAc at 100 µM for 3 h was selected as the sub-lethal concentration for further analysis.

Treatment with two reference polyphenols, 50 µM Q3G for 3 h and 50 µg/ml C3G for 3 h, were chosen for the comparisons. Both compounds were present in the selected haskap extracts.

4.6 Viability of BEAS-2B cells

The ACP and MTS assays were used to determine the viability of the BEAS-2B cells following each treatment. Based on the ACP assay, NNK, NNKOAc or any of the polyphenol compounds were not cytotoxic to BEAS-2B cells at the studied concentrations. Nearly 100% viability was seen in all treatments (Figure 9A). However, the MTS assay data showed few deviations, in that the viability of C3G-treated cells was significantly ($p< 0.0001$) reduced (45%) compared to the medium control (99%) and all other test compounds. The NNK (89%), NNKOAc (79%), H(E) (82%) and H(A) (86%) treatments resulted in similar cell viability values, but Q3G treatment resulted in 99% cell viability (Figure 9B). The viability assays demonstrated that any of the compounds at tested doses and time points were not cytotoxic to BEAS-2B cells.

4.7 Morphology of BEAS-2B cells

The morphological changes of BEAS-2B cells subjected to NNK- and NNKOAc-induced carcinogenesis, with or without adding test compounds [H(E), H(A), Q3G and C3G], were determined using an inverted phase contrast microscope at 100× magnification (Figure 10). Cells were well attached to the culture plates and showed their epithelial characteristics (cuboidal shape) in all treatments. No visible morphological characteristics of cell apoptosis, such as membrane blebbing, cell shrinkage, or floating cells, were seen among any of the treatments compared to the medium and DMSO controls.

4.8 Haskap extracts significantly reduced NNK-and NNKOAc-induced DSBs

The protective effect of haskap polyphenol-rich extracts, Q3G and C3G, was assessed by measuring the DSBs in BEAS-2B cells using the γH2AX assay.

Immunostaining of the phosphorylated histone H2AX protein gave an indication of DSBs and was detected by fluorescence microscopy (Figure 11A-C). Based on the quantitative data presented in Figure 11 D and E, NNKOAc-induced DSBs (40 γH2AX foci/nucleus) were significantly higher ($p < 0.0001$) in BEAS-2B cells, compared to that of NNK-treated cells (8 foci/nucleus). The HK(E) and HK(A) extracts, and C3G significantly ($p < 0.0001$) suppressed the NNK-induced DSBs, except Q3G (Figure 11D). However, pre-incubation with Q3G reduced the NNK-induced DSBs by 17%. Polyphenol-rich haskap extracts (50 µg/ml) did not form a significant ($p > 0.0001$) level of DSBs in BEAS-2B cells, compared to the DMSO vehicle control, but Q3G and C3G did (Figure 11D). Both ethanol and aqueous extracts of the haskap berry, Q3G, and C3G, significantly reduced NNKOAc-induced DSBs ($p < 0.0001$) in BEAS-2B cells. Compared to the ethanolic extract (51%), the aqueous extract of haskap showed a significant (75%) protective effect against NNKOAc-induced DNA damage (Figure 11E). Based on the γH2AX assay, NNKOAc was more genotoxic for BEAS-2B cells than NNK. Pre-incubation of BEAS-2B cells with H(E) and H(A) extracts reduced the DSBs induced by NNK and NNKOAc.

4.9 Haskap extracts reduced NNKOAc-induced DNA SSBs and DSBs

The comet assay is another well-established method of detecting DNA damage in single cells. Two indices, percent DNA in tail and olive tail moment, were used to determine the DNA damage in treated cells. The SSBs and DSBs were not significant ($p = 0.134$) in BEAS-2B cells treated with the H(E), H(A), Q3G and C3G, in comparison to the DMSO vehicle control. Representative comet images are presented in Figure 12A (top). The comet tail moment in NNKOAc-treated cells had a mean value of 17. Therefore, NNKOAc exposure resulted in a significant ($p < 0.0001$) increase in DSBs

and SSBs in BEAS-2B cells. Pre-incubation of BEAS-2B cells with the haskap extracts, Q3G and C3G, significantly ($p < 0.0001$) reduced the NNKOAc-induced damage to single and double stranded DNA. The damage reduction was as follows; H(A) extracts (75%) > H(E) extracts (67%) > Q3G (60%) > C3G (57%) in BEAS-2B cells. Compared to Q3G and C3G, both haskap extracts showed a higher level of protection against NNKOAc. The higher protective effect of the haskap extracts could be attributed to the synergistic effect of multiple polyphenols present in the extracts.

4.10 Haskap extracts reduced NNKOAc-induced DNA fragmentation

DNA fragmentation and the protective effect of polyphenols on DNA fragmentation were detected by ELISA assay and agarose gel electrophoresis (Figure 13A and B). DNA fragmentation was not significant ($p = 0.791$) in cells incubated with H(E), H(A), Q3G, C3G and the DMSO control. Moreover, haskap extracts and other flavonoids suppressed NNKOAc-induced fragmentation significantly ($p < 0.0001$). DNA fragmentation was reduced by 50% in the cells pre-incubated with polyphenols and was almost similar to DNA fragmentation in the DMSO control. However, agarose gel electrophoresis did not show DNA fragmentation following any of the treatments. Nuclear DNA remained on the top of the gel as a high molecular weight band representing intact DNA (Figure 13B).

4.11 Haskap extracts regulated the formation of ROS in BEAS-2B cells

Polyphenol-rich haskap extracts showed antioxidant capacity in DPPH and FRAP assays. Therefore, the ability of haskap extracts to scavenge NNK- and NNKOAc-induced intracellular ROS in BEAS-2B cells was of interest to investigate. Cellular oxidative stress was quantified using DCFDA, which was oxidized to DCF in the cells

and measured using a plate reader, as a probe. The H(E) and H(A) extracts, Q3G and C3G, completely abolished NNKOAc-induced intracellular ROS production, as indicated by the decrease in DCF fluorescence intensity (Figure 14). The intracellular ROS level was significantly lower ($p < 0.0001$) in BEAS-2B cells incubated with H(E) and H(A) extracts, Q3G and C3G alone. However, only Q3G could significantly suppress ($p < 0.0001$) NNK-induced oxidative stress in BEAS-2B cells.

Table 5 The concentration of major polyphenols (mg/100 g fresh fruits) in ethanolic and aqueous extracts of the two commercially grown haskap varieties in Nova Scotia.

Compound	**Indigo-gem**		**Tundra**	
	(E)	(A)	(E)	(A)
Anthocyanin				
Cyanidin-3-*O*-glucoside	192 ± 19	205 ± 14	162 ± 2	172 ± 3
Petunidin-3-*O*-glucoside	0.003 ± 0	0.002 ± 0	0.002 ± 0	0.002 ± 0
Delphinidin-3-*O*-glucoside	0.2 ± 0	0.1 ± 0	0.2 ± 0	0.2 ± 0
Peonidin-3-*O*-glucoside	9 ± 1	8 ± 0.3	9 ± 1	7 ± 0
Malvidin-3-*O*-glucoside	2 ± 0	2 ± 0	1 ± 0	2 ± 0
Delphinidin-3-*O*-rutinoside	0.1 ± 0	0.3 ± 0	0.7 ± 0	0.6 ± 0
Cyanidin-3-*O*-rutinoside	12 ± 1	10 ± 0	10 ± 1	10 ± 0
Total	*215*	*226*	*184*	*192*
Flavonols				
Quercetin-3-*O*-galactoside	0.02 ± 0	0.02 ± 0	0.02 ± 0	0.02 ± 0
Quercetin-3-*O*-glucoside	2 ± 0	2 ± 0	3 ± 0	2 ± 0
Quercetin-3-*O*-rhamnoside	0.2 ± 0	0.1 ± 0	0.2 ± 0	0.2 ± 0
Quercetin	0.2 ± 0	0.1 ± 0	0.2 ± 0	0.1 ± 0
Quercetin-3-*O*-rutinoside	12 ± 1	10 ± 0	9 ± 1	10 ± 0
Total	*14*	*12*	*13*	*13*
Flavanols				
EGC	0.1 ± 0	0.04 ± 0	0.02 ± 0	0.03 ± 0
Catechin	0.8 ± 0	0. 8 ± 0	0.7 ± 0	0.8 ± 0
Epicatechin	0.1 ± 0	0.1 ± 0	0.5 ± 0	0.5 ± 0
EGCG	0.1 ± 0	0.1 ± 0	0.01 ± 0	0.2 ± 0
ECG	0.1 ± 0	0.4± 0	0.002 ± 0	0.003 ± 0
Total	*1*	*1*	*1*	*2*
Phenolic acids				
Chlorogenic Acid	16 ± 2	16 ± 1	15 ± 2	17 ± 1
Phloridzin	0.3 ± 0	0.2 ± 0	0.3 ± 0	0.2 ± 0
Phloritin	0.01 ± 0	0.01 ± 0	0.01 ± 0	0.01 ± 0
Isoferulic Acid	0.3 ± 0	0.3 ± 0	0.4 ± 0	0.4 ± 0
Cafeic acid	0.04 ± 0	0.1 ± 0	0.1 ± 0	0.03 ± 0
Ferulic acid	0.1 ± 0	0.1 ± 0	0.1 ± 0	0.1 ± 0
Total	*16*	*17*	*16*	*18*
Total polyphenol content	***246***	***255***	***213***	***224***

*E, ethanolic extract; A, aqueous extract; EGC, epigallocatechin; ECG, epicatechin gallate. The results represent the mean ± SE of three (n = 3) independent extractions.

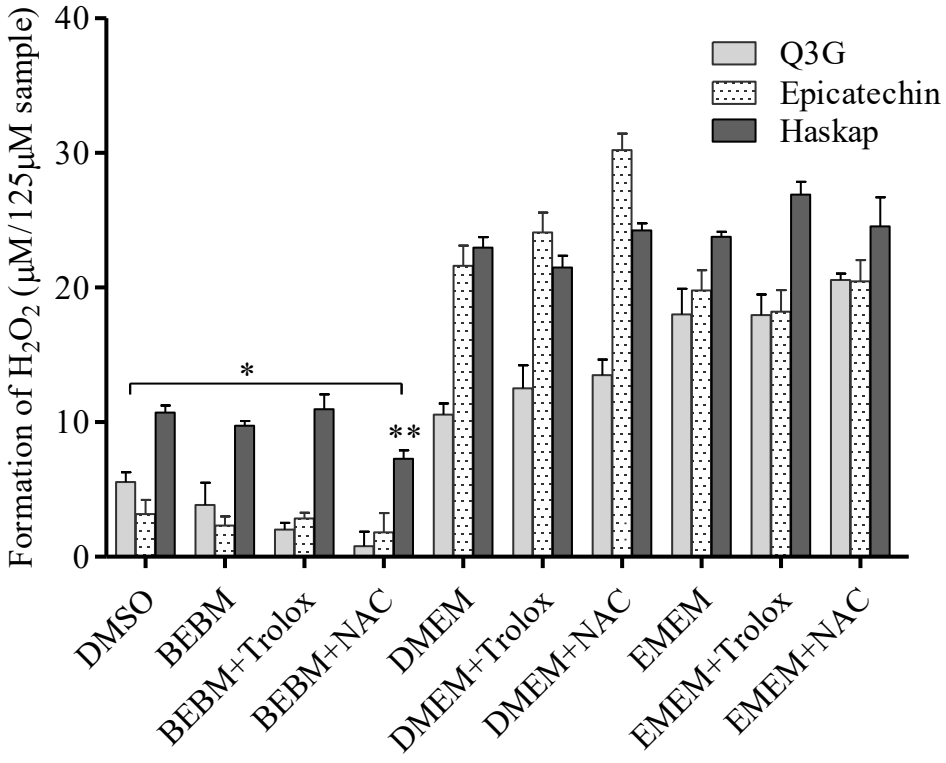

Figure 7 The BEBM medium did not generate H_2O_2 by reacting with test compounds.

The formation of H_2O_2 by haskap extracts and its polyphenol constituents (Q3G and epicatechin) in the cell culture medium was determined by Amplex® Red H_2O_2 assay kit. The formation of resorufin was measured at 570 nm excitation/585 nm emission after 8 h incubation of the haskap extracts (250 μg/ml) or pure polyphenols (250 μM) in selected culture medium, separately. The level of H_2O_2 in cell culture medium was calculated based on the H_2O_2 standard curve (0 – 5 μM, $r^2 = 0.9865$). One Way Analysis of Variance was performed with Duncan's multiple range test (at $\alpha = 0.05$) compared to DMSO vehicle control.

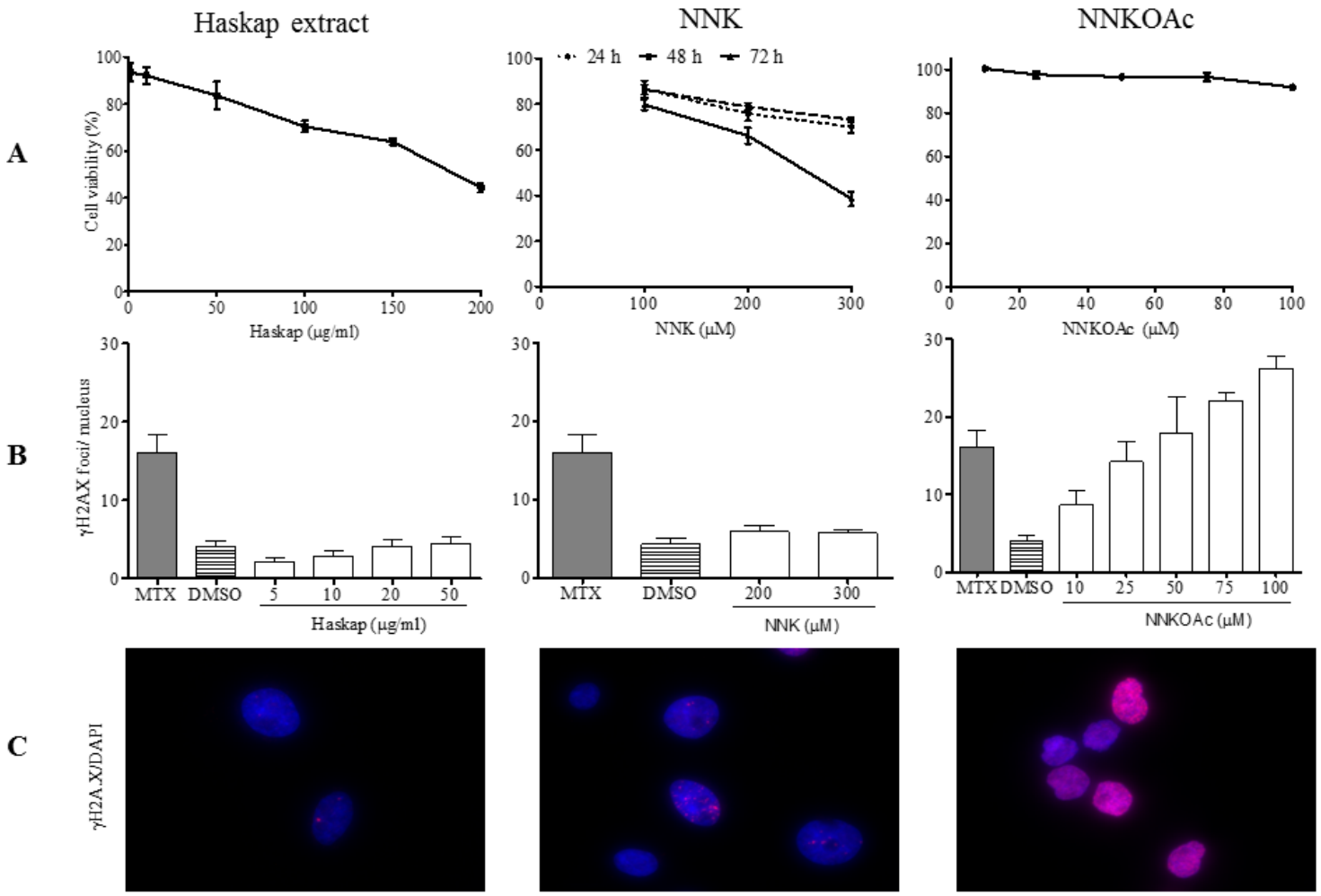

Figure 8 The optimization of NNK- and NNKOAc-induced lung carcinogenesis model using BEAS-2B cells.

Cell viability (MTS assay) and DSBs (γH2A.X assay) were used as two parameters to determine the sub-lethal concentrations of NNK and NNKOAc, and the cytoprotective concentrations of haskap extracts in BEAS-2B cells. A: Concentration- and time-dependent cell viability of BEAS-2B cells treated with test compounds. Haskap extracts (1 – 200 µg/ml, 3 h), NNK (100 – 300 µM, 24, 48 and 72 h) and NNKOAc (10 – 100 µM, 3 h) were tested to find the effect on cell viability. B: Concentration- and time-dependent DSBs. Cells were incubated with haskap (5 – 50 µg/ml, 3 h), NNK (200 – 300 µM, 72 h) and NNKOAc (10 – 100 µM, 3 h) to determine an appropriate time and dose for each tested compound to develop the experimental model. C: The variation of DSBs among each tested compound. Immunocytochemistry for γH2AX (Serine 139, red and DNA counterstaining performed with DAPI, blue). The phosphorylation of serine at histone H2AX protein was labeled using donkey anti-mouse IgG coupled to Alexa 594 and imaged. The fluorescence microscopic images were taken and quantified using Fiji ImageJ software (40 – 50 cells/treatment). MTX, a standard chemotherapeutic drug was used as a positive control (200 µM, 24 h) to compare the DSBs. The concentration of MTX was determined on cell viability. All the compounds dissolved in DMSO (0.05% final concentration), which. was used as the vehicle control.

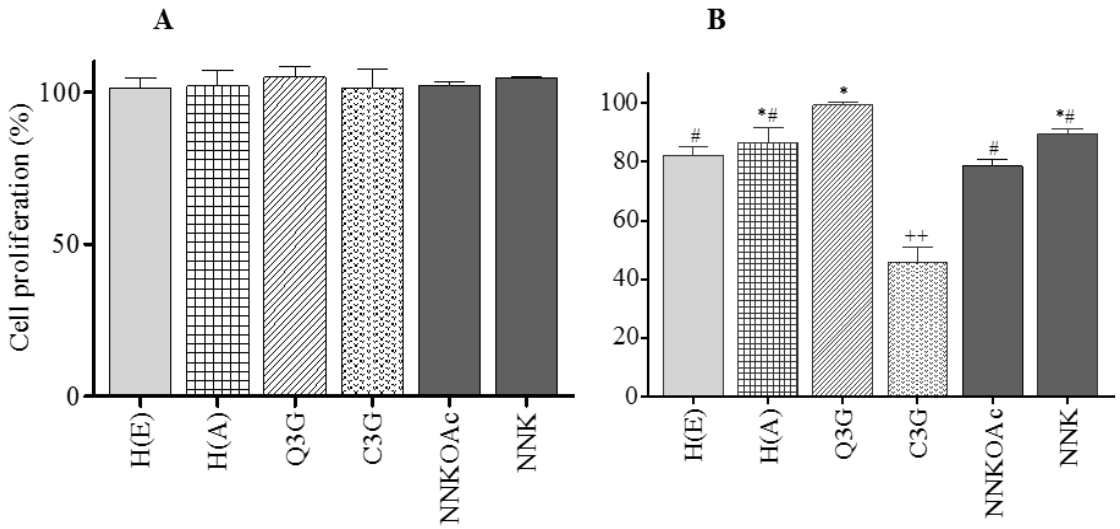

H(E) – 50 µg/ml, 3 h H(A) – 50 µg/ml, 3 h NNK – 200 µM, 72 h
Q3G – 50 µM, 3 h C3G – 50 µg/ml, 3 h NNKOAc – 50 µM/ 3 h

Figure 9 The H(E), H(A), Q3G, C3G, NNKOAc and NNK at the optimized concentrations were not cytotoxic for BEAS-2B cells.

Cytotoxicity was determined by ACP (A) and MTS (B) assays. A) The cell viability was determined as the percent acid phosphatase activity by measuring the absorbance at 405 nm. B) The cell viability was determined by measuring the color intensity of formazan at 490 nm. The studied concentrations of each compound have presented above. The results represent three independent experiments (n=3 with quadruplicate). One Way Analysis of Variance was performed ($p < 0.0001$) with Tukey pairwise comparison (at $\alpha = 0.05$) for mean comparison.

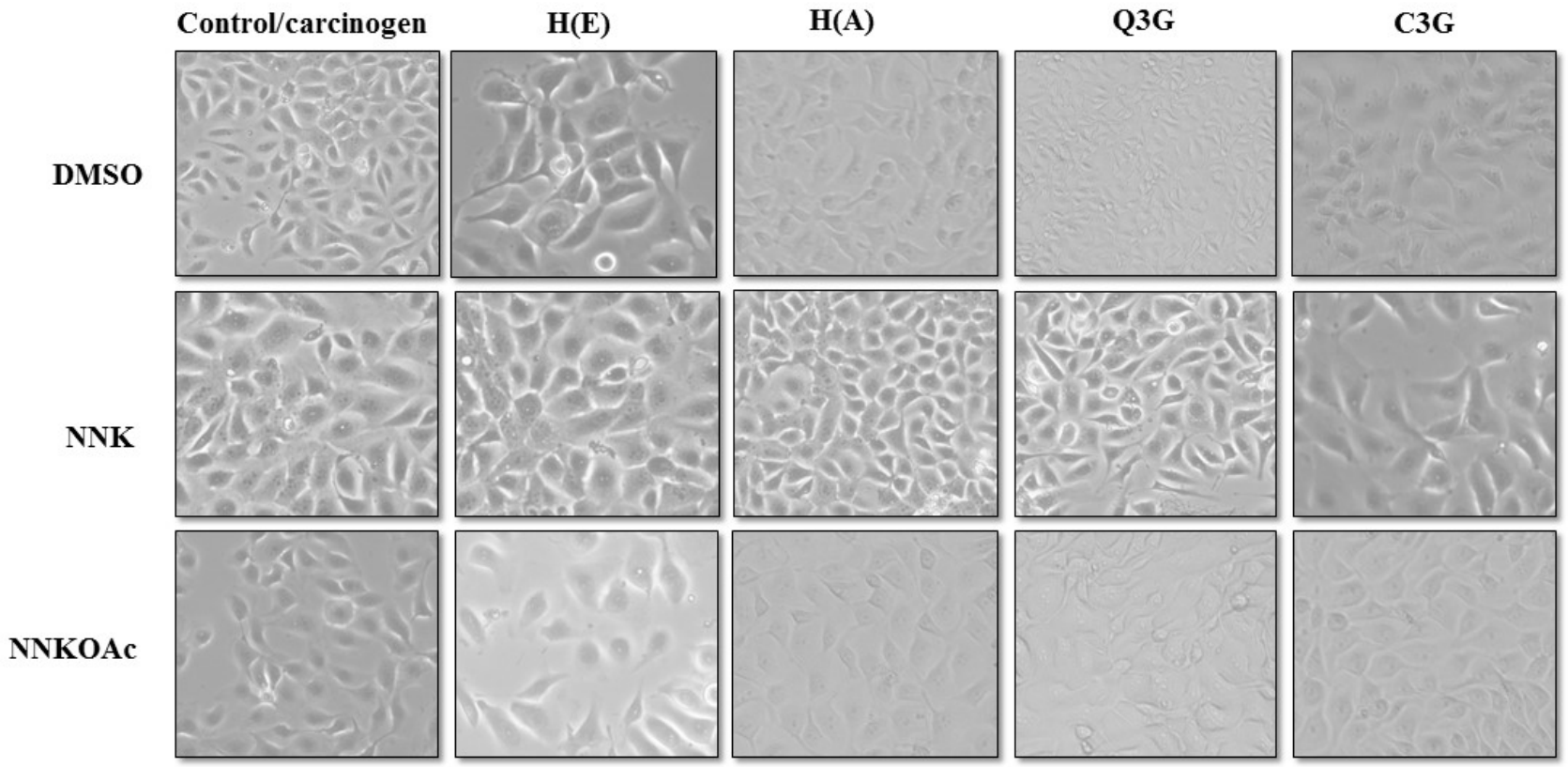

H(E) – 50 µg/ml, 3 h
H(A) – 50 µg/ml, 3 h
NNK – 200 µM, 72 h
Q3G – 50 µM, 3 h
C3G – 50 µg/ml, 3 h
NNKOAc – 50 µM/ 3 h

Figure 10 The morphology of BEAS-2B cells were not different from the DMSO control after each treatment combination.

Images were taken with the inverted phase contrast microscope at 100× magnification. The concentrations of tested compounds were presented above.

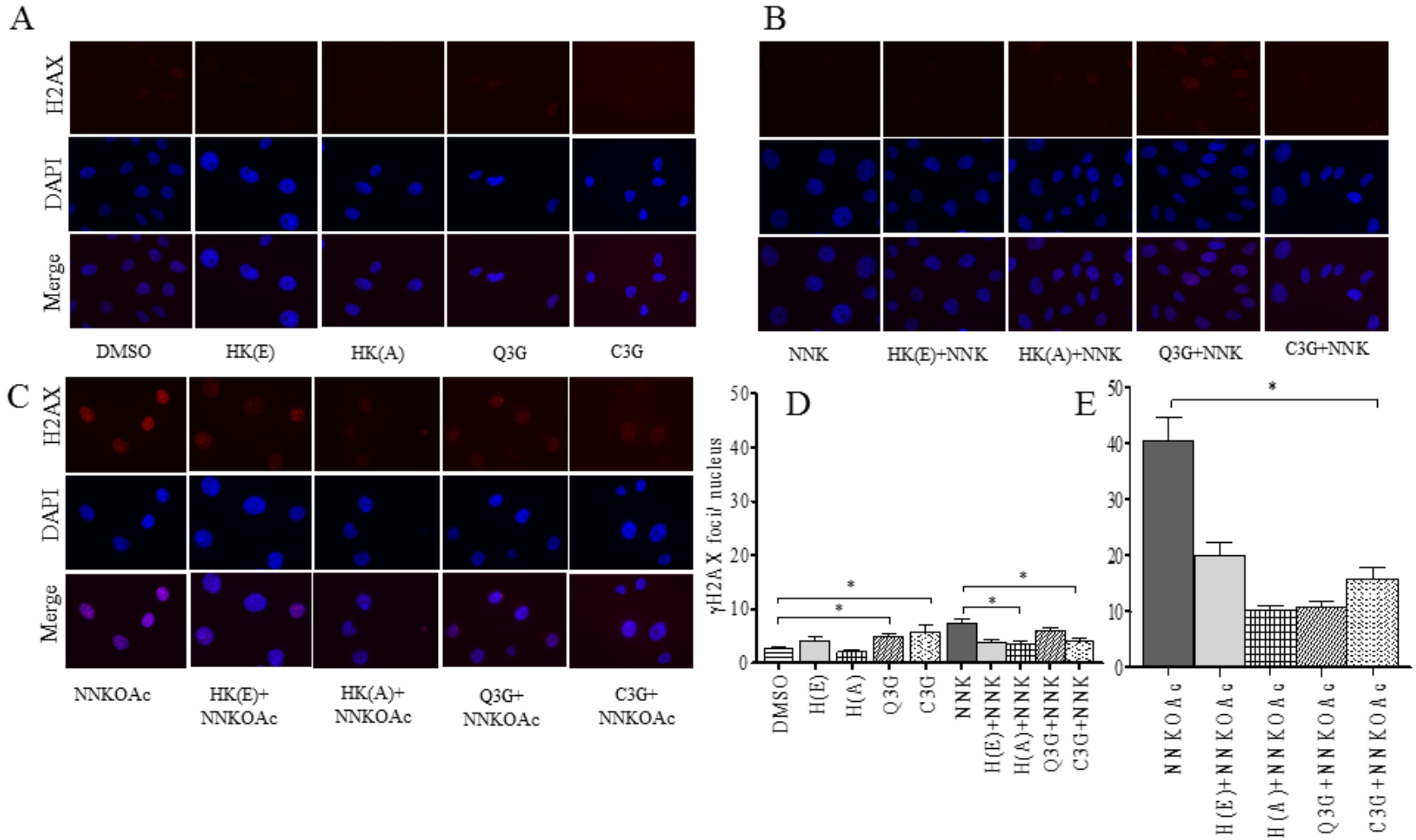

Figure 11 The polyphenol-rich haskap extracts significantly reduced NNK- and NNKOAc-induced DSBs in BEAS-2B cells (γH2A.X assay)

A) Variation of the DSBs among each tested compound. B and C) The protective effect of H(E) and H(A) extracts against NNK and NNKOAc, respectively. D and E). γH2A.X foci were quantified using Fiji ImageJ software in fluorescence microscopic images (100×). The results represent three independent experiments (n=3) and analysis of 100-120 nucleus from each treatment. One Way Analysis of Variance was performed ($p < 0.0001$) with Tukey pairwise comparison (at $\alpha = 0.05$) for mean comparison.

A

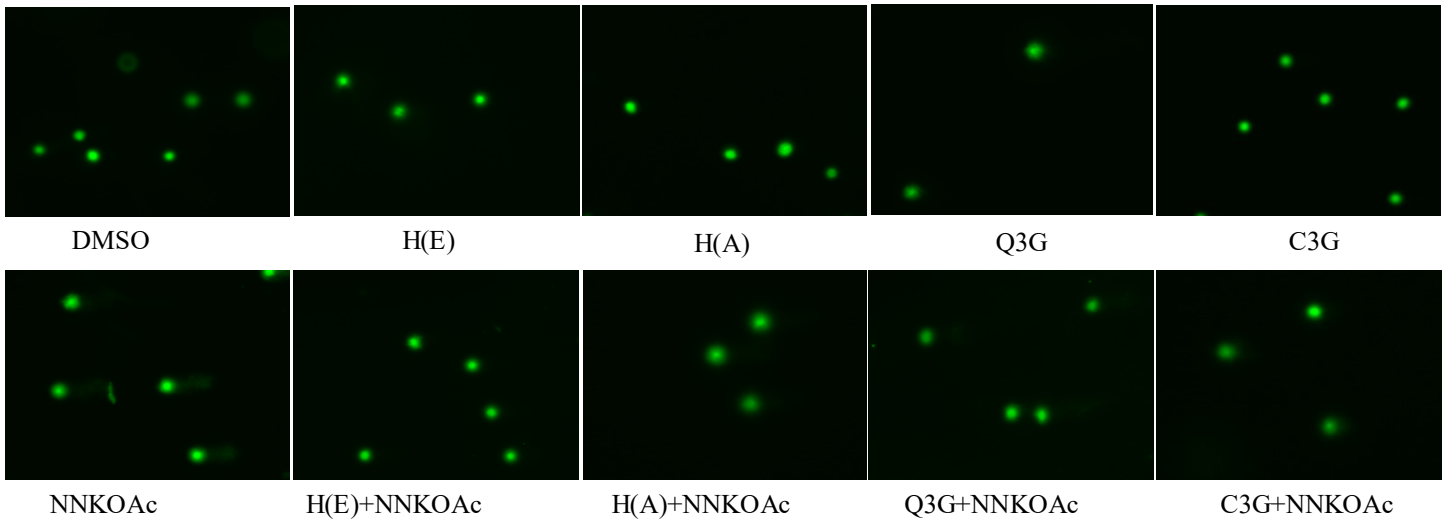

B

Treatment	Comet Tail moment ± SE	Tail DNA (%) ± SE	Tail length	Olive moment
DMSO	5.4 ± 1.5^{d}	12.2 ± 2.0^{c}	13.6 ± 1.7^{de}	4.2 ± 0.8^{bc}
NNKOAc	30.3 ± 4.7^{a}	33.0 ± 3.6^{a}	77.1 ± 9.0^{a}	16.7 ± 2.1^{a}
H(E)	16.5 ± 4.3^{bcd}	22.0 ± 3.9^{bc}	30.4 ± 5.2^{bcd}	10.6 ± 2.5^{b}
H(A)	7.3 ± 2.1^{cd}	13.3 ± 2.8^{c}	18.5 ± 3.4^{cde}	5.7 ± 1.5^{bc}
Q3G	3.8 ± 1.2^{cd}	9.3 ± 1.7^{c}	16.1 ± 2.5^{cde}	3.7 ± 0.9^{bc}
C3G	3.5 ± 1.0^{d}	9.5 ± 1.7^{c}	10.6 ± 1.3^{e}	3.0 ± 0.5^{c}
H(E)+NNKOAc	7.6 ± 1.9^{bcd}	15.2 ± 3.2^{bc}	28.1 ± 3.9^{bcd}	5.7 ± 1.0^{bc}
H(A)+NNKOAc	5.1 ± 2.3^{bcd}	9.5 ± 2.6^{c}	24.6 ± 4.3^{bcd}	4.1 ± 1.0^{bc}
Q3G+NNKOAc	9.1 ± 2.0^{abc}	15.9 ± 3.3^{bc}	37.7 ± 5.5^{ab}	6.5 ± 1.1^{b}
C3G+NNKOAc	11.9 ± 2.7^{bc}	28.8 ± 5.3^{ab}	29.0 ± 6.1^{abc}	7.6 ± 1.4^{bc}

Single and double strand DNA damage in BEAS-2B cells as determined by comet assay

Figure 12 The polyphenol-rich haskap extracts significantly reduced NNKOAc-induced SSBs and DSBs in BEAS-2B cells.

A) Nuclear DNA stained with SYBR Green I dye and images were taken (A) to measure the DNA damage. Fluorescence microscopic images (200×) were used to quantify the DNA damage as the percent DNA in tail and tail moment (tail moment = measure of tail length x measure of DNA in the tail) using Fiji ImageJ and Open Comet Version 1.3 software. The nuclear DNA is intact without a DNA tail (DMSO 0.05%). The bigger the DNA tail area (%) or the longer the DNA tail length indicates more significant DNA damage. B) Data in the table represent three independent experiments (n = 3) and 120 – 140 cells were analyzed for each treatment. One Way Analysis of Variance was performed ($p < 0.0001$) with Tukey pairwise comparison (at $\alpha = 0.05$) for mean comparison. Means that do not share a similar letter are significantly different.

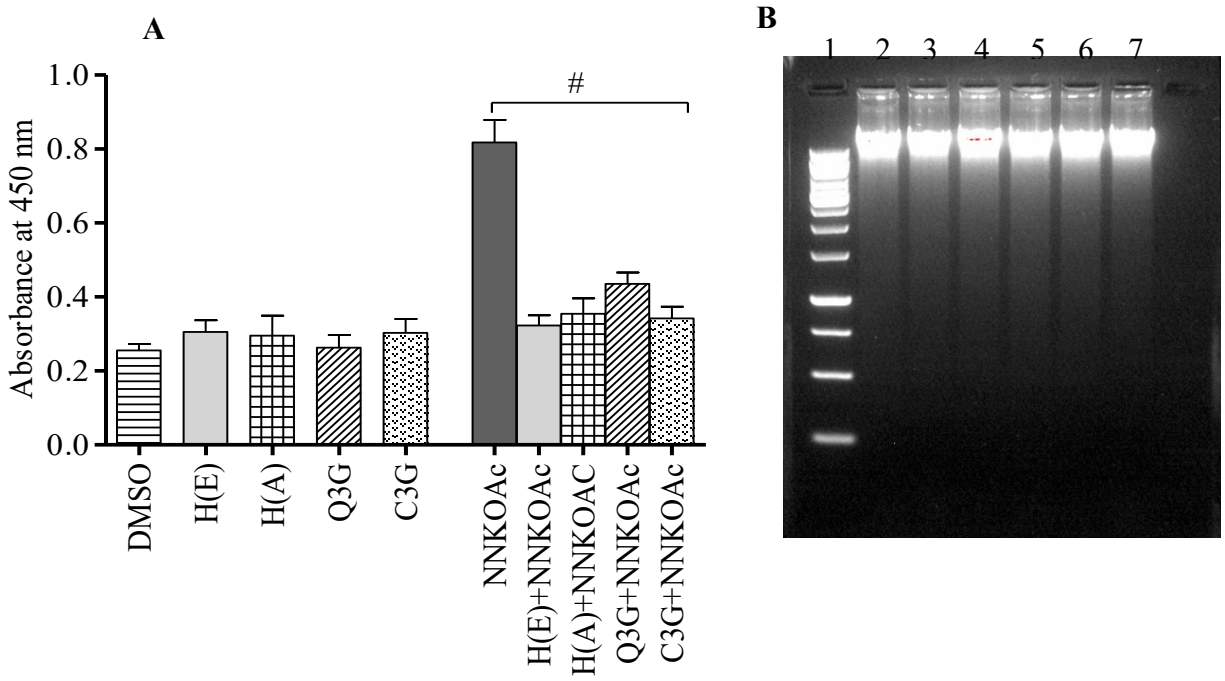

Figure 13 The polyphenol-rich haskap extracts reduced NNKOAc-induced DNA fragmentation.

DNA fragmentation was tested by ELISA (A) and agarose gel electrophoresis (B). A) DNA fragments present in cell lysates were quantified photometrically (at 450 nm) using a monoclonal antibody against BrdU. B) Agarose gel electrophoresis. Treatments found in each well as follows: 1, DNA marker; 2, NNKOAc (100 µM, 3 h); 3, H(E) (50 µg/ml, 3 h); 4, H(A) (50 µg/ml, 3 h); 5, NNK (200 µM, 72 h); 6, DMSO (0.01%) vehicle control, and 7, no treatment (BEGM medium). The results represent three independent experiments (n = 3). For the ELISA assay, each experiment was conducted with four sub-replicates. One Way Analysis of Variance was performed ($p < 0.0001$) with Tukey pairwise comparison (at $\alpha = 0.05$) for mean comparison.

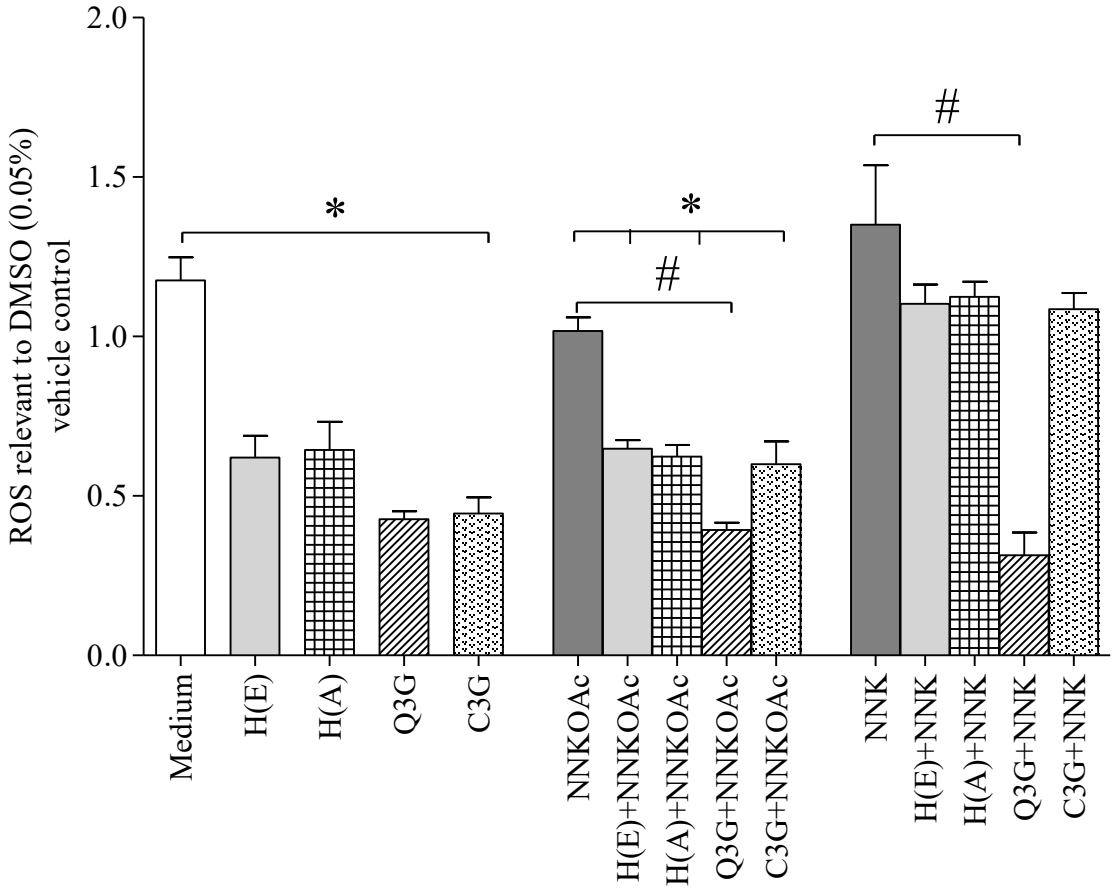

Figure 14 The reduction of ROS formation in BEAS-2B cells, in relation to tested compounds and extractions.

Intracellular ROS levels were determined by using DCFDA ROS detection assay kit. The cells were pre-incubated with and without each polyphenol prior to NNK and NNKOAc exposure and DCF status measured at 495 nm excitation and 529 nm emission by fluorescence spectrophotometer. The results represent three independent experiments (n=3) and each test comprised with four sub replicates. One Way Analysis of Variance was performed ($p < 0.0001$) with Tukey pairwise comparison (at $\alpha = 0.05$) for mean comparison.

CHAPTER 5. DISCUSSION

Polyphenol-rich diets have gained recent attention due to their beneficial health values. In particular, fruits and vegetables rich in polyphenols have been investigated extensively, and reviewed regarding their useful physiological functions including cancer preventive properties (Block et al., 2015; George et al., 2017; Rupasinghe et al., 2014; Shih et al., 2010; Tan et al., 2011). The focus of the current study was to explore the efficacy of polyphenol-rich haskap berry extracts in the reduction of DNA damage in relation to carcinogen-induced normal lung epithelial cells.

Haskap is notable for its abundant polyphenols, greater antioxidant capacity than other fruits and beneficial health effects (Celli et al. 2014; Khattab et al. 2016; Rupasinghe et al. 2012; Rupasinghe et al. 2015; Takahashi et al. 2014). Haskap berry provides significantly high levels of TPC, flavonoids, and antioxidant capacity, compared to popular berries, such as blueberry, raspberry, strawberry, partridgeberry, blackberry and grapes (Rupasinghe et al., 2012). The Group I carcinogen, NNK, is present in cigarette smoke and contributes to high lung cancer incidences (Canadian Cancer Society 2015; Gulland 2014; Yang et al. 2002). Carcinogenicity of NNK has thoroughly investigated using *in vitro* and *in vivo* experimental models (Hecht & Hoffmann 1988; IARC 2012; Lin et al. 2011). The beas-2b normal human lung epithelial cell is an established model, which has extensively tested with NNK to understand its role in lung carcinogenesis (Boo et al. 2016; Demizu et al. 2008; Hang et al. 2013; Lonardo et al. 2002).

The effect of polyphenol-rich haskap extracts in reducing the NNK- and NNKOAc-induced DNA damage was investigated in BEAS-2B normal lung epithelial

cells. Since C3G is the potent polyphenol found in haskap fruit, followed by Q3G, they were included as reference positive controls. A precursor, NNKOAc, which metabolizes into similar cytosolic carcinogenic metabolites (Figure 3) as of NNK, was also included (Ma et al., 2015). DNA damage was determined using γH2AX, comet, and DNA fragmentation ELISA assays, since compromising genetic stability is an initial step in lung carcinogenesis. The highly sensitive γH2AX assay can detect the direct effect of genotoxic compounds, such as chemical carcinogens (Garcia-Canton et al. 2013). It measures the DSBs in the nuclear genome of cells. The alkali comet assay determines a broad spectrum of DNA damage, such as the level of DNA SSBs, DSBs, and DNA cross-links (Hang et al., 2013).

Polyphenols present in haskap berries were extracted using ethanol and water to obtain lipophilic and hydrophilic compounds, respectively. These solvents allow one to justify the use of haskap extracts in food and pharmaceutical industry owing to their non-toxic nature, and ability to enhance the solubility of polyphenols as they are polar solvents (Dai and Mumper, 2010; Nicoué et al., 2007; Salamon et al., 2015). The extracts primarily consisted of C3G, Q3G and chlorogenic acid. The C3G content was 82 – 85% of total anthocyanin and agreement with the literature findings of 82 – 91% (Khattab et al. 2016) and 76% (Rupasinghe et al. 2015). The TPC and anthocyanin contents were higher in H(A) than the H(E). This may be related to poor oxidative degradation, weak hydrogen bonds and strong hydrophilic nature of anthocyanin in water (Wissam et al., 2012).

It is reported, that the medium constituents, such as inorganic ions, bicarbonate ions, 4-(2-hydroxyethyl)-1-piperazineethanesulfonic acid (HEPES) buffer, foetal bovine

serum (FBS), glucose, and hyperoxia conditions can trigger the oxidative degradation of polyphenols in cell culture medium (Halliwell, 2014; Kern et al., 2007). The consequential oxidized compounds can give false positive or negative data and interfere with research findings. A similar observation was noted in the present study in relation to DMEM and EMEM media. However, as presented in Figure 7, haskap extracts were not oxidized and degraded in BEBM tissue culture medium, which lacks FBS but contains selenium, an antioxidant which may protect haskap extracts from oxidative degradation (Halliwell, 2014). Alternatively, short periods of incubation at lower concentrations (3 h and 50 μg/ml) of haskap extracts could have minimized oxidative degradation.

The lung carcinogenesis model was developed to determine sub-lethal concentrations of NNK and NNKOAc, and non-cytotoxic concentrations of polyphenol-rich haskap extracts. NNK showed a dose- and time-dependent inhibitory effects on BEAS-2B cell viability (Figure 8). The IC_{50} value was not reached at a NNK concentration of up to 200 μM even after 72 h, suggesting that NNK is not very toxic to BEAS-2B cells, though DSBs were observed in the γH2AX assay. Similarly, Chen et al. (2010) noted high levels of DNA damage in BEAS-2B cells incubated with NNK (150 μM for 72 h), without affecting its cell viability. Confirming the observations of Wang et al. (2012), a concentration-dependent increase in DSBs was seen in NNKOAc-treated BEAS-2B cells (Figure 8). At the studied concentrations (0 – 100 μM), NNKOAc did not inhibit BEAS-2B cell viability, even though it significantly induced (82% higher γH2AX foci) DSBs in comparison to NNK. Justifying the findings of the current study, Cloutier et al. (2001) have reported that NNKOAc can damage all four DNA bases guanine > adenine > cytosine > thymine in decreasing order, whereas NNK primarily damages

guanine bases. In addition, the limited activity of CYP450 enzymes in BEAS-2B cells may have led to lower DSBs in NNK-treated cells than following exposure to NNKOAc, which is activated by esterase (Ma et al., 2015; Wang et al., 2012). However, moderately higher levels of CYP1A1, 1A2, and 1B1 were reported with chemical-induction (Garcia-Canton et al. 2013). Conversely, Courcot et al. (2012) noted higher levels of CYP1B1 activity in BEAS-2B cells. Moreover, they also noted the significant expression of esterase (ESD gene). Since the activation of NNKOAc is cytochrome-independent and catalyzed by esterase activity, a higher level of DSBs and DNA fragmentation is expected in NNKOAc-treated cells. Therefore, the significant level of NNKOAc-induced DNA damage and lower level of DNA DSBs in NNK-treated cells are agreeable with the limited expression of CYP450 enzymes in BEAS-2B cells.

Anthocyanin-rich haskap extracts showed dose-dependent loss of BEAS-2B cell viability, but less cytotoxicity at lower concentrations (0 – 50 µg/ml). Similarly, Chen et al., (2006) observed > 90% lung cancer cell viability when cells were treated with cyanidin-rich mulberry fruit extracts (0 - 100 µM for 24 h). Therefore, 50 µg/ml concentration agrees with literature findings and was further confirmed with the γH2AX assay for its non-genotoxicity to BEAS-2B cells.

The data presented in Figures 10 - 14 validate the protective effect of polyphenol-rich haskap extracts against NNK- and NNKOAc-induced DNA damage in BEAS-2B cells. Haskap extracts did not induce DNA damage in epithelial cells. NNKOAc-induced DNA fragmentation was not significant in agarose gel electrophoresis. However, when the ELISA assay was performed, the presence of cytoplasmic DNA fragments (BrdU-labelled DNA fragments as nucleosomes) and early apoptosis in NNKOAc treated

BEAS-2B cells were observed. Concentration-dependent DNA fragmentation at higher concentrations of NNKOAc (0.25 – 25 mM) was reported by Cloutier et al. (2001) in neutral agarose gel electrophoresis. Many studies have demonstrated the efficacy of polyphenols-rich plant extracts and individual polyphenols in attenuating DNA damage induced by various carcinogenic factors. Blueberry (*Vaccinium corymbosum*), which is also abundant in anthocyanins gives a protection against UV radiation. Its anthocyanin-rich extracts (75 µg for 24 h) reduces the UV radiation (4 mJ/cm^2)-induced SSBs and DSBs in HepG2 cells (Liu et al., 2013) via scavenging ROS and restoring oxidative stress. Similarly, a DNA protective effect of 20 µM chlorogenic acid against UVB (30 mJ/cm^2) has recorded in HaCa keratinocytes (Cha et al., 2014). Incubation of A459 cells with quercetin, rutin, and naringin reduces NNK-induced DNA damage (Yeh et al., 2006). In contrast, two flavonols, quercetin, and apigenin have a synergistic effect with doxorubicin- and etoposide-induced DSBs in Jurkat leukemia cells (Mahbub et al., 2015). Combination treatment reduces the glutathione levels in Jurkat cells, resulting oxidative stress in cells leading to DNA damage. Interestingly, they found that this effect depends on the cell type, where polyphenols reduce the cytotoxicity of doxorubicin and etoposide on normal cell lines. Thus, the reported protective effects of haskap extracts in the present study may be related to the higher TPC, in particular, richness in anthocyanin.

The cytoprotective effect of fruit extracts and polyphenols is largely associated with their antioxidant capacity. However, oxidative stress was not significant (Figure 14) in lung epithelial cells treated with either NNK or NNKOAc compared to the medium control, but cells treated with polyphenol-rich haskap extracts, Q3G and C3G showed a significant reduction in the formation of ROS compared to the medium and NNKOAc-

treated cells. Only Q3G could effectively reduce ROS in NNK-treated BEAS-2B cells. Likewise, Demizu et al. (2008) noted a moderately higher level of superoxide radicals in NNK-treated BEAS-2B cells, but ROS, such as hydrogen peroxide, hydroxyl radicals, and nitric oxide. In the present model, ROS concentration was determined using H_2DCFDA, which can detect ROS and RNS, such as hydrogen peroxide, hydroxyl radicals, and nitric oxide. However, the method cannot detect superoxide radicals (Demizu et al., 2008). Therefore, the reason for the lower level of ROS found in this study could be due to the inability to measure superoxide radicals by the method used in this experiment. Enzymatic antioxidants such as SOD, CAT, glutathione peroxidase (GPx) and non-enzymatic antioxidant glutathione (GSH) work together in oxidative stress conditions and balance the ROS in the cells (Rugina et al. 2015). The pre-treatment of cells with quercetin, naringin and rutin markedly reduce NNK-induced ROS formation (Yeh et al., 2006) in A549 Cells. Cyanidin-rich chokeberry extracts increase the activity of SOD, CAT, GPx and GSH in H_2O_2-induced pancreatic β-cells (Rugina et al., 2015). Pre-incubation of primary human colon cells (HT29 clone 19A) with anthocyanin-rich elderberry and *Arnonia melanocarpa* berry extracts (25 µg/ml) for 15 min suppresses H_2O_2-induced DNA oxidative damage (Pool-Zobel et al., 1999). Alternatively, anthocyanins extracted from *Arnonia melanocapa*, significantly reduce the B(a)P-induced superoxide radical formation in human granulocytes (Gąsiorowski et al., 1997). Gasiorowski and colleagues also have found that the anthocyanins are effective against superoxide radicals but their hydroxyl radical scavenging efficiency is moderate. This suggests that the anthocyanins and anthocyanin-rich extracts scavenge superoxide radicals and block the free radical cascade at the beginning.

Since the BEAS-2B cells were pre-incubated with the haskap extracts, the possible preventive mechanism could be via the activation of enzymatic and non-enzymatic antioxidants in BEAS-2B cells. The cytoprotective effect of extracts might be diminished with a longer exposure of NNK (200 μM) for 72 h. Therefore, a time course treatment regime will provide a proper understanding of the effect of haskap extracts against NNK-induced oxidative stress in BEAS-2B cells.

It is useful to review the possible protective mechanism of the haskap extracts against NNK- and NNKOAc-induced DNA damage in BEAS-2B cells. NNK and NNKOAc are activated by CYP450 and esterase enzymes, respectively (Figure 3). However, both compounds form similar electrophilic metabolites, which react with DNA and form DNA adducts (Ma et al., 2015). Haskap extracts were abundant with a diversity of polyphenols, including phenolic acids and flavonoids (Table 1), and many of them have the potential to suppress phase I enzyme activity induced by carcinogens. Hot water infusion of guava, rich in quercetin, actively inhibits CYP1A1 expression in lung epithelial cells (Badal et al., 2012). Grape seed proanthocyanidin suppresses NNK-induced CYP1A1 and 1B1 expression (Song et al. 2010). Quercetin and phloretin inhibit the CYP3A4 in an *ex vivo* experimental model (Kimura et al., 2010). Also, kaempferol (*Gingko biloba*) suppresses CYP1B1 expression and acts as an antagonist for B(a)P-induced AhR in normal MCF10A mammary cells (Rajaraman et al., 2009). Furthermore, caffeic acid and quercetin inhibit the α-hydroxylation capacity of CYP2A6 activity by chelating the benzoic hydroxyl groups with a ferric portion of the CYP2A6 site (Woodward, 2008). However, the effect of polyphenols on the activity of esterase has been barely investigated. Mangiferin, quercetin, catechin and gallic acid-rich mango bark

extract, and its quercetin-rich fraction inhibit the activity of esterase in an *ex vivo* experimental model separately (Chieli et al., 2009).

Phase II enzymes are involved in the detoxification of NNK and NNKOAc and their electrophilic metabolites. Carbonyl reductase involves in converting NNK to NNAL, which later conjugates with glutathione and forms less toxic NNAL-N-glucuronide. Anthocyanin and proanthocyanidin-rich cranberry extracts enhance the activity of carbonyl reductase and UGT in Wistar rat hepatic tissues (Bártíková et al., 2014). UGT and GST catalyze the glucuronidation of NNAL (Crampsie et al., 2011). GST removes electrophilic metabolites by conjugating them with glutathione (Castell et al., 2005). Many polyphenols present in the haskap extracts are effective in activating the UGT and GST *in vitro* and *in vivo*. The anthocyanins, cyanidin, delphinidin, malvidin and peonidin, significantly induce the expression of GST in rat liver clone 9 cells (Shih et al., 2007). Chlorogenic acid enhances the activity of GST in JB6 mouse epidermal cells and HT29 human colorectal adenocarcinoma cells by activating NrF2 translocation (Boettler et al. 2011; Feng et al. 2005). The flavanols EGCG, ECG and EGC, enhance GST expression by 40-60% in B(a)P-induced BEAS-2B cells (Steele et al., 2000). Grape extracts and delphinidin significantly improve the expression of GST activity in MCF-10F breast epithelial cells and suppress the B(a)P-induced DNA adducts formation (Singletary et al., 2007).

Ethanolic and aqueous extracts of haskap berries contain a diversity of polyphenols, including anthocyanins, such as cyanidin-3-*O*-glucoside, delphinidin, peonidin, malvidin; quercetin-like flavonols; flavanols, such as EGCG and catechin, and phenolic acids, such as chlorogenic acid, caffeic acid, and phloretin. The extracts also

showed high antioxidant capacity. The observed protective effect of the haskap extracts against NNK- and NNKOAc-induced DNA damage in BEAS-2B cells could be through two main pathways. Firstly, the polyphenols present in haskap extracts may effectively suppress the phase I and esterase enzymes, resulting in less electrophilic metabolites. The second possible mechanism of polyphenol-rich haskap in DNA damage reduction could be related to their ability to activate phase II detoxification enzymes. The upregulation of GST by haskap extracts could have induced the conjugation of NNK- and NNKOAc-derived electrophilic metabolites, preventing their subsequent reactions with nuclear DNA. Phase II enzymes may have detoxified the NNAL and suppressed the α-hydroxylation of NNK and NNAL. Hence, the pre-treatment of BEAS-2B cells with haskap extract could facilitate detoxification of NNK and NNKOAc, and inactivation of electrophilic metabolites (Figure 15). In addition, the haskap extract-induced oxidative protection in cells could have additionally enhanced the protection against NNK and NNKOAc-induced DNA damage (Figure 15). Thus, the ability of haskap extracts in reducing NNK- and NNOAc-induced DNA damage could be related to the diversity of polyphenols present in each extract and higher antioxidant capacity.

The activation of *KRAS* oncogene and inactivation of *TP53* tumor suppressor and DNA repair genes due to DNA adducts are common in lung cancer patients with smoking history. The accumulation of mutated oncogenes and tumor suppressor genes in lung epithelium leads to uncontrolled cell proliferation, and are prominent in the early stage of lung carcinogenesis. Maintaining genomic stability is a key chemopreventive strategy against smoking-induced lung carcinogenesis.

The present study shows the potential use of polyphenol-rich haskap extracts in the reduction of NNK-induced DNA damage in BEAS-2B lung epithelial cells. NNK is a predominant lung carcinogen present in tobacco smoke. Therefore, polyphenol-rich haskap berry extracts could be a potential dietary and nutraceutical source in suppressing or preventing tobacco-specific lung carcinogenesis. Further investigations using experimental mouse model could be used to understand the chemopreventive potential and mechanism of polyphenol-rich haskap extracts against NNK-induced lung tumorigenesis.

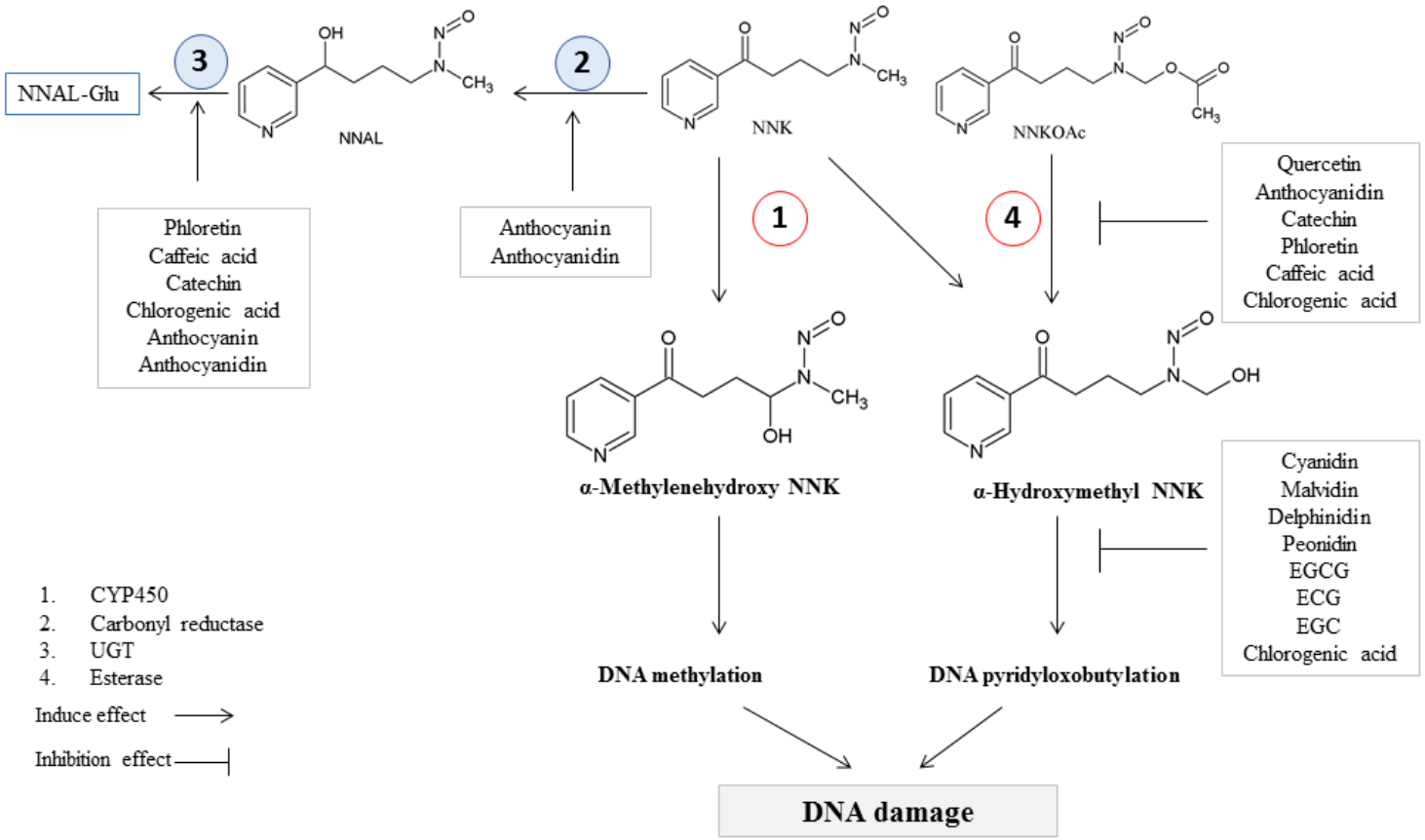

Figure 15 The potential protective mechanism of the polyphenol-rich haskap extracts against NNK- and NNKOAc-induced DNA damage in BEAS-2B cells.

1) The formation of cytochrome- and esterase-induced electrophilic metabolite from NNK and NNKOAc respectively (the activation of procarcinogen). 2) The conversion of NNK to NNAL by carbonyl reductase (the beginning of detoxification cascade). 3) The detoxification resulted in NNAL by glucuronidation and sulfation (formation of the nontoxic excretable compounds). Adapted from Cloutier et al. 2001. (Literature is cited in the text)

References

Acehan, D., Jiang, X., Morgan, D.G., Heuser, J.E., Wang, X., Akey, C.W., and Louis, S. (2002). Three-dimensional structure of the apoptosome: Implications for assembly, procaspase-9 binding, and activation. Mol. Cell *9*, 423–432.

Ajiboye, T.O., Salawu, N.A., Yakubu, M.T., Oladiji, A.T., Akanji, M.A., and Okogun, J.I. (2011). Antioxidant and drug detoxification potentials of *Hibiscus sabdariffa* anthocyanin extract. Drug Chem. Toxicol. *34*, 109–115.

Akopyan, G., and Bonavida, B. (2006). Understanding tobacco smoke carcinogen NNK and lung tumorigenesis (Review). Int. J. Mol. Sci. *29*, 745–752.

Al-Wadei, H., and Schuller, H.M. (2009). Nicotinic receptor-associated modulation of stimulatory and inhibitory neurotransmitters in NNK-induced adenocarcinoma of the lungs and pancreas. J. Pathol. *218*, 437–445.

Appelt, L.C., and Reicks, M.M. (1997). Soy feeding induces phase II enzymes in rat tissues. Nutr. Cancer *28*, 270–275.

ATCC (2016). ATCC product sheet BEAS-2B (ATCC ® CRL- 9609 ™). 1–3.

B'chir, F., Laouani, A., Ksibi, S., Arnaud, M.J., and Saguem, S. (2007). Cigarette filter and the incidence of lung adenocarcinoma among Tunisian population. Lung Cancer *57*, 26–33.

Badal, S., Shields, M., and Delgoda, R. (2012). Cytochrome P450 enzyme inhibitors from nature. In Enzyme Inhibition and Bioapplications, R. Sharma, ed. (Rijeka, Croatia: In Tech), pp. 39–56.

Bailey-Wilson, J.A. (2008). Lung cancer susceptible genes. In Lung Cancer, J.A. Roth, J.D. Cox, and W.K. Hong, eds. (Malden, Massachusetts, USA: Blackwell Publishing), pp. 20–32.

Banin, S., Moyal, L., Shieh, S., Taya, Y., Anderson, C.W., Chessa, L., Smorodinsky, N.I., Prives, C., Reiss, Y., Shiloh, Y., et al. (1998). Enhanced phosphorylation of p53 by ATM in response to DNA damage. Science *281*, 1674–1677.

Bártíková, H., Boušová, I., Jedličková, P., Lněničková, K., Skálová, L., and Szotáková, B. (2014). Effect of standardized cranberry extract on the activity and expression of selected biotransformation enzymes in rat liver and intestine. Molecules *19*, 14948–14960.

BC Cancer Agency (2006). Methotrexate Drug Monograph. BC Cancer Agency Drug Man. 1–16.

Bear, W.L., and Teel, R.W. (2000). Effects of citrus phytochemicals on liver and lung cytochrome P450 activity and on the *in vitro* metabolism of the tobacco-specific nitrosamine NNK. Anticancer Res. *20*, 3323–3329.

Bellik, Y., Boukraâ, L., Alzahrani, H.A., Bakhotmah, B.A., Abdellah, F., Hammoudi, S.M., and Iguer-Ouada, M. (2012). Molecular mechanism underlying anti-inflammatory and anti-allergic activities of phytochemicals: An update. Molecules *18*, 322–353.

Benzie, I.F., and Strain, J.J. (1996). The ferric reducing ability of plasma (FRAP) as a measure of "antioxidant power": The FRAP assay. Anal. Biochem. *239*, 70–76.

Block, K.I., Gyllenhaal, C., Lowe, L., Amedei, A., Amin, A.R., Amin, A., Aquilano, K., Arbiser, J., Arreola, A., Arzumanyan, A., et al. (2015). A broad-spectrum integrative design for cancer prevention and therapy. Semin. Cancer Biol. *35*, S276–S304.

Blois, M. (1958). Antioxidant determinations by the use of a stable free radical. Nature *181*, 1199–1200.

Boettler, U., Volz, N., Pahlke, G., Teller, N., Kotyczka, C., Somoza, V., Stiebitz, H., Bytof, G., Lantz, I., Lang, R., et al. (2011). Coffees rich in chlorogenic acid or N-methylpyridinium induce chemopreventive phase II-enzymes via the Nrf2/ARE pathway *in vitro* and *in vivo*. Mol. Nutr. Food Res. *55*, 798–802.

Boo, H.-J., Min, H.-Y., Jang, H.-J., Yun, H.J., Smith, J.K., Jin, Q., Lee, H.-J., Liu, D., Kweon, H.-S., Behrens, C., et al. (2016). The tobacco-specific carcinogen-operated calcium channel promotes lung tumorigenesis via IGF2 exocytosis in lung epithelial cells. Nat. Commun. *7*, 1–16.

Bravo, L. (1998). Polyphenols: Chemistry, dietary sources, metabolism, and nutritional significance. Nutr. Rev. *56*, 317–333.

Brooks, D.R., Austin, J.H.M., Heelan, R.T., Ginsberg, M.S., Shin, V., Olson, S.H., Muscat, J.E., and Stellman, S.D. (2005). Influence of type of cigarette on peripheral versus central lung cancer. Cancer Epidemiol. Biomarkers Prev. *14*, 576–581.

Büchner, F.L., Bueno-de-Mesquita, H.B., Ros, M.M., Overvad, K., Dahm, C.C., Hansen, L., Tjønneland, A., Clavel-Chapelon, F., Boutron-Ruault, M.C., Touillaud, M., et al. (2010). Variety in fruit and vegetable consumption and the risk of lung cancer in the European prospective investigation into cancer and nutrition. Cancer Epidemiol. Biomarkers Prev. *19*, 2278–2286.

Canadian Cancer Society (2015). Canadian cancer statistics special topic: Predictions of the future burden of cancer in Canada.

Carbone, D. (1992). Smoking and cancer. Am. J. Med. *93*, S13–S17.

Carmella, S.G., Akerkar, S., Hecht, S.S., and Cannella, S.G. (1993). Metabolites of the tobacco-specific nitrosamine 4-(methylnitrosamino)-1-(3-pyridyl)-1-butanone in smokers' urine. Cancer Epidemiol. Biomarkers Prev. *53*, 721–724.

Carmella, S.G., Borukhova, A., Akerkar, S.A., and Hecht, S.S. (1997). Analysis of human urine for pyridine-N-oxide metabolites of 4-(methylnitrosamino)-1-(3-pyridyl)-1-butanone, a tobacco specific lung carcinogen. Cancer Epidemiol. Biomarkers Prev. *6*, 113–120.

Castell, J. V., Donato, M.T., and Gómez-Lechón, M.J. (2005). Metabolism and bioactivation of toxicants in the lung. The *in vitro* cellular approach. Exp. Toxicol. Pathol. *57*, 189–204.

Celli, G.B., Ghanem, A., and Brooks, M.S.L. (2014). Haskap berries (*Lonicera caerulea* L.)-a critical review of antioxidant capacity and health-related studies for potential value-added products. Food Bioprocess Technol. *7*, 1541–1554.

Cha, J.W., Piao, M.J., Kim, K.C., Yao, C.W., Zheng, J., Kim, S.M., Hyun, C.L., Ahn, Y.S., and Hyun, J.W. (2014). The polyphenol chlorogenic acid attenuates UVB-mediated oxidative stress in human HaCaT keratinocytes. Biomol. Ther. (Seoul). *22*, 136–142.

Chang, H.C., Huang, Y.C., and Hung, W.C. (2003). Antiproliferative and chemopreventive effects of adlay seed on lung cancer *in vitro* and *in vivo*. J. Agric. Food Chem. *51*, 3656–3660.

Charpantier, E. (2005). Alpha 7 neuronal nicotinic acetylcholine receptors are negatively regulated by tyrosine phosphorylation and Src-family kinases. J. Neurosci. *25*, 9836–9849.

Chem, F., Ros, W., and Dox, A. (2010). A major green tea component, (-)-epigallocatechin-3-gallate, ameliorates doxorubicin-mediated cardiotoxicity in cardiomyocytes of neonatal rats. J. Agric. Food Chem. *58*, 8977–8982.

Chen, L., Shao, C., Cobos, E., Wang, J.-S., and Gao, W. (2010). 4-(Methylnitro-samino)-1-(3-pyridyl)-1-butanone induces CRM1-dependent P53 nuclear accumulation in human bronchial epithelial cells. Toxicol. Sci. *116*, 206–215.

Chen, P.N., Chu, S.C., Chiou, H.L., Kuo, W.H., Chiang, C.L., and Hsieh, Y.S. (2006). Mulberry anthocyanins, cyanidin 3-rutinoside and cyanidin 3-glucoside, exhibited an inhibitory effect on the migration and invasion of a human lung cancer cell line. Cancer Lett. *235*, 248–259.

Cheynier, V. (2005). Polyphenols in food are more complex then often thought. Am. J. Clin. Nutr. *81*, 223–229.

Chieli, E., Romiti, N., Rodeiro, I., and Garrido, G. (2009). *In vitro* effects of *Mangifera indica* and polyphenols derived on ABCB1/P-glycoprotein activity. Food Chem. Toxicol. *47*, 2703–2710.

Chung, F.L., Wang, M., Rivenson, A., Iatropoulos, M.J., Reinhardt, J.C., Pittman, B., Ho, C.T., and Amin, S.G. (1998). Inhibition of lung carcinogenesis by black tea in fischer rats treated with a tobacco-specific carcinogen: Caffeine as an important constituent. Cancer Res. *58*, 4096–4101.

Clancy, L. (2014). Reducing lung cancer and other tobacco-related cancers in Europe: Smoking cessation is the key. Oncologist *19*, 16–20.

Cloutier, J.F., Drouin, R., Weinfeld, M., O'Connor, T.R., and Castonguay, A. (2001). Characterization and mapping of DNA damage induced by reactive metabolites of 4-(methylnitrosamino)-1-(3-pyridyl)-1-butanone (NNK) at nucleotide resolution in human genomic DNA. J. Mol. Biol. *313*, 539–557.

Cooper, D.N. (2005). The molecular genetics of lung cancer (NewYork: Springer Berlin Heidelberg).

Cos, P., Ying, L., Calomme, M., Hu, J.P., Cimanga, K., Poel, B. Van, Pieters, L., Vlietinck, A.J., and Berghe, D. Vanden (1998). Structure-activity relationship and classification of flavonoids as inhibitors of xanthine oxidase and superoxide scavengers. J. Nat. Prod. *61*, 71–76.

Crampsie, M.A., Jones, N., Das, A., Aliaga, C., Desai, D., Lazarus, P., Shantu, A., and Sharma, A.K. (2011). Phenylbutyl isoselenocyanate modulates phase I and II enzymes and inhibits 4-(methylnitrosamino)-1-(3-pyridyl)-1-butanone induced DNA adducts in mice. Cancer Prev. Res. (Phila). *4*, 1884–1894.

Dai, J., and Mumper, R.J. (2010). Plant phenolics: Extraction, analysis and their antioxidant and anticancer properties. Molecules *15*, 7313–7352.

Dasgupta, P., Rastogi, S., Pillai, S., Ordonez-ercan, D., Morris, M., Haura, E., and Chellappan, S. (2006). Nicotine induces cell proliferation by β-arrestin–mediated activation of Src and Rb –Raf-1 pathways. J. Clin. Invest. *116*, 2208–2217.

Demizu, Y., Sasaki, R., Trachootham, D., Pelicano, H., Colacino, J.A., Liu, J., and Huang, P. (2008). Alterations of cellular redox state during NNK-induced malignant transformation and resistance to radiation. Antioxid. Redox Signal. *10*, 951–961.

Denison, M.S., and Nagy, S.R. (2003). Activation of the aryl hydrocarbon receptor by structurally diverse exogenous and endogenous chemicals. Annu. Rev. Pharmacol. Toxicol. *43*, 309–334.

Denison, M.S., Pandini, A., Nagy, S.R., Baldwin, E.P., and Bonati, L. (2002). Ligand binding and activation of the Ah receptor. Chem Biol.Interact. *141*, 3–24.

Devereux, T.R., Anderson, M.W., and Belinsky, S.A. (1988). Factors regulating activation and DNA alkylation by 4-(N-methyl-N-nitrosamino)-1-(3-pyridyl)-1-butanone and nitrosodimethylamine in rat lung and isolated lung cells, and the relationship to carcinogenicity. Cancer Res. *48*, 4215–4221.

Dhillon, A.S., Hagan, S., Rath, O., and Kolch, W. (2007). MAP kinase signalling pathways in cancer. Oncogene *26*, 3279–3290.

Ding, L., Getz, G., Wheeler, D., and Mardis, E. (2008). Somatic mutations affect key pathways in lung adenocarcinoma. Nature *455*, 1069–1075.

Duthie, S.J. (2007). Berry phytochemicals, genomic stability and cancer: Evidence for chemoprotection at several stages in the carcinogenic process. Mol. Nutr. Food Res. *51*, 665–674.

El-Kenawy, A.E.-M., Elshama, S.S., and Osman, H.-E.H. (2015). Effects of *Physalis peruviana* L. on toxicity and lung cancer induction by nicotine derived nitrosamine ketone in rats. Asian Pac. J. Cancer Prev. *16*, 5863–5868.

Fan, M.-J., Wang, I.-C., Hsiao, Y.-T., Lin, H.-Y., Tang, N.-Y., Hung, T.-C., Quan, C., Lien, J.-C., and Chung, J.-G. (2015). Anthocyanins from black rice (*Oryza sativa* L.) demonstrate antimetastatic properties by reducing MMPs and NF-κB expressions in human oral cancer CAL 27 cells. Nutr. Cancer *67*, 327–338.

Feng, R., Lu, Y., Bowman, L.L., Qian, Y., Castranova, V., and Ding, M. (2005). Inhibition of activator protein-1, NF-kB, and MAPKs and induction of phase 2 detoxifying enzyme activity by chlorogenic acid. J. Biol. Chem. *280*, 27888–27895.

Ferlay, J., Soerjomataram, I., Dikshit, R., Eser, S., Mathers, C., Rebelo, M., Parkin, D.M., Forman, D., and Bray, F. (2015). Cancer incidence and mortality worldwide: Sources, methods and major patterns in GLOBOCAN 2012. Int. J. Cancer *136*, E359–E386.

Fernández-medarde, A., and Santos, E. (2011). Ras in cancer and developmental diseases. Genes and Cancer *2*, 344–358.

Ferrazzano, G.F., Amato, I., Ingenito, A., Zarrelli, A., Pinto, G., and Pollio, A. (2011). Plant polyphenols and their anti-cariogenic properties: A review. Molecules *16*, 1486–1507.

Feskanich, D., Ziegler, R.G., Michaud, D.S., Giovannucci, E.L., Speizer, F.E., Willett, W.C., and Colditz, G. a (2000). Prospective study of fruit and vegetable consumption and risk of lung cancer among men and women. J. Natl. Cancer Inst. *92*, 1812–1823.

Franco, R. Di, Calvanese, M., Murino, P., Manzo, R., Guida, C., Gennaro, D. Di, Anania, C., and Ravo, V. (2012). Skin toxicity from external beam radiation therapy in breast cancer patients: Protective effects of resveratrol, lycopene, Vitamin C and anthocianin (Ixor ®). Radiat. Oncol. *7*, 12.

Fridman, J.S., and Lowe, S.W. (2003). Control of apoptosis by p53. Oncogene *22*, 9030–9040.

Froyen, E.B., Reeves, J.L.R., Mitchell, A.E., and Steinberg, F.M. (2009). Regulation of phase II enzymes by genistein and daidzein in male and female Swiss Webster mice. J. Med. Food *12*, 1227–1237.

Garcia-Canton, C., Anadon, A., and Meredith, C. (2013a). Assessment of the *in vitro* γH2AX assay by High Content Screening as a novel genotoxicity test. Mutat. Res. *757*, 158–166.

Garcia-Canton, C., Minet, E., Anadon, A., and Meredith, C. (2013b). Metabolic characterization of cell systems used in *in vitro* toxicology testing: Lung cell system BEAS-2B as a working example. Toxicol. Vitr. *27*, 1719–1727.

Gąsiorowski, K., Szyba, K., Brokos, B., Kołaczyńska, B., Jankowiak-Włodarczyk, M., and Oszmiański, J. (1997). Antimutagenic activity of anthocyanins isolated from *Aronia melanocarpa* fruits. Cancer Lett. *119*, 37–46.

George, V.C., Dellaire, G., and Rupasinghe, H.P.V. (2017). Plant flavonoids in cancer chemoprevention: Role in genome stability. J. Nutr. Biochem. *45*, 1–14.

Gnagnarella, P., Maisonneuve, P., Bellomi, M., Rampinelli, C., Bertolotti, R., Spaggiari, L., Palli, D., and Veronesi, G. (2013). Red meat, mediterranean diet and lung cancer risk among heavy smokers in the cosmos screening study. Ann. Oncol. *24*, 2606–2611.

Gruia, M.I., Oprea, E., Gruia, I., Negoita, V., and Farcasanu, I.C. (2008). The antioxidant response induced by *Lonicera caerulaea* berry extracts in animals bearing experimental solid tumors. Molecules *13*, 1195–1206.

Gulland, A. (2014). Global cancer prevalence is growing at "alarming pace," says WHO. BMJ *348*, g1338.

Guo, Q., Zhao, B., Li, M., Shen, S., and Wenjuan, X. (1996). Studies on protective mechanisms of four components of green tea polyphenols against lipid peroxidation in synaptosomes. Biochim. Biophys. Acta - Lipids Lipid Metab. *1304*, 210–222.

Halliwell, B. (2014). Cell culture, oxidative stress, and antioxidants: Avoiding pitfalls. Biomed. J. *37*, 99–105.

Hang, B., Sarker, A.H., Havel, C., Saha, S., Hazra, T.K., Schick, S., Jacob, P., Rehan, V.K., Chenna, A., Sharan, D., et al. (2013). Thirdhand smoke causes DNA damage in human cells. Mutagenesis *28*, 381–391.

Health Canada (2011). Carcinogens in tobacco smoke. 1–2.

Hecht, S.S. (1998). Biochemistry, biology, and carcinogenicity of tobacco-specific N-nitrosamines. Chem. Res. Toxicol. *11*, 559–603.

Hecht, S.S. (1999). Tobacco smoke carcinogen and lung cancer. J. Natl. Cancer Inst. *91*, 1194–1210.

Hecht, S.S., and Hoffmann, D. (1988). Tobacco-specific nitrosamines, an important group of carcinogens in tobacco and tobacco smoke. *9*, 875–884.

Hecht, S.S., Trushin, N., Reid-Quinn, C.A., Burak, E.S., Jones, A.B., Southers, J.L., Gombar, C.T., Carmella, S.G., Anderson, L.M., and Rice, J.M. (1993). Metabolism of the tobacco-specific nitrosamine 4-(methylnitrosamino)-1-(3-pyridyl)-1-butanone in the patas monkey: Pharmacokinetics and characterization of glucuronide metabolites. Carcinogenesis *14*, 229–236.

Hecht, S.S., Stepanov, I., and Carmella, S.G. (2016). Exposure and metabolic activation biomarkers of carcinogenic tobacco-specific nitrosamines. Acc. Chem. Res. *49*, 106–114.

Hoffmann, D., and Hecht, S.S. (1985). Nicotine-derived N-nitrosamines and tobacco-related cancer: Current status and future directions. Cancer Res. *45*, 935–944.

Hoffmann, D., Brunnemann, K.D., Prokopczyk, B., and Djordjevic, M. V (1994). Tobacco-specific N-nitrosamines and *Areca*-derived N-nitrosamines: Chemistry, biochemistry, carcinogenicity, and relevance to humans. J. Toxicol. Environ. Health *41*, 1–52.

Hoffmann, D., Hoffmann, I., and El-Bayoumy, K. (2001). The less harmful cigarette: A controversial issue. A tribute to Ernst L. Wynder. Chem. Res. Toxicol. *14*, 767–790.

Hu, Y., Cao, J.J., Liu, P., Guo, D.H., Wang, Y.P., and Yin, J. (2011). Protective role of tea polyphenols in combination against radiation-induced haematopoietic and biochemical alterations in mice. Phyther. Res. *1769*, 1761–1769.

Hummer, K. (2006). Blue honeysuckle: A new berry crop for North America. J. Am. Pomol. Soc. *60*, 3–8.

IARC (2012). N'-Nitrosonornicotine and 4-(methylnitrosamino)-1-(3-pyridyl)-1-butanone. In IARC Monographs on the Evaluation of Carcinogenic Risks to Humans, pp. 323–335.

Improgo, M.R., Soll, L.G., Tapper, A.R., and Gardner, P.D. (2013). Nicotinic acetylcholine receptors mediate lung cancer growth. Front. Physiol. *4*, 1–6.

Jancova, P., Anzenbacher, P., and Anzenbacherova, E. (2010). Phase II drug metabolizing enzymes. Biomed. Pap. *154*, 103–116.

Jin, H., Chen, J.X., Wang, H., Lu, G., Liu, A., Li, G., Tu, S., Lin, Y., and Yang, C.S. (2015). NNK-induced DNA methyltransferase 1 in lung tumorigenesis in A/J mice and inhibitory effects of (-)-epigallocatechin-3-gallate. Nutr. Cancer *67*, 167–176.

Jin, X.H., Ohgami, K., Shiratori, K., Suzuki, Y., Koyama, Y., Yoshida, K., Ilieva, I., Tanaka, T., Onoe, K., and Ohno, S. (2006a). Effects of blue honeysuckle (*Lonicera caerulea* L.) extract on lipopolysaccharide-induced inflammation *in vitro* and *in vivo*. Exp. Eye Res. *82*, 860–867.

Jin, Z., Gao, F., Flagg, T., and Deng, X. (2004). Tobacco-specific nitrosamine 4-(methylnitrosamino)-1-(3-pyridyl)-1-butanone promotes functional cooperation of Bcl2 and c-Myc through phosphorylation in regulating cell survival and proliferation. J. Biol. Chem. *279*, 40209–40219.

Jin, Z., May, W.S., Gao, F., Flagg, T., and Deng, X. (2006b). Bcl2 suppresses DNA repair by enhancing c-Myc transcriptional activity. J. Biol. Chem. *281*, 14446–14456.

Kaczmarska, E., Gawronski, J., Dyduch-Sieminska, M., Najda, A., Marecki, W., and Zebrowska, J. (2015). Genetic diversity and chemical characterization of selected Polish and Russian cultivars and clones of blue honeysuckle (*Lonicera caerulea*). Turkish J. Agric. For. *39*, 394–402.

Kawabuchi, B., Moriyama, S., Hironaka, M., Fujii, T., Koike, M., Moriyama, H., Nishimura, Y., Mizuno, S., and Fukayama, M. (1999). p16 Inactivation in small-sized lung adenocarcinoma: Its association with poor prognosis. Int. J. Cancer *84*, 49–53.

Keohavong, P., Kahkonen, B., Kinchington, E., Yin, J., Jin, J., Liu, X., Siegfried, J.M., and Di, Y.P. (2011). K-ras mutations in lung tumors from NNK-treated mice with lipopolysaccharide-elicited lung inflammation. Anticancer Res. *31*, 2877–2882.

Kern, M., Fridrich, D., Reichert, J., Skrbek, S., Nussher, A., Hofem, S., Vatter, S., Pahlke, G., Rüfer, C., and Marke, D. (2007). Limited stability in cell culture medium and hydrogen peroxide formation affect the growth inhibitory properties of delphinidin and its degradation product gallic acid. Mol. Nutr. Food Res. *51*, 1163–1172.

Khan, N., Afaq, F., Khusro, F.H., Adhami, V.M., Suh, Y., and Mukhtar, H. (2012). Dual inhibition of PI3/AKT and mTOR signaling in human non-small cell lung cancer cells by a dietary flavonoid fisetin. Int. J. Cancer *130*, 1695–1705.

Khan, N., Syed, D.N., Ahmad, N., and Mukhtar, H. (2013). Fisetin: A dietary antioxidant for health promotion. Antioxidants & Redox Signal. *19*, 151–162.

Khattab, R., Celli, G.B., Ghanem, A., and Brooks, M.S.-L. (2015). Effect of frozen storage on polyphenol content and antioxidant activity of haskap berries (*Lonicera caerulea* L.). J. Berry Res. *5*, 231–242.

Khattab, R., Brooks, M.S.-L., and Ghanem, A. (2016). Phenolic analyses of haskap berries (*Lonicera caerulea* L.): Spectrophotometry versus high performance liquid chromatography. Int. J. Food Prop. *19*, 1708–1725.

Kimura, Y., Ito, H., Ohnishi, R., and Hatano, T. (2010). Inhibitory effects of polyphenols on human cytochrome P450 3A4 and 2C9 activity. Food Chem. Toxicol. *48*, 429–435.

Knaul, F.M., Arreola-Ornelas, H., and Guerrero, R. (2012). Investing in cancer care and control. In A Report of the Global Task Force on Expanded Access to Cancer Care and Control. In Developing Contries, F.M. Knaul, J.R. Gralow, R. Atun, and B. A, eds. (Boston, MA, USA: Harvard Global Equity Initiative, Secretatiat), pp. 63–70.

Kohno, H., Taima, M., Sumida, T., Azuma, Y., Ogawa, H., and Tanaka, T. (2001). Inhibitory effect of mandarin juice rich in beta-cryptoxanthin and hesperidin on 4-(methylnitrosamino)-1-(3-pyridyl)-1-butanone-induced pulmonary tumorigenesis in mice. Cancer Lett. *174*, 141–150.

Landau, J.M., Wang, Z.Y., Yang, G.Y., Ding, W., and Yang, C.S. (1998). Inhibition of spontaneous formation of lung tumors and rhabdomyosarcomas in A/J mice by black and green tea. Carcinogenesis *19*, 501–507.

Lane, D.P. (1992). Cancer. p53, guardian of the genome. Nature *358*, 15–16.

Lecumberri, E., Marc, Y., Miralbell, R., and Pichard, C. (2013). Green tea polyphenol epigallocatechin-3-gallate (EGCG) as adjuvant in cancer therapy. Clin. Nutr. *32*, 894–903.

Lees-Miller, S.P., Chen, Y.R., and Anderson, C.W. (1990). Human cells contain a DNA-activated protein kinase that phosphorylates simian virus 40 T antigen, mouse p53, and the human Ku autoantigen. Mol. Cell. Biol. *10*, 6472–6481.

Lefol, E.B. (2007). Haskap market development-The Japanese opportunity-feasibility study August 2007.

Li, H., Wu, S., Shi, N., Lin, W., You, J., and Zhou, W. (2011). NF-E2-related factor 2 activation in PC12 cells: Its protective role in manganese-induced damage. Arch. Toxicol. *85*, 901–910.

Lin, P., Chen, R.J., Chang, L.W., and Wang, Y.J. (2011). Epigenetic effects and molecular mechanisms of tumorigenesis induced by cigarette smoke: An overview. J. Oncol. *2011*.

Linnoila, R.I., and Aisner, S.C. (1995). Pathology of lung cancer: An exercise in classification. In Lung Cancer, B.E. Johnson, and D.H. Johnson, eds. (NewYork: Wiley-Liss Inc), pp. 73–95.

Linseisen, J., Rohrmann, S., Miller, A.B., Bueno-De-Mesquita, H.B., Buchner, F.L., Vineis, P., Agudo, A., Gram, I.T., Janson, L., Krogh, V., et al. (2007). Fruit and vegetable consumption and lung cancer risk: Updated information from the European prospective investigation into cancer and nutrition (EPIC). Int. J. Cancer *121*, 1103–1114.

Liu, L., and Castonguay, A. (1991). Inhibition of the metabolism and genotoxicity of 4-(methylnitrosamino)-1-(3-pyridyl)-1-butanone (nnk) in rat hepatocytes by (+)-catechin. Carcinogenesis *12*, 1203–1208.

Liu, W., Lu, X., He, G., Gao, X., Li, M., Wu, J., Li, Z., Wu, J., Wang, J., and Luo, C. (2013). Cytosolic protection against ultraviolet induced DNA damage by blueberry anthocyanins and anthocyanidins in hepatocarcinoma HepG2 cells. Biotechnol. Lett. *35*, 491–498.

Loechler, E.L., Green, C.L., and Essigmann, J.M. (1984). *In vivo* mutagenesis by O^6-methylguanine built into a unique site in a viral genome. Proc. Natl. Acad. Sci. U. S. A. *81*, 6271–6275.

Lu, G., Liao, J., Yang, G., Reuhl, K.R., Hao, X., and Yang, C.S. (2006). Inhibition of adenoma progression to adenocarcinoma in a 4-(methylnitrosamino)-1-(3-pyridyl)-1-butanone-induced lung tumorigenesis model in A/J mice by tea polyphenols and caffeine. Cancer Res. *66*, 11494–11501.

Ma, B., Villalta, P.W., Zarth, A.T., Kotandeniya, D., Upadhyaya, P., Stepanov, I., and Hecht, S.S. (2015). Comprehensive high-resolution mass spectrometric analysis of DNA phosphate adducts formed by the tobacco-specific lung carcinogen 4-(methylnitrosamino)-1-(3-pyridyl)-1-butanone. Chem. Res. Toxicol. *28*, 2151–2159.

MacDonald, V. (2009). Chemotherapy: Managing side effects and safe handling. Can. Vet. J. *50*, 665–668.

Maeda, R., Yoshida, J., Hishida, T., Aokage, K., Nishimura, M., Nishiwaki, Y., and Nagai, K. (2010). Late recurrence of non-small cell lung cancer more than 5 years after complete resection: Incidence and clinical implications in patient follow-up. Chest *138*, 145–150.

Mahbub, A., Le Maitre, C., Haywood-Small, S., Cross, N., and Jordan-Mahy, N. (2015). Polyphenols act synergistically with doxorubicin and etoposide in leukaemia cell lines. Cell Death Discov. *1*, 15043.

Le Marchand, L., Murphy, S.P., Hankin, J.H., Wilkens, L.R., and Kolonel, L.N. (2000). Intake of flavonoids and lung cancer. J. Natl. Cancer Inst. *92*, 154–160.

Markakis, P.C., Jurd, L., Nayak, C. a., Rastogi, N.K., Ferreira, D.S., Faria, A.F., Grosso, C.R.F., Mercadante, A.Z., Shiga, H., Yoshii, H., et al. (2015). Health benefits of anthocyanins and their encapsulation for potential use in food systems: A review. Dry. Technol. *28*, 1385–1395.

Mascaux, C., Iannino, N., Martin, B., Paesmans, M., Berghmans, T., Dusart, M., Haller, A., Lothaire, P., Meert, A.-P., Noel, S., et al. (2005). The role of RAS oncogene in survival of patients with lung cancer: A systematic review of the literature with meta-analysis. Br. J. Cancer *92*, 131–139.

Maser, E., Richter, E., and Friebertshäuser, J. (1996). The identification of 11 beta-hydroxysteroid dehydrogenase as carbonyl reductase of the tobacco-specific nitrosamine 4-(methylnitrosamino)-1-(3-pyridyl)-1-butanone. Eur. J. Biochem. *238*, 484–489.

Mcilwain, D.R., Berger, T., and Mak, T.W. (2013). Caspase functions in cell death and disease. In Cold Spring Harbor Prospectives in Biology, H. Eric, D.R. Baehrecke, S.K. Green, and G.S. Salvesen, eds. (Dusseldorf, Germany: Colds Spring Harbor Laboratory Press), pp. 1–28.

Meloche, S., and Pouysse, J. (2007). The ERK1/2 mitogen-activated protein kinase pathway as a master regulator of the G1- to S-phase transition. Oncogene *26*, 3227–3239.

Morgan, E. (2007). Cancer control: Knowledge into action: WHO guide for effective programmes; module 2.

Morse, M.A., Eklind, K.I., Toussaint, M., Amin, S.G., and Chung, F. (1990). Characterization of a glucuronide metabolite of 4-(methyl-nitrosamino)-l-(3-pyridyl)-1-butanone (NNK) and its dose-dependent excretion in the urine of mice and rats. Carcinogenesis *11*, 1819–1823.

Murakami, A., Ashida, H., and Terao, J. (2008). Multitargeted cancer prevention by quercetin. Cancer Lett. *269*, 315–325.

Nakano, K., Bálint, E., Ashcroft, M., and Vousden, K.H. (2000). A ribonucleotide reductase gene is a transcriptional target of p53 and p73. Oncogene *19*, 4283–4289.

National Cancer Institute (2012). Support for people with cancer-Radiation therapy and you (National Institutes of Health).

National Center for Biotechnology Information. PubChem Compound Database; CID=47289. *https://pubchem.ncbi.nlm.nih.gov/compound (Accessed Nov 17.2016)*

Nicoué, E.É., Savard, S., and Belkacemi, K. (2007). Anthocyanins in wild blueberries of Quebec: Extraction and identification. J. Agric. Food Chem. *55*, 5626–5635.

O'Kennedy, N., Crosbie, L., Van Lieshout, M., Broom, J.I., Webb, D.J., and Duttaroy, A.K. (2006). Effects of antiplatelet components of tomato extract on platelet function *in vitro* and *ex vivo*: A time-course cannulation study in healthy humans. Am. J. Clin. Nutr. *84*, 570–579.

Ochmian, I., Skupień;, K., Grajkowski, J., Smolik, M., and Ostrowska, K. (2012). Chemical composition and physical characteristics of fruits of two cultivars of blue honeysuckle (*Lonicera caerulea* L.) in relation to their degree of maturity and harvest date. Not. Bot. Horti Agrobot. Cluj-Napoca *40*, 155–162.

Ohtani, N., Yamakoshi, K., Takahashi, A., and Hara, E. (2004). The p16INK4a-RB pathway: Molecular link between cellular senescence and tumor suppression. J. Med. Investig. *Vol. 51 (2*, 146–153.

Pan, W., Ikeda, K., Takebe, M., and Yamori, Y. (2001). Genistein, daidzein and glycitein inhibit growth and DNA synthesis of aortic smooth muscle cells from stroke-prone spontaneously hypertensive rats. J Nutr *131*, 1154–1158.

Pandey, K.B., and Rizvi, S.I. (2009). Plant polyphenols as dietary antioxidants in human health and disease. Oxid. Med. Cell. Longev. *2*, 270–278.

Parr, A.J., and Bolwell, G.P. (2000). Phenols in the plant and in man. The potential for possible nutritional enhancement of the diet by modifying the phenols content or profile. J. Sci. Food Agric. *80*, 985–1012.

Patel, D., Shukla, S., and Gupta, S. (2007). Apigenin and cancer chemoprevention: Progress, potential and promise (Review). Int. J. Oncol. *30*, 233–245.

Patten, C.J., Smith, T.J., Murphy, S.E., Wang, M.H., Lee, J., Tynes, R.E., Koch, P., and Yang, C.S. (1996). Kinetic analysis of the activation of 4-(methylnitrosamino)-1-(3-pyridyl)-1-butanone by heterologously expressed human P450 enzymes and the effect of P450-specific chemical inhibitors on this activation in human liver microsomes. Arch. Biochem. Biophys. *333*, 127–138.

Pegg, A.E. (2000). Repair of O^6-alkylguanine by alkyltransferases. Mutat. Res. *462*, 83–100.

Peterson, L.A. (2010). Formation, repair, and genotoxic properties of bulky DNA adducts formed from tobacco-specific nitrosamines. J. Nucleic Acids *2010*, 284935 (1-11).

Peterson, L.A., Mathew, R., and Hecht, S.S. (1991). Quantitation of microsomal alpha-hydroxylation of the tobacco-specific nitrosamine, 4-(methylnitrosamino)-1-(3-pyridyl)-1-butanone. Cancer Res. *51*, 5495–5500.

Pool-Zobel, B.L., Bub, A., Schröder, N., and Rechkemmer, G. (1999). Anthocyanins are potent antioxidants in model systems but do not reduce endogenous oxidative DNA damage in human colon cells. Eur. J. Nutr. *38*, 227–234.

Proulx, L.I., Gaudreault, M., Turmel, V., Augusto, L.A., Castonguay, A., and Bissonnette, É.Y. (2005). 4-(Methylnitrosamino)-1-(3-pyridyl)-1-butanone, a component of tobacco smoke, modulates mediator release from human bronchial and alveolar epithelial cells. Clin. Exp. Immunol. *140*, 46–53.

Pulling, L.C., Divine, K.K., Klinge, D.M., Gilliland, F.D., Kang, T., Schwartz, A.G., Bocklage, T.J., and Belinsky, S.A. (2003). Promoter hypermethylation of the O^6-methylguanine-DNA methyltransferase gene: More common in lung adenocarcinomas from never-smokers than smokers and associated with tumor progression. Cancer Res. *63*, 4842–4848.

Rajaraman, G., Yang, G., Chen, J., and Chang, T.K.H. (2009). Modulation of CYP1B1 and CYP1A1 gene expression and activation of aryl hydrocarbon receptor by *Ginkgo biloba* extract in MCF-10A human mammary epithelial cells. Can. J. Physiol. Pharmacol. *87*, 674–683.

Rayess, H., Wang, M.B., and Srivatsan, E.S. (2012). Cellular senescence and tumor suppressor gene p16. Int. J. Cancer *130*, 1715–1725.

Revel, A., Raanani, H., Younglai, E., Xu, J., Rogers, I., Han, R., Savouret, J.F., and Casper, R.F. (2003). Resveratrol, a natural aryl hydrocarbon receptor antagonist, protects lung from DNA damage and apoptosis caused by benzo[a]pyrene. J. Appl. Toxicol. *23*, 255–261.

Rugina, D., Diaconeasa, Z., Coman, C., Bunea, A., Socaciu, C., and Pintea, A. (2015). Chokeberry anthocyanin extract as pancreatic β-cell protectors in two models of induced oxidative stress. Oxid. Med. Cell. Longev. *2015*, 1–10.

Rupasinghe, H.P. V, Yu, L.J., Bhullar, K.S., and Bors, B. (2012). Haskap: A new berry crop with high antioxidant capacity. Can. J. Plant Sci. *3*, 1311–1317.

Rupasinghe, H.P.V., Nair, S.V.G., and Robinson, R.A. (2014). Chemopreventive properties of fruit phenolic compounds and their possible mode of actions. In Studies in Natural Products Chemistry, *42*, 229–266.

Rupasinghe, H.P.V., Boehm, M.M.A., Sekhon-Loodu, S., Parmar, I., Bors, B., Jamieson, A.R., Breitenbach, M., and Eckl, P. (2015). Anti-inflammatory activity of haskap cultivars is polyphenols-dpendent. Biomolecules *5*, 1079–1098.

Rupasinghe, V.H.P., Embree, C., Forsline, P.L., and Huber, G.M. (2010). Red-fleshed apple as a source for functional beverages. Can. J. Plant Sci. 95–100.

Salamon, I., Mariychuk, R., and Grulova, D. (2015). Optimal extraction of pure anthocyanins from fruits of *Sambucus nigra*. Acta Hortic. *1061*, 73–78.

Schuller, H.M., Plummer III, H.K., and Jull, B.A. (2003). Receptor-mediated effects of nicotine and its nitrosated derivative NNK on pulmonary neuroendocrine cells. Anat. Rec. Part A *270A*, 51–58.

Shames, D. V., Sato, M., and Minna, J.D. (2008). The molecular genetics of lung cancer. In Lung Cancer, J.A. Roth, J.D. Cox, and W.K. Hong, eds. (Malden, Massachusetts, USA: Blackwell Publishing), pp. 61–83.

Sheets, W.C., Mugnier, E., Barnabe, A., Marks, T.J., and Poeppelmeier, K.R. (2006). Methylating agents and DNA repair responses: Methylated bases and sources of strand breaks. Chem. Res. Toxicol. *19*, 7–20.

Shih, P., Yeh, C., and Yen, G. (2007). Anthocyanins induce the activation of phase II enzymes through the antioxidant response element pathway against oxidative stress-induced apoptosis. J. Agric. Food Chem. *2*, 9427–9435.

Shih, Y.L., Liu, H.C., Chen, C.S., Hsu, C.H., Pan, M.H., Chang, H.W., Chang, C.H., Chen, F.C., Ho, C.T., Yang, Y.I.Y., et al. (2010). Combination treatment with luteolin and quercetin enhances antiproliferative effects in nicotine-treated MDA-MB-231 cells by down-regulating nicotinic acetylcholine receptors. J. Agric. Food Chem. *58*, 235–241.

Shukla, Y., and Taneja, P. (2002). Anticarcinogenic effect of black tea on pulmonary tumors in Swiss albino mice. Cancer Lett. *176*, 137–141.

Singletary, K.W., Jung, K.J., and Giusti, M. (2007). Anthocyanin-rich grape extract blocks breast cell DNA damage. J. Med. Food *10*, 244–251.

Skupień, K., Ochmian, I., and Grajkowski, J. (2009). Influence of ripening time on fruit chemical composition of two blue honeysuckle cultigens. J. Fruit Ornam. Plant Res. *17*, 101–111.

Song, X., Siriwardhana, N., Rathore, K., Lin, G., and Wang, H.R. (2010). Grape seed proanthocyanidin suppression of breast cell carcinogenesis induced by chronic exposure to combined 4-(methylnitrosamino)-1-(3-pyridyl)-1-butanone and benzo[a]pyrene. Mol. Carcinog. *49*, 450–463.

Soria, J., Kim, E.S., Fayette, J., Lantuejoul, S., Deutsch, E., and Hong, W.K. (2003). Chemoprevention of lung cancer. Lancet Oncol. *4*, 659–669.

Steele, V.E., Kelloff, G.J., Balentine, D., Boone, C.W., Mehta, R., Bagheri, D., Sigman, C.C., Zhu, S., and Sharma, S. (2000). Comparative chemopreventive mechanisms of green tea, black tea and selected polyphenol extracts measured by *in vitro* bioassays. Carcinogenesis *21*, 63–67.

Suwannakul, N., Punvittayagul, C., Jarukamjorn, K., and Wongpoomchai, R. (2015). Purple rice bran extract attenuates the aflatoxin B1-induced initiation stage of hepatocarcinogenesis by alteration of xenobiotic metabolizing enzymes. Asian Pacific J. Cancer Prev. *16*, 3371–3376.

Svobodova, A., Rambouskova, J., Walterova, D., and Vostalova, J. (2008). Protective effects of phenolic fraction of blue honeysuckle fruits against UVA-induced damage to human keratinocytes. Arch Dermatol Res *300*, 225–233.

Takahashi, A., Okazaki, Y., Nakamoto, A., Watanabe, S., Sakaguchi, H., Tagashira, Y., Kagii, A., Nakagawara, S., Higuchi, O., Suzuki, T., et al. (2014). Dietary anthocyanin-rich haskap phytochemicals inhibit postprandial hyperlipidemia and hyperglycemia in rats. J. Oleo Sci. J. Oleo Sci *63*, 201–209.

Tam, K.W., Zhang, W., Soh, J., Stastny, V., Chen, M., Sun, H., Thu, K., Rios, J.J., Yang, C., Marconett, C.N., et al. (2013). CDKN2A/p16 inactivation mechanisms and their relationship to smoke exposure and molecular features in non-small-cell lung cancer. J. Thorac. Oncol. *8*, 1378–1388.

Tan, A.C., Konczak, I., Sze, D.M.-Y., and Ramzan, I. (2011). Molecular pathways for cancer chemoprevention by dietary phytochemicals. Nutr. Cancer *63*, 495–505.

Thompson, M.M. (2006). Introducing haskap, Japanese blue honeysuckle. J. Am. Pomol. Soc. *60*, 164–168.

Travis, W.D., Brambilla, E., Müller-Hermelink, H.K., and Harris, C.C. (2004). Pathology and genetics of tumours of the lung. Bull. World Health Organ. *50*, 9–19.

Travis, W.D., Brambilla, E., Nicholson, A.G., Yatabe, Y., Austin, J.H.M., Beasley, M.B., Chirieac, L.R., Dacic, S., Duhig, E., Flieder, D.B., et al. (2015). The 2015 World Health Organization classification of lung tumors: Impact of genetic, clinical and radiologic advances since the 2004 classification. J. Thorac. Oncol. *10*, 1243–1260.

Tsao, R. (2010). Chemistry and biochemistry of dietary polyphenols. Nutrients *2*, 1231–1246.

Tu, S.H., Ku, C.Y., Ho, C.T., Chen, C.S., Huang, C.S., Lee, C.H., Chen, L.C., Pan, M.H., Chang, H.W., Chang, C.H., et al. (2011). Tea polyphenol (-)-epigallocatechin-3-gallate inhibits nicotine- and estrogen-induced alpha9-nicotinic acetylcholine receptor upregulation in human breast cancer cells. Mol. Nutr. Food Res. *55*, 455–466.

Union for International Cancer Control (2014). The economics of cancer prevention and control. Data digest. 1–8.

Uramoto, H., and Tanaka, F. (2014). Recurrence after surgery in patients with NSCLC. Transl Lung Cancer Res *3*, 242–249.

Valentão, P., Fernandes, E., Carvalho, F., Andrade, P.B., Seabra, R.M., and Bastos, M.L. (2003). Hydroxyl radical and hypochlorous acid scavenging activity of small centaury (*Centaurium erythraea*) infusion. A comparative study with green tea (*Camellia sinensis*). Phytomedicine *10*, 517–522.

Vauzour, D., Rodriguez-Mateos, A., Corona, G., Oruna-Concha, M.J., and Spencer, J.P.E. (2010). Polyphenols and human health: Prevention of disease and mechanisms of action. Nutrients *2*, 1106–1131.

Vavilov, N.I., and Plekhanova, M.N. (2000). Blue honeysuckle (*Lonicera caerulea* L.) - A new commercial berry crop for temperate climate: Genetic resources and breeding. In Proc. EUCARPIA Symp. on Fruit Breed. and Genetics, M.F.& C.F. M. Geibel, ed. (Acta Hort. 538, ISHS), pp. 159–163.

Wang, X.Y., Jensen-Taubman, S.M., Keefe, K.M., Yang, D., and Linnoila, R.I. (2012). Achaete-scute complex homolog-1 promotes DNA repair in the lung carcinogenesis through matrix metalloproteinase-7 and $O^{(6)}$-methylguanine-DNA methyltransferase. PLoS One *7*, E52832.

Weitber, A.B., and Corvese, D. (1999). The effect of epigallocatechin galleate and sarcophytol A on DNA strand breakage induced by tobacco-specific nitrosamines and stimulated human phagocytes. J. Exp. Clin. Cancer Res. *18*, 433–437.

Wen, J., Fu, J., Zhang, W., and Guo, M. (2011). Genetic and epigenetic changes in lung carcinoma and their clinical implications. Mod. Pathol. *24*, 932–943.

West, K. A, Brognard, J., Clark, A.S., Linnoila, I.R., Yang, X., Swain, S.M., Harris, C., Belinsky, S., and Dennis, P. A (2003). Rapid Akt activation by nicotine and a tobacco carcinogen modulates the phenotype of normal human airway epithelial cells. J. Clin. Invest. *111*, 81–90.

WHO (2016). WHO | Cancer (World Health Organization).

Wiener, D., Doerge, D.R., Fang, J., Upadhyaya, P., and Lazarus, P. (2004). Characterization of N- glucuronidation of the lung carcinogen 4-(methylnitrosamino)-1-(3-pyridyl)-1-butanol (NNAL) in human liver: Importance of UDP-glucuronosyltransferase 1A4. Drug Metab. Dispos. *32*, 72–79.

Wissam, Z., Ghada, B., Wassim, A., and Warid, K. (2012). Effective extraction of polyphenols and proanthocyanidins from pomegranate's peel. Int. J. Pharm. Pharm. Sci. *4*, 675–682.

Woodward, G.M. (2008). The potential effect of excessive coffee consumption on nicotine metabolism: CYP2A6 inhibition by caffeic acid and quercetin. Biosci. Horizons *1*, 98–103.

Wu, Q., Nadesalingam, J., Moodley, S., Bai, X., and Liu, M. (2015). XB130 translocation to microfilamentous structures mediates NNK-induced migration of human bronchial epithelial cells. Oncotarget *6*, 18050–18065.

Wu, X., Yang, H., Lin, J., and Spitz, M.R. (2008). Lung cancer susceptibility and risk assessment models. In Lung Can, J.A. Roth, C.J. D, and W.K. Hong, eds. (New Jersey, USA: Blackwell Publishing), pp. 33–60.

Xu, Y., Ho, C., Amin, S.G., Han, C., and Chung, F. (1992). Inhibition of tobacco-specific nitrosamine-induced lung tumorigenesis. Cancer Res. *52*, 3875–3879.

Xue, J., Yang, S., and Seng, S. (2014). Mechanisms of cancer induction by tobacco-specific NNK and NNN. Cancers (Basel). *6*, 1138–1156.

Yalcin, E., and Monte, S. de la (2016). Tobacco nitrosamines as culprits in disease: Mechanisms reviewed. J. Physiol. Biochem. *72*, 107–120.

Yang, G.Y., Liu, Z., Seril, D.N., Liao, J., Ding, W., Kim, S., Bondoc, F., and Yang, C.S. (1997). Black tea constituents, theaflavins, inhibit 4-(methylnitrosamino)-1-(3-pyridyl)-1-butanone (NNK)-induced lung tumorigenesis in A/J mice. Carcinogenesis *18*, 2361–2365.

Yang, P., Cerhan, J.R., Vierkant, R.A., Olson, J.E., Vachon, C.M., Limburg, P.J., Parker, A.S., Anderson, K.E., and Sellers, T.A. (2002). Adenocarcinoma of the lung is strongly associated with cigarette smoking: Further evidence from a prospective study of women. Am. J. Epidemiol. *156*, 1114–1122.

Yeh, S.L., Wang, W.Y., Huang, C.S., and Hu, M.L. (2006). Flavonoids suppresses the enhancing effect of beta-carotene on DNA damage induced by 4-(methylnitrosamino)-1-(3-pyridyl)-1-butanone (NNK) in A549 cells. Chem. Biol. Interact. *160*, 175–182.

Zafarullah, M., Li, W.Q., Sylvester, J., and Ahmad, M. (2003). Molecular mechanisms of N-acetylcysteine actions. Cell. Mol. Life Sci. *60*, 6–20.

Zannini, L., Delia, D., and Buscemi, G. (2014). CHK2 kinase in the DNA damage response and beyond. J. Mol. Cell Biol. *6*, 442–457.

Zhai, X., Lin, M., Zhang, F., Hu, Y., Xu, X., Li, Y., Liu, K., Ma, X., Tian, X., and Yao, J. (2013). Dietary flavonoid genistein induces Nrf2 and phase II detoxification gene expression via ERKs and PKC pathways and protects against oxidative stress in Caco-2 cells. Mol. Nutr. Food Res. *57*, 249–259.

Zhan, J., Zhu, X., Guo, Y., Wang, Y., Wang, Y., Qiang, G., Niu, M., Hu, J., Du, J., Li, Z., et al. (2012). Opposite Role of Kindlin-1 and Kindlin-2 in Lung Cancers. PLoS One *7*.

Zhan, Q., Carrier, F., and Fornace, a J. (1993). Induction of cellular p53 activity by DNA-damaging agents and growth arrest. Mol. Cell. Biol. *13*, 4242–4250.

Zhan, Q., Antinore, M.J., Wang, X.W., Carrier, F., Smith, M.L., Harris, C.C., and Fornace, a J. (1999). Association with Cdc2 and inhibition of Cdc2/Cyclin B1 kinase activity by the p53-regulated protein Gadd45. Oncogene *18*, 2892–2900.

Zhang, G., Wang, Y., Zhang, Y., Wan, X., Li, J., Wang, F., Liu, K., Liu, Q., Yang, C., Yu, P., et al. (2012). Anti-cancer activities of tea epigallocatechin-3-gallate in breast cancer patients under radiotherapy. Curr. Mol. Med. *12*, 163–176.

Zhang, H., Jiang, H., Hu, X., and Jia, Z. (2015). Aidi injection combined with radiation in the treatment of non-small cell lung cancer: A meta-analysis evaluation the efficacy and side effects. J. Cancer Res. Ther. *11*, 118–121.

Zhu, S., Wu, J., Du, G., Zhou, J., and Chen, J. (2014). Efficient synthesis of eriodictyol from L-tyrosine in Escherichia coli. Appl. Environ. Microbiol. *80*, 3072–3080.

Appendix 1: Viability of BEAS-2B cells after 24 h incubation with haskap ethanol extract

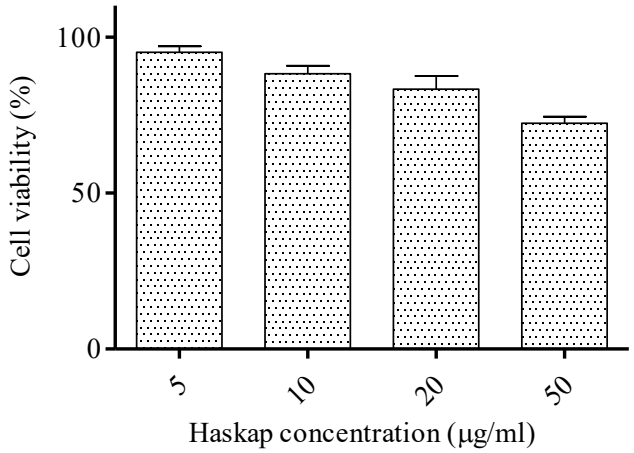

Appendix 2: Viability of BEAS-2B cells after 24 h incubation with NNK at different concentrations.

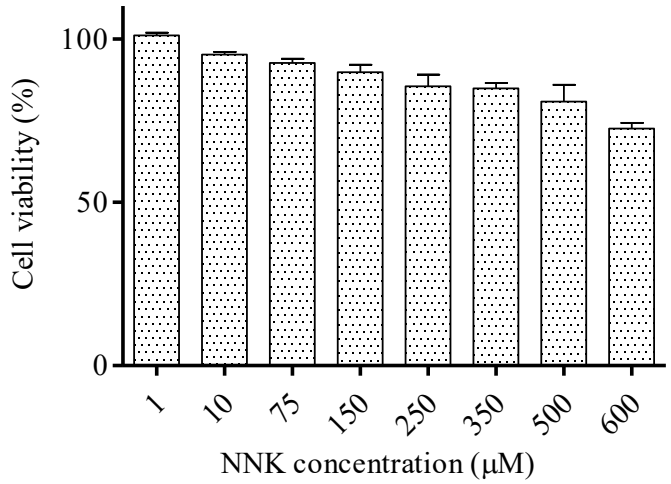

Appendix 3: The formation of γH2AX foci was greater in BEAS-2B cells after treating cells with 200 µM of NNKOAc for 4 h.

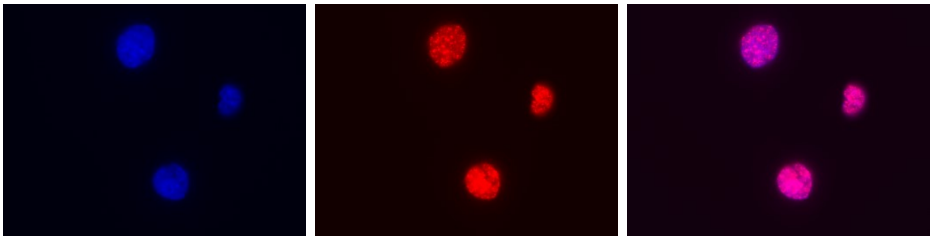

DAPI γH2AX Merge